# Regulation of Survival and Synaptic Connectivity in the Adult Brain by Cell-Intrinsic Excitability

by

Shuyin Sim

B.S. Biology
Duke University, 2005



Submitted to the Department of Biology in Partial Fulfillment of the Requirements for the Degree of

Doctor of Philosophy in Biology
at the
Massachusetts Institute of Technology

June 2011



Signature of Author.....
Department of Biology
April 18, 2011

Certified by..... .....
Carlos Lois
Professor of Neurobiology
Thesis Supervisor

Accepted by..... .....
Robert T. Sauer
Salvador E. Luria Professor of Biology
Chairman, Committee for Graduate Students

# Regulation of Survival and Synaptic Connectivity in the Adult Brain by Cell-Intrinsic Excitability

by

Shuyin Sim

Submitted to the Department of Biology
on May 20, 2011 in Partial Fulfillment of the
Requirements for the Degree of Doctor of Philosophy in
Biology

## ABSTRACT

Although the lifelong addition of new neurons to the olfactory bulb and dentate gyrus of mammalian brains is by now an accepted fact, the function of adult-generated neurons still largely remains a mystery. The ability of new neurons to form synapses with preexisting neurons without disrupting circuit function is central to the hypothesized role of adult neurogenesis as a substrate for learning and memory.

In this doctoral thesis, I present work done in collaboration with other scientists that advance knowledge in our understanding of how the cell-intrinsic excitability of new neurons governs their incorporation into mature circuits in the adult brain. Contrary to the notion that adult neurogenesis represents continual addition of the same type of neurons that are incorporated during brain development, we have obtained data that suggests adult-born neurons have distinct characteristics and may perform a distinct function. Results we have obtained in the olfactory bulb show that an increase in cell-intrinsic activity increases survival of adult-born olfactory granule neurons and that precise spiking of these neurons is not critical for integration. Our observations in the dentate gyrus demonstrate that an increase in cell-intrinsic activity is sufficient to effect alterations in synaptic connectivity with the surrounding circuit and that input connectivity is regulated in an activity-dependent manner by Npas4 signaling.

Progress in the field of adult neurogenesis is beginning to shed light on the flexibility that adult-born neurons offer to mature circuits and their potential contribution toward circuit refinement and adaptation to changing environmental demands. I am pleased to present this work as a small step towards reaching the ultimate goal of understanding the biology of lifelong learning and memory.

Thesis Supervisor: Carlos Lois
Title: Professor of Neurobiology

## Acknowledgements

I thank God for this amazing journey.
To my dear mentor, colleagues, beloved friends and family who have showered me with support, laughter and love through both good and rough times, you have made this possible. Thanks for being there for me—I am so blessed.

# Regulation of Survival and Synaptic Connectivity in the Adult Brain by Cell-Intrinsic Excitability

## CONTENTS

Introduction

# Watching Synaptogenesis in the Adult Brain

The manuscript enclosed in this Introduction has been published in pages 131 – 149 of the 33rd volume of the journal *Annual Review of Neuroscience* dated June 2010 and is reproduced with permission from Annual Reviews.

# Watching Synaptogenesis in the Adult Brain

Wolfgang Kelsch*, Shuyin Sim* and Carlos Lois

*These authors contributed equally to this work

## ABSTRACT

Although the lifelong addition of new neurons to the olfactory bulb and dentate gyrus of mammalian brains is by now an accepted fact, the function of adult-generated neurons still largely remains a mystery. The ability of new neurons to form synapses with preexisting neurons without disrupting circuit function is central to the hypothesized role of adult neurogenesis as a substrate for learning and memory. With the development of several new genetic labeling and imaging techniques, the study of synapse development and integration of these new neurons into mature circuits both in vitro and in vivo is rapidly advancing our insight into their structural plasticity. Investigators' observation of synaptogenesis occurring in the adult brain is beginning to shed light on the flexibility that adult neurogenesis offers to mature circuits and the potential contribution of the transient plasticity that new neurons provide toward circuit refinement and adaptation to changing environmental demands.

## INTRODUCTION

Adult neurogenesis in mammals was first described in the early 1960s (Altman & Das 1965), but it was not until much later that investigators broadly accepted that the addition of new neurons occurs throughout life in both the olfactory bulb (OB) (Lois & Alvarez-Buylla 1993, Luskin 1993) and the dentate gyrus (DG) (Bayer 1980, Bayer et al. 1982, Gage et al. 1995). Although most neurons in the brain are added to immature circuits during assembly, neurons generated in adulthood face an additional challenge as they integrate into mature, fully functional circuits. Relatively little is known about the mechanisms that regulate the synaptic development of adult-born neurons and their connectivity within mature circuits. This review aims to present key aspects of the emerging understanding of synaptogenesis in adult-born neurons, as well as how activity in the brain modulates this process.

Synapse formation during adult neurogenesis raises several intriguing questions. Does synapse formation in adult-born neurons simply recapitulate the steps that occur during embryonic and neonatal development, or is it regulated by specific mechanisms specialized for integration into functioning circuits? How do new neurons make synapses with mature circuits without disrupting existing connectivity? An understanding of synaptogenesis in the adult brain will not only shed light on the putative function of adult neurogenesis in information processing and storage, but also provide new insights to develop strategies for successful neuronal replacement therapies to treat brain injury and neurodegenerative conditions.

We begin this review by discussing some of the techniques currently being used to study synaptogenesis in adult-born neurons. Next, we proceed to critically examine current literature on how the various types of adult-born neurons develop synaptic connections with their respective circuits and how this process is modulated by activity. We also discuss the

functional properties of new neurons and their potential contribution toward refining the existing circuit. Finally, we conclude by reflecting on recent trends and discoveries in this dynamic field and exploring future directions toward understanding the integration of new neurons into adult circuits and the role of adult-born neurons in brain function.

## TECHNIQUES FOR OBSERVING SYNAPTOGENESIS

Recent technical advances have accelerated the study of synapse formation in adult neurogenesis. In particular, two genetic methods that facilitate the selective labeling of new neurons with fluorescent proteins have been especially useful. First, oncoretroviral vectors can be used to label new neurons genetically (Jessberger et al. 2007, Kelsch et al. 2007), as they exclusively infect actively dividing cells, such as neuronal progenitors, but are unable to infect postmitotic cells, such as neurons (Roe et al. 1993). Second, investigators have developed several transgenic mouse lines that enable selective labeling of adult-born neurons. In two of these transgenic lines, expression of a fluorescent protein, either green fluorescent protein (GFP) or red fluorescent protein (dsRed), is driven by promoters that are active only in immature neurons, namely doublecortin (Wang et al. 2007) and nestin (Mignone et al. 2004). This process results in specific labeling of immature neurons in both the OB and the DG (Brown et al. 2003, Yamaguchi et al. 2000). In another line, the proopiomelanocortin (POMC) promoter drives GFP expression, which, unexpectedly, labels new neurons in the DG (Overstreet et al. 2004).

### Genetic Labeling of Synapses of Adult-Born Neurons

Synapse formation has traditionally been studied in three main ways. First, in some cases, synapses can be easily identified on the basis of their association with neuronal structural specializations. For instance, many excitatory input synapses are located in dendritic spines,

in which case spines may be used as a morphological

substitute for synapses. One limitation of this method is that a large proportion of

synapses, such as excitatory input synapses on cell somata and inhibitory synapses, are simply not associated with spines (Price & Powell 1970, Woolf et al. 1991). In addition, it is not possible to accurately quantify the density and measure the size of output synapses by simple morphological analyses. Second, antibody labeling against synaptic markers is a powerful method to label synapses in cultured neurons. However, this method is suboptimal in brain sections because the large number of synapses present severely complicates the attribution of synapses to individual new neurons. Emerging imaging techniques, however, may be able to overcome some of these problems soon (Micheva & Smith 2007). Third, synapses can be unambiguously identified by electron microscopy, but this technique is labor intensive and has yet to be sufficiently developed for high-throughput analysis. Labeling synapses with genetically encoded markers addresses some of the limitations of the above-mentioned techniques and significantly simplifies the quantification of synaptic development in new neurons (Kelsch et al. 2008, Livneh et al. 2009, Meyer & Smith 2006, Niell et al. 2004). The visualization of pre and postsynaptic terminals can be achieved via expression of fluorescent proteins fused to proteins specifically located in synapses. For instance, synaptophysin is a protein located in neurotransmitter vesicles that is selectively localized at presynaptic terminals (Sudhof & Jahn 1991) and can be used to identify release sites on axon terminals (**Figures 1*d*, 2*b***). To identify postsynaptic terminals, PSD95, a scaffolding protein restricted to clusters in the postsynaptic density of most glutamatergic synapses (Ebihara et al. 2003, Gray et al. 2006, Niell et al. 2004, Sassoe-Pognetto et al. 2003, Sheng 2001, Washbourne et al. 2002), can be used (**Figures 1*c*,*d*** and **2*c***). When introducing these genetically encoded markers, it is critical to ensure that only modest levels of overexpression are achieved because excessive levels of these proteins may interfere with synaptic

development or function (El-Husseini et al. 2000). Fortunately, retroviral vectors, which deliver single copies of transgenes into their target cells, produce sufficiently low levels of expression that leave synapse number and strength unperturbed (Kelsch et al. 2008). With genetically encoded markers, one can, in principle, analyze the complete set of a neuron's excitatory input synapses and output synapses, including those not associated with spines or axon terminals, respectively. This method also allows for software-aided quantification of synapses (Kelsch et al. 2008). Furthermore, viral vectors can be engineered such that in addition to synaptic markers other genes of interest, such as those coding for ion channels, growth factors, or cell adhesion molecules, can be introduced in the same vector to assess the effects of various manipulations on synapse formation and dynamics.

The labeling methods mentioned above allow investigators to observe synapse development in combination with a variety of imaging and recording techniques. Here we briefly discuss the strengths and limitations of four major techniques currently used in the field.

**Two-photon laser scanning fluorescence microscopy in vivo**

Two-photon microscope technology has taken off considerably in recent years and is still the only technique that allows for synapse imaging in vivo. This technique is extremely useful for observing real-time changes to experimental manipulations and allows investigators to visualize synapse dynamics. Owing to detection limits, only neurons up to ~800 μm below the brain's surface can be imaged (Helmchen & Denk 2005), largely restricting this technology to the study of adult-born periglomerular neurons (PGNs) in the glomerular layer of the OB and distal dendrites of OBgranule neurons, which are located in the external plexiform layer (**Figure 1*a***) (Mizrahi 2007). By removing part of the neocortex and white

matter above the hippocampus, superficial dendrites of neurons in CA1 of the hippocampus can be imaged with two-photon technology (Mizrahi et al. 2004). However, adult-born granule cells in the DG cannot be imaged in the same manner without damaging a substantial part of the hippocampus. There has been great interest in using two-photon microscopy associated with endoscope lenses to image deep within the brain, but several technical obstacles need to be solved before this method can be routinely used (Barretto et al. 2009).

**Confocal laser scanning microscopy**

Because deep structures of the brain, such as the DG where adult-born granule cells are added, are beyond the depth limitation of two-photon microscopy in vivo, in vitro time-lapse confocal imaging of brain slices is sometimes carried out to study the dynamics of synapse formation (Galimberti et al. 2006, Toni et al. 2007). This technique is not widely used because of concerns about the integrity of cultured adult brain slices over long time periods with currently available culture techniques (Berdichevsky et al. 2009), as well as the possibility of abnormal synapse rearrangement due to fluctuations in culture conditions (Kirov et al. 2004). Confocal

imaging of fixed slices is much more commonly used to study synaptogenesis, especially because this method of observation is technically straightforward and enables investigators to analyze many neurons at one time. Time course experiments can be performed to observe spine formation over days and months, but because only an instantaneous snapshot of the synapses can be obtained in fixed slices, this technique cannot be used to analyze the short-term dynamics of synapse formation in real time.

**Electron microscopy**

Electron microscopy is more technically challenging than confocal imaging but allows for

simultaneous analysis of pre- and postsynaptic sites by visualizing synaptic vesicles and postsynaptic sites, respectively. Electron microscopy can also be used for three-dimensional high-resolution analysis of individual synapses on adult-born neurons and their synaptic partners (Toni et al. 2007). Recent developments within the past few years hint at the possibility of semiautomated sectioning and imaging of large neuropil volumes (Briggman& Denk 2006), thus facilitating high-throughput ultrastructural analyses of synapses.

### Electrophysiology

lectrophysiological recording provides a functional confirmation of structural observations in studies of adult-born neurons. The frequency and amplitude of excitatory and inhibitory synaptic inputs help scientists understand changes in connectivity of new neurons during their maturation and the effects of diverse manipulations. Carleton et al. (2003) and van Praag et al. (2002) have used electrophysiology to describe synaptic properties of new neurons as they mature and integrate into their circuits. One of the most significant contributions of electrophysiology to the study of adult neurogenesis is the demonstration that new neurons display enhanced synaptic plasticity compared with fully mature neurons in both the OB and the DG (Nissant et al. 2009, Schmidt-Hieber et al. 2004). Scharfman et al. (2000) also used electrophysiological methods to study how different manipulations affect neuronal integration into the adult brain, such as the effects of seizures on synaptic properties of adult-born dentate granule neurons.

## SYNAPTOGENESIS IN NEURONS ADDED TO THE ADULT MAMMALIAN BRAIN

The three main types of neurons added to the adult brain are the granule cells ($GC_{OB}$) and PGNs in the OB and the granule cells in the DG ($GC_{DG}$). $GC_{OB}$ constitute the largest

population of adult-born neurons. They are GABAergic interneurons that connect to the lateral dendrites of the OB's principal neurons (mitral and tufted cells; **Figure 1*a***). PGNs are GABAergic and/or dopaminergic interneurons that modulate incoming information from olfactory sensory axons that connect to the apical dendrites of the olfactory bulb's principal neurons (**Figure 1*a***). Granule neurons in the DG are excitatory neurons that receive input from the entorhinal cortex and project to the CA3 region of the hippocampal formation (**Figure 2*a***).

## SYNAPTOGENESIS IN ADULT-BORN OLFACTORY BULB GRANULE NEURONS

### Stages of Synaptic Development

Adult-born $GC_{OB}$ arise from neural progenitors in the subventricular zone (SVZ), which lines the walls of the lateral ventricles (Lois & Alvarez-Buylla 1994). Neuroblasts travel long distances via the rostral migratory stream (RMS) into the OB where they migrate radially into the granule cell layer (Lois & Alvarez- Buylla 1994). Of the ~30,000 new neurons produced daily in an adult mouse, more than 97% differentiate into $GC_{OB}$ while the remaining develop into PGNs (Lois & Alvarez-Buylla 1994, Winner et al. 2002). $GC_{OB}$ are axonless neurons that have a basal and an apical dendrite (**Figure 1*d***). Their apical dendrite is composed of an unbranched segment emerging from the soma followed by a branched segment and can be divided into proximal and distal synaptic domains. The proximal synaptic domain is a region on the unbranched dendrite segment with a high concentration of glutamatergic input synapses. The distal domain consists of the branched dendritic segment and possesses spines containing bidirectional dendro-dendritic synapses, where input and output synapses are colocalized and functionally coupled. These bidirectional synapses receive glutamatergic input synapses from the lateral dendrites of principal neurons and release GABA back onto

the same neurons (**Figure 1*b***) (Mori 1987). Dendro-dendritic synapses are the only output of $GC_{OB}$ and are responsible for local inhibition of principal neurons in the OB (Chen et al. 2000, Halabisky & Strowbridge 2003, Mori 1987). The basal dendrite, or basal domain, and unbranched apical dendrite receive glutamatergic input from axon collaterals of the OB's principal neurons and olfactory cortex (Balu et al. 2007, Davis & Macrides 1981, Luskin & Price 1983, Mori et al. 1983). The developmental stages of adult-born $GC_{OB}$ have been defined according to morphological criteria (Petreanu & Alvarez-Buylla 2002). Stage one neurons are those in the process of migration in the RMS. At stage two, new $GC_{OB}$ reach the granule cell layer and begin to extend their first neurites. At stage three, about ten days after the birth of $GC_{OB}$ in the SVZ, the main dendritic arbor of new $GC_{OB}$ continues to grow and cells start to receive inhibitory synaptic input (Carleton et al. 2003). At stage four, or about two weeks after their birth, new$GC_{OB}$ start receiving excitatory synaptic input (Carleton et al. 2003). In adultborn $GC_{OB}$, excitatory synapses appear first on the proximal segment of the apical dendrite at this stage (Kelsch et al. 2008). At this time there are few spines and synaptic sites on the distal branches of the apical dendrite (Petreanu & Alvarez-Buylla 2002). Finally, at stage five, between three and four weeks after birth of $GC_{OB}$, the distal branches of their apical dendrites develop dense spines, achieving full spine density in these dendrites by four weeks of development (Petreanu & Alvarez-Buylla 2002). During this final stage of maturation, new $GC_{OB}$ acquire the ability to fire fast action potentials (Carleton et al. 2003) and form most of the input and output synapses on their distal branches (Kelsch et al. 2008). Although synaptic development is mostly complete by four weeks after the generation of adult-born $GC_{OB}$ (Carleton et al. 2003, Kelsch et al. 2008, Mizrahi 2007, Petreanu&Alvarez-Buylla 2002, Whitman & Greer 2007a), Mizrahi (2007) has observed rearrangement of spines after this time, which suggests that $GC_{OB}$ may maintain some capacity for synaptic modification even when they are mature.

Adult-born granule neurons first develop input synapses in their proximal dendritic domain, which lacs output synapses, before developing most of their dendro-dendritic output synapses and prior to acquiring the ability to fire action potentials (Kelsch et al. 2008), i.e., they "listen" before they can "speak." This sequential pattern of synaptic development of adult-born $GC_{OB}$ sharply contrasts with the maturation of cells born during neonatal development, which is when most $GC_{OB}$ are generated (Lemasson et al. 2005). First, neonatal-born $GC_{OB}$ develop the ability to fire action potentials early in their development, during stage three, around the same time they start receiving synaptic inputs (Carleton et al. 2003). Second, neurons added to the neonatal brain also develop input and output synapses on the distal and proximal regions of apical dendrites simultaneously (Kelsch et al. 2008). The different modes of synaptic development between adult and neonatal neurons could be due to intrinsic properties of new $GC_{OB}$ already determined in their respective precursors. Alternatively, local cues in the neonatal and adult OB environment may be responsible for these differences. Heterochronic transplantation of postmitotic precursors could be helpful to clarify which aspects of synaptic development are governed by cell-autonomous versus external cues.

**Synapse Connectivity Within Olfactory Circuits**

The lateral dendrites of mitral and tufted cells, which form dendro-dendritic synapses with $GC_{OB}$, are located in the deep and superficial external plexiform layers, respectively (**Figure 1*a***). Most $GC_{OB}$ ramify distal dendritic branches only in either location within the external plexiform layer, not in both (Kelsch et al. 2007, Mori et al. 1983), and this phenomenon is genetically predetermined in neuronal progenitors as demonstrated by fate-mapping and transplantation studies (Kelsch et al. 2007, Merkle et al. 2007). The OB may have "independent microcircuits" such that specific populations of $GC_{OB}$ target only one class of

principal neurons (Mori 1987); $GC_{OB}$ with superficial or deep dendrites may exclusively form synapses with tufted or mitral cells, respectively. However, the existence of these independent microcircuits has yet to be proven functionally. The concept of microcircuit-specific targeting of new neurons in the adult brain is consistent with the protomap model of circuit assembly (Rakic et al. 2009) and raises the possibility of genetically engineering stem cells to generate specific neuronal types to replace those lost to disease or injury.

**Neuronal Addition and Turnover**

The functional differences between deep and superficial $GC_{OB}$ also extend to neuronal survival. Whereas neonatal-born $GC_{OB}$ often reside in the superficial granule cell layers, adult-born neurons tend to localize within the deep layers (Imayoshi et al. 2008, Lemasson et al. 2005). Although most superficial and neonatal-born $GC_{OB}$ survive for long periods approaching the animal's lifetime, deep and adult-born $GC_{OB}$ tend to be short-lived (Imayoshi et al. 2008, Lemasson et al. 2005). A recent study using a transgenic labeling technique suggests that almost all

deep, adult-born neurons are turned over and thus continuously replaced (Imayoshi et al. 2008), which supports Bayer's (1980) original observations. Two long-term studies suggest that cell death in adult-born $GC_{OB}$ is limited to the first month after neuron birth (Lemasson et al. 2005, Winner et al. 2002), whereas another study suggests there is a further drop in cell survival after the first two months (Petreanu & Alvarez-Buylla 2002). However, the latter study has low temporal resolution after the two-month time point, and this result may also be caused by the high variability

between samples. At least some of the adult-born $GC_{OB}$ that persist throughout life

maintain a synaptic density similar to the one they displayed a month after their birth (W. Kelsch & C. Lois, unpublished observations). In summary, the question of neuronal addition

or turnover of adult-born $GC_{OB}$ remains unresolved and warrants further clarification, especially in light of the implications on the potential role of adult neurogenesis for long-term memory storage.

**Activity-Dependent Neuronal Survival**

Only 50% of new $GC_{OB}$ generated in the adult successfully integrate into the bulb's circuits and survive for extended time periods, and abundant evidence indicates that neuronal activity is important in determining their survival. Synaptic maturation in $GC_{OB}$ occurs mostly in the third and fourth week of development (Carleton et al. 2003, Kelsch et al. 2008, Whitman & Greer 2007b). This period coincides with a time window during which the survival of $GC_{OB}$ is most sensitive to sensory deprivation, when the proportion of surviving neurons is further reduced by half in a deprived bulb (Petreanu & Alvarez-Buylla 2002, Yamaguchi et al. 2000, Yamaguchi&Mori 2005). Silencing the circuit with pharmacologically enhanced inhibition also reduces survival of adult-born neurons during this critical period (Yamaguchi & Mori 2005). Rochefort et al. (2002) reported that exposure to an odor-enriched environment increases survival, particularly when the animal is rewarded for performing an odor discrimination task (Alonso et al. 2006). However, the enhanced survival reported in these works has not been observed in other studies (Magavi et al. 2005). Although the source of this disparity is unclear, the enhanced survival reported may not be due solely to exposure to enriched odors, but also to the fact that the behavioral demand of the task may raise animals' attention levels (Alonso et al. 2006). These observations suggest that odor information processing via nascent synapses plays a critical role in the stable integration of new neurons in the adult olfactory system.

**Activity-Dependent Synaptogenesis**

Activity in the OB not only influences the survival of adult-born $GC_{OB}$, but also regulates their synaptic connectivity. When postnatal-born $GC_{OB}$ are subject to sensory deprivation during the critical period, they display fewer synaptic spines (Saghatelyan et al. 2005). Kelsch et al. (2009) recently confirmed this finding using genetically encoded markers for excitatory synapses in adult-born $GC_{OB}$. The loss of input and output synapses triggered by sensory deprivation occurs only during early synaptic development and is not seen when sensory deprivation is performed

after synaptic development is completed. This observation suggests that the critical period during which the survival of new neurons is dependent on sensory input coincides with a stage in which neurons have a high degree of plasticity, which facilitates the shaping of their synaptic organization. Similarly, a recent study by Nissant et al. (2009) has demonstrated that long-term potentiation can be induced in adult-born neurons during early stages of their maturation, but not after this period. It will be interesting to examine whether this critical period also applies to other forms of plasticity in adult-born neurons. The effects of olfactory deprivation on synaptic development are complex: Adult-born $GC_{OB}$ that survive after sensory deprivation display an increased density of proximal input synapses in the unbranched apical dendrite (Kelsch et al. 2009). This observation suggests that neurons may compensate for the absence of sensory input by receiving additional excitatory drive, which elevates their activity level above the threshold required for survival. The relationship between cell-intrinsic excitability and synapse formation is not well understood. Recent experiments indicate that increasing the intrinsic excitability of adult-born $GC_{OB}$ by expressing a voltage gated bacterial sodium channel does not affect synapse formation or maintenance (Kelsch et al. 2009) and promotes stable integration of adult-born $GC_{OB}$ (Lin et al. 2010). However, genetically increased excitability blocks sensory deprivation–triggered synaptic changes. $GC_{OB}$ expressing this sodium channel that are born in a bulb deprived of

sensory input develop a normal organization of glutamatergic input synapses, as measured by the density of their PSD95:GFP-positive clusters (Kelsch et al. 2009). Similarly, dampening the excitability of new $GC_{OB}$ by overexpressing the potassium channel Kir2.1 does not affect the synapse numbers of the surviving neurons (Lin et al. 2010). Taken together with the finding that increased inhibition in the circuit decreases the survival of adult-born GCs (Yamaguchi & Mori 2005), these observations demonstrate that synaptogenesis in adult-born $GC_{OB}$ is sensitive to changes in synaptic input and suggest that both survival selection and synaptic development are driven by a minimum threshold excitation level, to which several factors can contribute: first, local glutamatergic excitatory inputs from mitral or tufted cells, whose activity is regulated primarily by sensory experience; second, centrifugal glutamatergic inputs originating in other regions of the brain, such as the olfactory cortex, which act on the olfactory bulb; third, centrifugal inputs of neuromodulators such as acetylcholine, noradrenaline, or neuropeptides, which modulate neuronal activity on a longer timescale. For instance, cholinergic stimulation, which causes sustained depolarizations in $GC_{OB}$ (Pressler et al. 2007), enhances the survival of new neurons both in the dentate gyrus and in the OB (Kaneko et al. 2006) and may be responsible for the reported enhanced survival of adult-born neurons when olfactory tasks involved increased attention levels (Alonso et al. 2006). Hence, phasic excitation provided by synaptic input from mitral and tufted cells is only one of the many determinants of survival and integration of new GCs into the bulb's circuits. We hope future studies will resolve the ambiguities surrounding the regulation of neuronal survival by centrifugal and sensory-driven inputs. Meanwhile, the transient synaptic plasticity displayed during synaptic development of new $GC_{OB}$ may be an attractive model with which to study how neuronal connectivity during circuit assembly is regulated by activity.

## SYNAPTOGENESIS IN ADULT-BORN OLFACTORY BULB PERIGLOMERULAR NEURONS

The second class of neurons generated throughout life in the OB is the PGN, which surrounds glomeruli, where olfactory sensory axons connect to the apical dendrites of the OB's principal neurons (**Figure 1*a***). PGNs receive excitatory synaptic input both from olfactory sensory axons as well as from the apical dendrites of principal neurons via dendro-dendritic synapses. The outputs of PGNs occur both through dendrodendritic synapses and axonal output synapses with principal neurons, although not all PGNs have axons (Pinching & Powell 1971). PGNs are a highly diverse group of neurons and can be broadly divided into two groups: those whose dendrites synapse on only one or two glomeruli and those that synapse on many (Whitman & Greer 2007a). These neurons can be dopaminergic and/or GABAergic, and different subsets of GABAergic neurons also express different calcium-binding proteins such as calbindin and calretinin (Whitman & Greer 2007a). Different subtypes of PGNs are generated in the OB during embryogenesis, neonatal development, and adulthood (Batista-Brito et al. 2008, De Marchis et al. 2007). Much less is known about the synaptic development of adult-born PGNs as compared with $GC_{OB}$. Given the diversity of adult-born PGNs, one would expect heterogeneity in their synaptic development and organization as well. Indeed, the maturational sequence of spontaneous inputs is not stereotypical for PGNs: Some neurons develop GABAergic inputs first, whereas others develop glutamatergic inputs first (Grubb et al. 2008). Excitatory inputs to PGNs appear early during their development, and their frequency continues to increase until six weeks after their birth (Grubb et al. 2008). During the first six weeks after their birth, adult-born PGNs develop a full dendritic arbor. In vivo two-photon imaging has shown that the spines of adult-born PGNs become more stable as they mature (Livneh et al. 2009). During the

maturation of PGNs, strong functional changes occur in the synapses between sensory neurons and PGNs. These changes appear to be mostly restricted to the postsynaptic sites on the PGNs, whereas the characteristically high release probability at olfactory sensory neuron terminals (Murphy et al. 2004) is already present as soon as functional synapses are formed (Grubb et al. 2008). The highly dynamic rearrangement of input synapses in PGNs may be attributed to the continuous turnover of olfactory sensory axons (Zou et al. 2004), from which they receive their primary input, or could simply be an intrinsic property of these neurons.

### Activity-Dependent Neuronal Survival and Synaptogenesis

Because PGNs are the first relay station of olfactory sensory input, it is hardly surprising that, akin to $GC_{OB}$, adult-born PGNs also display activity-dependent survival. Investigators have reported that sensory deprivation decreases (Mandairon et al. 2006), whereas olfactory enrichment (Rochefort et al. 2002) and olfactory discrimination tasks (Alonso et al. 2006) increase, adult-born PGN survival. Also, sensory enrichment accelerates the development of their glutamatergic input synapses as visualized by genetic synaptic markers (Livneh et al. 2009). PGNs may be an attractive model with which to study the formation of synaptic connections and how they are affected by activity in real time, since their superficial location in the olfactory bulb makes them the only adult-born neurons amenable to in vivo two-photon imaging with sufficient spatial resolution to visualize these changes (Livneh et al. 2009).

## SYNAPTOGENESIS IN ADULT-BORN DENTATE GYRUS GRANULE NEURONS

### Stages of Synaptic Development

The third type of adult-born neurons in mammals is the DG granule cell ($GC_{DG}$), which arises from progenitors in the subgranular zone just beneath the granular layer where mature neurons eventually reside. About 9000 new granule cells are produced daily in the DG of

young rats (Cameron & McKay 2001). These neurons receive their main excitatory input from the entorhinal cortex and provide glutamatergic input primarily to the excitatory pyramidal neurons and inhibitory interneurons in the CA3 region of the hippocampus (**Figure 2*a***). In this manner, the DG acts as the main entry point for entorhinal cortex input into the hippocampus, relaying the information to CA3 for further processing before it is returned to the entorhinal cortex via CA1. The distinct stages of neuronal maturation of adult-born $GC_{DG}$ largely recapitulate those that occur during perinatal development, but at a slower pace (Overstreet-Wadiche et al. 2006a, Zhao et al. 2006). This observation could be due to the upregulation of DISC1 protein in the adult DG, which slows the increase in spine density of $GC_{DG}$ during their development (Duan et al. 2007). The new $GC_{DG}$ first receive GABAergic input to their dendrites approximately one week after they are generated. This innervation is initially depolarizing until two to four weeks, when it becomes hyperpolarizing (Esposito et al. 2005), owing to the transient expression of the inward chloride transporter NKCC1 in immature neurons, which results in an elevated intracellular chloride concentration as compared with mature neurons (Ge et al. 2006). Expression of this transporter is necessary for normal development because its ablation leads to severely delayed neuronal maturation (Ge et al. 2006). In the second week after their birth, dendrites of $GC_{DG}$ start to form spines and to receive glutamatergic input, and their GABAergic input becomes predominantly perisomatic (**Figure 2*d***) (Esposito et al. 2005, Ge et al. 2006). Concurrently, axonal projections from new neurons reach the CA3 region and begin to form contacts that continue to mature for months (Toni et al. 2008). By two months of age, adult-born neurons have similar morphological and electrophysiological properties to those formed during perinatal development (Ge et al. 2007; Laplagne et al. 2006, 2007).

**Activity-Dependent Neuronal Survival**

Akin to GCs in the OB, 50% of new $GC_{DG}$ born in the adult die by four weeks of age (Kempermann et al. 1997a), and their survival is most sensitive to environmental influences between the first and third weeks of development (Tashiro et al. 2006). Levels of neurogenesis and subsequent survival of $GC_{DG}$ are strongly influenced by neuronal activity. Increased levels of adult neurogenesis in the DG accompany changes in experiences through exercise or enriched environments (Kempermann et al. 1997b, van Praag et al. 1999). New neurons that are activated during learning are preferentially selected for incorporation into active DG circuits (Kee et al. 2007). Conversely, new $GC_{DG}$ whose N-methyl-D-aspartate (NMDA) receptor-mediated input is eliminated experience a drastic reduction in survival rates (Tashiro et al. 2006). These observations illustrate that, as described in the OB, neuronal activity plays a role in selecting new neurons that eventually survive and integrate into the DG circuits.

**Activity-Dependent Synaptogenesis and Pathology: Excitability-Induced Rewiring of Adult-Born Neurons in the Dentate Gyrus**

The functional maturation of adult-born $GC_{DG}$ is highly sensitive to changes in activity, and the strongest perturbations of synapse formation in new $GC_{DG}$ are caused by seizures (Parent et al. 1997). Experimentally induced seizures accelerate synaptic development of new neurons such that new $GC_{DG}$ added to an epileptic brain start receiving GABAergic input to their dendrites prior to two weeks after their birth, significantly earlier than in the unperturbed DG (Overstreet-Wadiche et al. 2006b). In experimental seizure models, the DG exhibits network changes that resemble those observed in human pathology of temporal lobe epilepsy. This reorganization of connectivity may be attributed to anomalous integration of new neurons, in addition to other changes in preexisting neurons. Differentiating neurons are most susceptible to develop aberrant connectivity, and some morphological changes are seen

only in new neurons generated within days of the onset of seizure, but not in neurons born a week before (Jessberger et al. 2007). Seizure-induced synaptic alterations to $GC_{DG}$ in animal models include increased numbers of mushroom spines (spines with characteristically large heads) and spiny, branched basal dendrites that extend into the polymorphic cell layer (Jessberger et al. 2007). Seizures also perturb the migration of new $GC_{DG}$. The cell bodies of new $GC_{DG}$ born during seizures aberrantly localize within the hilus and these neurons fire in synchrony with CA3 pyramidal neurons, which suggest that they contribute to increased excitability within the hippocampus (Scharfman et al. 2000). Seizures can also result in mossy fiber sprouting, axonal projection by $GC_{DG}$ to the supragranular molecular layer. The consequences of sprouting are controversial; electrophysiological studies have proposed that this aberrant connectivity produces either recurrent excitatory circuits and subsequent hippocampal hyperexcitability (Okazaki et al. 1995), or conversely, recurrent inhibition by preferentially targeting inhibitory neurons in the molecular layer (Sloviter 1992). Preliminary analyses of the addition of individual new neurons with genetically enhanced excitability into the adult dentate gyrus in vivo suggest that these neurons experience increased perisomatic inhibition as well as a reduction in the frequency of excitatory inputs and density of glutamatergic input synapses (S. Sim, C.W. Lin, and C. Lois, unpublished observations). Notably, these neurons display many of the seizure-induced alterations such as larger dendritic spines and basal dendrites, but they lack mossy fiber sprouting. Investigators have also observed synaptic rearrangements in these neurons' axon terminals. Normal $GC_{DG}$ have axonal specializations known as large mossy terminals, where they form complex synapses with pyramidal neurons in theCA3region of the hippocampus. Neurons with genetically enhanced excitability lose many of their large mossy terminals, suggesting a reduction in inputs to excitatory CA3 neurons. These results support previous findings in hippocampal cultures showing that these axonal connections are fairly dynamic, since synaptic

rearrangements as well as changes in the size of large mossy terminals have been documented in response to changes in spiking activity (Galimberti et al. 2006).

### Synaptic Plasticity During a Critical Period

Similar to the situation described for $GC_{OB}$, there is a critical period within which new neurons in the adult DG display increased synaptic plasticity compared with mature neurons as demonstrated by an enhanced propensity for long-term potentiation (Schmidt-Hieber et al. 2004). This enhanced synaptic plasticity lasts until the second month after new neurons are generated and then decreases to levels comparable to those of the surrounding mature neurons (Ge et al. 2007). Long-term potentiation during this critical period possesses several defining characteristics: It is dependent on the presence of the NR2B subunit of the NMDA receptor and can be induced in the presence of intact inhibition (Ge et al. 2007). Similarly, a low-threshold calcium spike can boost fast sodium action potentials and contribute to long-term potentiation during this critical period (Schmidt-Hieber et al. 2004). Investigating how the flow of information through the hippocampus can shape the synaptic organization of new neurons will help investigators elucidate the role of adult neurogenesis in learning and memory.

## PERSPECTIVES ON THE FUTURE

We conclude this review by raising several open questions that, we hope, may inspire future research.

First, adult neurogenesis is a widespread phenomenon in most vertebrates. It is interesting to note that mammals appear to be an exception among vertebrates: Their brains are composed mostly of long-lived, nonrenewable neurons born during the embryonic

development. Why has a phenomenon that is common in so many classes of animals become less prevalent in mammals? Why is the human cerebellum or neocortex capable of processing, acquiring, and storing information for decades using a single set of neurons, whereas the dentate gyrus and olfactory bulb require the continuous addition of neurons into their circuits throughout life to perform their functions? Second, in contrast with circuit assembly during embryonic development, which involves integration of new neurons in a mostly constant environment in utero, adult-born neurons integrate into mature, functioning circuits. This observation poses additional challenges because adult brain activity is constantly modulated by the ever-changing conditions of the outside world. Furthermore, because adult-generated neurons integrate into the brains of behaving animals, these neurons must form new synapses with minimal disruption to existing connectivity so that behavior is unperturbed. Do specialized mechanisms exist for synaptic integration in adult-born neurons, which differ from those used during embryonic brain development? Third, synaptic plasticity of adult-born neurons is likely restricted to a specific time window early during their maturation. This phenomenon supports the idea that new neurons provide the mature circuit with a transient form of heightened plasticity, acting as a substrate for circuit refinement and adaptation. After this critical window, the neurons mature, become stably integrated into the brain, and partially lose their activity-dependent plasticity. The addition of cells endowed with such an initial short-lived flexibility and longterm stability enables information processing in the brain to be both versatile and reliable while faced with changing behavioral demands. The transient plasticity of new cells generated during adult neurogenesis may explain the requirement for additional new neurons to facilitate lifelong plasticity and reshaping of memory circuits. Which molecular mechanisms are responsible for this transient plasticity? Most mammalian brain regions, such as the thalamus, striatum, and neocortex do not receive any new neurons after birth. Do neurons in these brain areas maintain their

plasticity for longer periods of time compared with adult-born neurons added into the OB and DG?

Investigating these unanswered questions will shed some light on the mystery of why mammalian brain circuits are composed of two classes of neurons: those that live as long as the individual harboring them and those that are continuously added throughout life.

## LITERATURE CITED


Alonso M, Viollet C, Gabellec MM, Meas-Yedid V, Olivo-Marin JC, Lledo PM. 2006. Olfactory discrimination learning increases the survival of adult-born neurons in the olfactory bulb. *J. Neurosci.* 26:10508–13

Altman J, Das GD. 1965. Autoradiographic and histological evidence of postnatal hippocampal neurogenesis in rats. *J. Comp. Neurol.* 124:319–35

Balu R, Pressler RT, Strowbridge BW. 2007. Multiple modes of synaptic excitation of olfactory bulb granule cells. *J. Neurosci.* 27:5621–32

Barretto RP, Messerschmidt B, Schnitzer MJ. 2009. In vivo fluorescence imaging with high-resolution microlenses. *Nat. Methods* 6:511–12

Batista-Brito R, Close J, Machold R, Fishell G. 2008. The distinct temporal origins of olfactory bulb interneuron subtypes. *J. Neurosci.* 28:3966–75

Bayer SA. 1980. Quantitative 3H-thymidine radiographic analyses of neurogenesis in the rat amygdala. *J. Comp. Neurol.* 194:845–75

Bayer SA, Yackel JW, Puri PS. 1982. Neurons in the rat dentate gyrus granular layer substantially increase during juvenile and adult life. *Science* 216:890–92

Berdichevsky Y, Sabolek H, Levine JB, Staley KJ, Yarmush ML. 2009. Microfluidics and multielectrode array-compatible organotypic slice culture method. *J. Neurosci. Methods* 178:59–64

Briggman KL, Denk W. 2006. Towards neural circuit reconstruction with volume electron microscopy techniques. *Curr. Opin. Neurobiol.* 16:562–70

Brown JP, Couillard-Despres S, Cooper-Kuhn CM, Winkler J, Aigner L, Kuhn HG. 2003. Transient expression of doublecortin during adult neurogenesis. *J. Comp. Neurol.* 467:1–10

Cameron HA, McKay RD. 2001. Adult neurogenesis produces a large pool of new granule cells in the dentate gyrus. *J. Comp. Neurol.* 435:406–17

Carleton A, Petreanu LT, Lansford R, Alvarez-Buylla A, Lledo PM. 2003. Becoming a new neuron in the adult olfactory bulb. *Nat. Neurosci.* 6:507–18 Chen WR, Xiong W, Shepherd GM. 2000. Analysis of relations betweenNMDAreceptors and GABA release at olfactory bulb reciprocal synapses. *Neuron* 25:625–33

Davis BJ, Macrides F. 1981. The organization of centrifugal projections from the anterior olfactory nucleus, ventral hippocampal rudiment, and piriform cortex to the main olfactory bulb in the hamster: an autoradiographic study. *J. Comp. Neurol.* 203:475–93 De Marchis S, Bovetti S, Carletti B, Hsieh YC, Garzotto D, et al. 2007. Generation of distinct types of periglomerular olfactory bulb interneurons during development and in adult mice: implication for intrinsic properties of the subventricular zone progenitor population. *J. Neurosci.* 27:657–64

Duan X, Chang JH, Ge S, Faulkner RL, Kim JY, et al. 2007. Disrupted-In-Schizophrenia 1

regulates integration of newly generated neurons in the adult brain. *Cell* 130:1146–58
Ebihara T, Kawabata I, Usui S, Sobue K, Okabe S. 2003. Synchronized formation and remodeling of postsynaptic densities: long-term visualization of hippocampal neurons expressing postsynaptic density proteins tagged with green fluorescent protein. *J. Neurosci.* 23:2170–81
El-Husseini AE, Schnell E, Chetkovich DM, Nicoll RA, Bredt DS. 2000. PSD-95 involvement in maturation
of excitatory synapses. *Science* 290:1364–68
Esposito MS, Piatti VC, Laplagne DA, Morgenstern NA, Ferrari CC, et al. 2005. Neuronal differentiation in the adult hippocampus recapitulates embryonic development. *J. Neurosci.* 25:10074–86
Gage FH, Coates PW, Palmer TD, Kuhn HG, Fisher LJ, et al. 1995. Survival and differentiation of adult neuronal progenitor cells transplanted to the adult brain. *Proc. Natl. Acad. Sci. USA* 92:11879–83
Galimberti I, Gogolla N, Alberi S, Santos AF, Muller D, Caroni P. 2006. Long-term rearrangements of hippocampal mossy fiber terminal connectivity in the adult regulated by experience. *Neuron* 50:749–63
Ge S, Goh EL, Sailor KA, Kitabatake Y, Ming GL, Song H. 2006. GABA regulates synaptic integration of newly generated neurons in the adult brain. *Nature* 439:589–93
Ge S, Yang CH, Hsu KS, Ming GL, Song H. 2007. A critical period for enhanced synaptic plasticity in newly generated neurons of the adult brain. *Neuron* 54:559–66
Gray NW, Weimer RM, Bureau I, Svoboda K. 2006. Rapid redistribution of synaptic PSD-95 in the neocortex in vivo. *PLoS Biol.* 4:e370
Grubb MS, Nissant A, Murray K, Lledo PM. 2008. Functional maturation of the first synapse in olfaction: development and adult neurogenesis. *J. Neurosci.* 28:2919–32
Halabisky B, Strowbridge BW. 2003. Gamma-frequency excitatory input to granule cells facilitates dendrodendritic inhibition in the rat olfactory Bulb. *J. Neurophysiol.* 90:644–54
Helmchen F, Denk W. 2005. Deep tissue two-photon microscopy. *Nat. Methods* 2:932–40
Imayoshi I, Sakamoto M, Ohtsuka T, Takao K, Miyakawa T, et al. 2008. Roles of continuous neurogenesis in the structural and functional integrity of the adult forebrain. *Nat. Neurosci.* 11:1153–61
Jessberger S, Zhao C, Toni N, Clemenson GD Jr, Li Y, Gage FH. 2007. Seizure-associated, aberrant neurogenesis in adult rats characterized with retrovirus-mediated cell labeling. *J. Neurosci.* 27:9400–7
Kaneko N, Okano H, Sawamoto K. 2006. Role of the cholinergic system in regulating survival of newborn neurons in the adult mouse dentate gyrus and olfactory bulb. *Genes Cells* 11:1145–59
Kee N, Teixeira CM, Wang AH, Frankland PW. 2007. Preferential incorporation of adult-generated granule cells into spatial memory networks in the dentate gyrus. *Nat. Neurosci.* 10:355–62
Kelsch W, Lin CW, Mosley CP, Lois C. 2009. A critical period for activity-dependent synaptic development during olfactory bulb adult neurogenesis. *J. Neurosci.* 29:11852–58
Kelsch W, Lin CW, Lois C. 2008. Sequential development of synapses in dendritic domains during adult neurogenesis. *Proc. Natl. Acad. Sci. USA* 105:16803–8
Kelsch W, Mosley CP, Lin CW, Lois C. 2007. Distinct mammalian precursors are committed to generate neurons with defined dendritic projection patterns. *PLoS Biol.* 5:e300
Kempermann G, Kuhn HG, Gage FH. 1997a. Genetic influence on neurogenesis in the dentate gyrus of adult mice. *Proc. Natl. Acad. Sci. USA* 94:10409–14
Kempermann G, Kuhn HG, Gage FH. 1997b. More hippocampal neurons in adult mice living

in an enriched environment. *Nature* 386:493–95
Kirov SA, Petrak LJ, Fiala JC, Harris KM. 2004. Dendritic spines disappear with chilling but proliferate excessively upon rewarming of mature hippocampus. *Neuroscience* 127:69–80
Laplagne DA, Esposito MS, Piatti VC, Morgenstern NA, Zhao C, et al. 2006. Functional convergence of neurons generated in the developing and adult hippocampus. *PLoS Biol.* 4:e409
Laplagne DA, Kamienkowski JE, Esposito MS, Piatti VC, Zhao C, et al. 2007. Similar GABAergic inputs in dentate granule cells born during embryonic and adult neurogenesis. *Eur. J. Neurosci.* 25:2973–81
Lemasson M, Saghatelyan A, Olivo-Marin JC, Lledo PM. 2005. Neonatal and adult neurogenesis provide two distinct populations of newborn neurons to the mouse olfactory bulb. *J. Neurosci.* 25:6816–25
Lin CW, Sim S, Ainsworth A, Okada M, Kelsch W, Lois C. 2010. Genetically increased cell-intrinsic excitability enhances neuronal integration into adult brain circuits. *Neuron* 65:32–39
Livneh Y, Feinstein N, Klein M, Mizrahi A. 2009. Sensory input enhances synaptogenesis of adult-born neurons. *J. Neurosci.* 29:86–97
Lois C, Alvarez-Buylla A. 1993. Proliferating subventricular zone cells in the adult mammalian forebrain can differentiate into neurons and glia. *Proc. Natl. Acad. Sci. USA* 90:2074–77
Lois C, Alvarez-Buylla A. 1994. Long-distance neuronal migration in the adult mammalian brain. *Science* 264:1145–48
Luskin MB. 1993. Restricted proliferation and migration of postnatally generated neurons derived from the forebrain subventricular zone. *Neuron* 1:173–89
Luskin MB, Price JL. 1983. The topographic organization of associational fibers of the olfactory system in the rat, including centrifugal fibers to the olfactory bulb. *J. Comp. Neurol.* 216:264–91
Magavi SS, Mitchell BD, Szentirmai O, Carter BS, Macklis JD. 2005. Adult-born and preexisting olfactory granule neurons undergo distinct experience-dependent modifications of their olfactory responses in vivo. *J. Neurosci.* 25:10729–39
Mandairon N, Sacquet J, Jourdan F, Didier A. 2006. Long-term fate and distribution of newborn cells in the adult mouse olfactory bulb: influences of olfactory deprivation. *Neuroscience* 141:443–51
Merkle FT, Mirzadeh Z, Alvarez-Buylla A. 2007. Mosaic organization of neural stem cells in the adult brain. *Science* 317:381–84
Meyer MP, Smith SJ. 2006. Evidence from in vivo imaging that synaptogenesis guides the growth and branching of axonal arbors by two distinct mechanisms. *J. Neurosci.* 26:3604–14
Micheva KD, Smith SJ. 2007. Array tomography: a new tool for imaging the molecular architecture and ultrastructure of neural circuits. *Neuron* 55:25–36
Mignone JL, Kukekov V, Chiang AS, Steindler D, Enikolopov G. 2004. Neural stem and progenitor cells in nestin-GFP transgenic mice. *J. Comp. Neurol.* 469:311–24
Mizrahi A. 2007. Dendritic development and plasticity of adult-born neurons in the mouse olfactory bulb. *Nat. Neurosci.* 10:444–52
Mizrahi A, Crowley JC, Shtoyerman E, Katz LC. 2004. High-resolution in vivo imaging of hippocampal dendrites and spines. *J. Neurosci.* 24:3147–51
Mori K. 1987. Membrane and synaptic properties of identified neurons in the olfactory bulb. *Prog. Neurobiol.* 29:275–320
Mori K, Kishi K, Ojima H. 1983. Distribution of dendrites of mitral, displaced mitral, tufted, and granule cells in the rabbit olfactory bulb. *J. Comp. Neurol.* 219:339–55
Murphy GJ, Glickfeld LL, Balsen Z, Isaacson JS. 2004. Sensory neuron signaling to the

brain: properties of transmitter release from olfactory nerve terminals. *J. Neurosci.* 24:3023–30
Niell CM, Meyer MP, Smith SJ. 2004. In vivo imaging of synapse formation on a growing dendritic arbor. *Nat. Neurosci.* 7:254–60
Nissant A, Bardy C, Katagiri H, Murray K, Lledo PM. 2009. Adult neurogenesis promotes synaptic plasticity
in the olfactory bulb. *Nat. Neurosci.* 12:728–30
Okazaki MM, Evenson DA, Nadler JV. 1995. Hippocampal mossy fiber sprouting and synapse formation after status epilepticus in rats: visualization after retrograde transport of biocytin. *J. Comp. Neurol.* 352:515–34
Overstreet LS, Hentges ST, Bumaschny VF, de Souza FS, Smart JL, et al. 2004. A transgenic marker for newly born granule cells in dentate gyrus. *J. Neurosci.* 24:3251–59
Overstreet-Wadiche LS, Bensen AL, Westbrook GL. 2006a. Delayed development of adult-generated granule cells in dentate gyrus. *J. Neurosci.* 26:2326–34
Overstreet-Wadiche LS, Bromberg DA, Bensen AL, Westbrook GL. 2006b. Seizures accelerate functional integration of adult-generated granule cells. *J. Neurosci.* 26:4095–103
Parent JM, Yu TW, Leibowitz RT, Geschwind DH, Sloviter RS, Lowenstein DH. 1997. Dentate granule cell neurogenesis is increased by seizures and contributes to aberrant network reorganization in the adult rat hippocampus. *J. Neurosci.* 17:3727–38
Petreanu L, Alvarez-Buylla A. 2002. Maturation and death of adult-born olfactory bulb granule neurons: role of olfaction. *J. Neurosci.* 22:6106–13
Pinching AJ, Powell TP. 1971. The neuropil of the periglomerular region of the olfactory bulb. *J. Cell Sci.* 9:379–409
Pressler RT, Inoue T, Strowbridge BW. 2007. Muscarinic receptor activation modulates granule cell excitability and potentiates inhibition onto mitral cells in the rat olfactory bulb. *J. Neurosci.* 27:10969–81
Price JL, Powell TP. 1970. The synaptology of the granule cells of the olfactory bulb. *J. Cell Sci.* 7:125–55
Rakic P, Ayoub AE, Breunig JJ, Dominguez MH. 2009. Decision by division: making cortical maps. *Trends Neurosci.* 32:291–301
Rochefort C, Gheusi G, Vincent JD, Lledo PM. 2002. Enriched odor exposure increases the number of newborn neurons in the adult olfactory bulb and improves odor memory. *J. Neurosci.* 22:2679–89
Roe T, Reynolds TC, Yu G, Brown PO. 1993. Integration of murine leukemia virus DNA depends on mitosis. *EMBO J.* 12:2099–108
Saghatelyan A, Roux P, Migliore M, Rochefort C, Desmaisons D, et al. 2005. Activity-dependent adjustments of the inhibitory network in the olfactory bulb following early postnatal deprivation. *Neuron* 46:103–16
Sassoe-Pognetto M, Utvik JK, Camoletto P, Watanabe M, Stephenson FA, et al. 2003. Organization of postsynaptic density proteins and glutamate receptors in axodendritic and dendrodendritic synapses of the rat olfactory bulb. *J. Comp. Neurol.* 463:237–48
Scharfman HE, Goodman JH, Sollas AL. 2000. Granule-like neurons at the hilar/CA3 border after status epilepticus and their synchrony with area CA3 pyramidal cells: functional implications of seizure-induced neurogenesis. *J. Neurosci.* 20:6144–58
Schmidt-Hieber C, Jonas P, Bischofberger J. 2004. Enhanced synaptic plasticity in newly generated granule cells of the adult hippocampus. *Nature* 429:184–87
Sheng M. 2001. Molecular organization of the postsynaptic specialization. *Proc. Natl. Acad. Sci. USA* 98:7058– 61
Sloviter RS. 1992. Possible functional consequences of synaptic reorganization in the dentate

gyrus of kainite treated rats. *Neurosci. Lett.* 137:91–96
Sudhof TC, JahnR. 1991. Proteins of synaptic vesicles involved in exocytosis and membrane recycling. *Neuron*
6:665–77
Tashiro A, SandlerVM, ToniN, Zhao C, Gage FH. 2006. NMDA-receptor-mediated, cell-specific integration of new neurons in adult dentate gyrus. *Nature* 442:929–33
Toni N, Laplagne DA, Zhao C, Lombardi G, Ribak CE, et al. 2008. Neurons born in the adult dentate gyrus form functional synapses with target cells. *Nat. Neurosci.* 11:901–7
Toni N, Teng EM, Bushong EA, Aimone JB, Zhao C, et al. 2007. Synapse formation on neurons born in the adult hippocampus. *Nat. Neurosci.* 10:727–34
van Praag H, Kempermann G, Gage FH. 1999. Running increases cell proliferation and neurogenesis in the adult mouse dentate gyrus. *Nat. Neurosci.* 2:266–70
van Praag H, Schinder AF, Christie BR, Toni N, Palmer TD, Gage FH. 2002. Functional neurogenesis in the adult hippocampus. *Nature* 415:1030–34
Wang X, Qiu R, Tsark W, Lu Q. 2007. Rapid promoter analysis in developing mouse brain and genetic labeling of young neurons by doublecortin-DsRed-express. *J. Neurosci. Res.* 85:3567–73
Washbourne P, Bennett JE, McAllister AK. 2002. Rapid recruitment of NMDA receptor transport packets to nascent synapses. *Nat. Neurosci.* 5:751–59
Whitman MC, Greer CA. 2007a. Adult-generated neurons exhibit diverse developmental fates. *Dev. Neurobiol.* 67:1079–93
Whitman MC, Greer CA. 2007b. Synaptic integration of adult-generated olfactory bulb granule cells: basal axodendritic centrifugal input precedes apical dendrodendritic local circuits. *J. Neurosci.* 27:9951–61
Winner B, Cooper-Kuhn CM, Aigner R, Winkler J, Kuhn HG. 2002. Long-term survival and cell death of newly generated neurons in the adult rat olfactory bulb. *Eur. J. Neurosci.* 16:1681–89 Woolf TB, Shepherd GM, Greer CA. 1991. Serial reconstructions of granule cell spines in the mammalian olfactory bulb. *Synapse* 7:181–92
Yamaguchi M, Mori K. 2005. Critical period for sensory experience-dependent survival of newly generated granule cells in the adult mouse olfactory bulb. *Proc. Natl. Acad. Sci. USA* 102:9697–702
Yamaguchi M, Saito H, Suzuki M, Mori K. 2000. Visualization of neurogenesis in the central nervous system using nestin promoter-GFP transgenic mice. *Neuroreport* 11:1991–96
Zhao C, Teng EM, Summers RG Jr, Ming GL, Gage FH. 2006. Distinct morphological stages of dentate granule neuron maturation in the adult mouse hippocampus. *J. Neurosci.* 26:3–11
Zou DJ, Feinstein P, Rivers AL, Mathews GA, Kim A, et al. 2004. Postnatal refinement of peripheral olfactory projections. *Science* 304:1976–79

## FIGURES

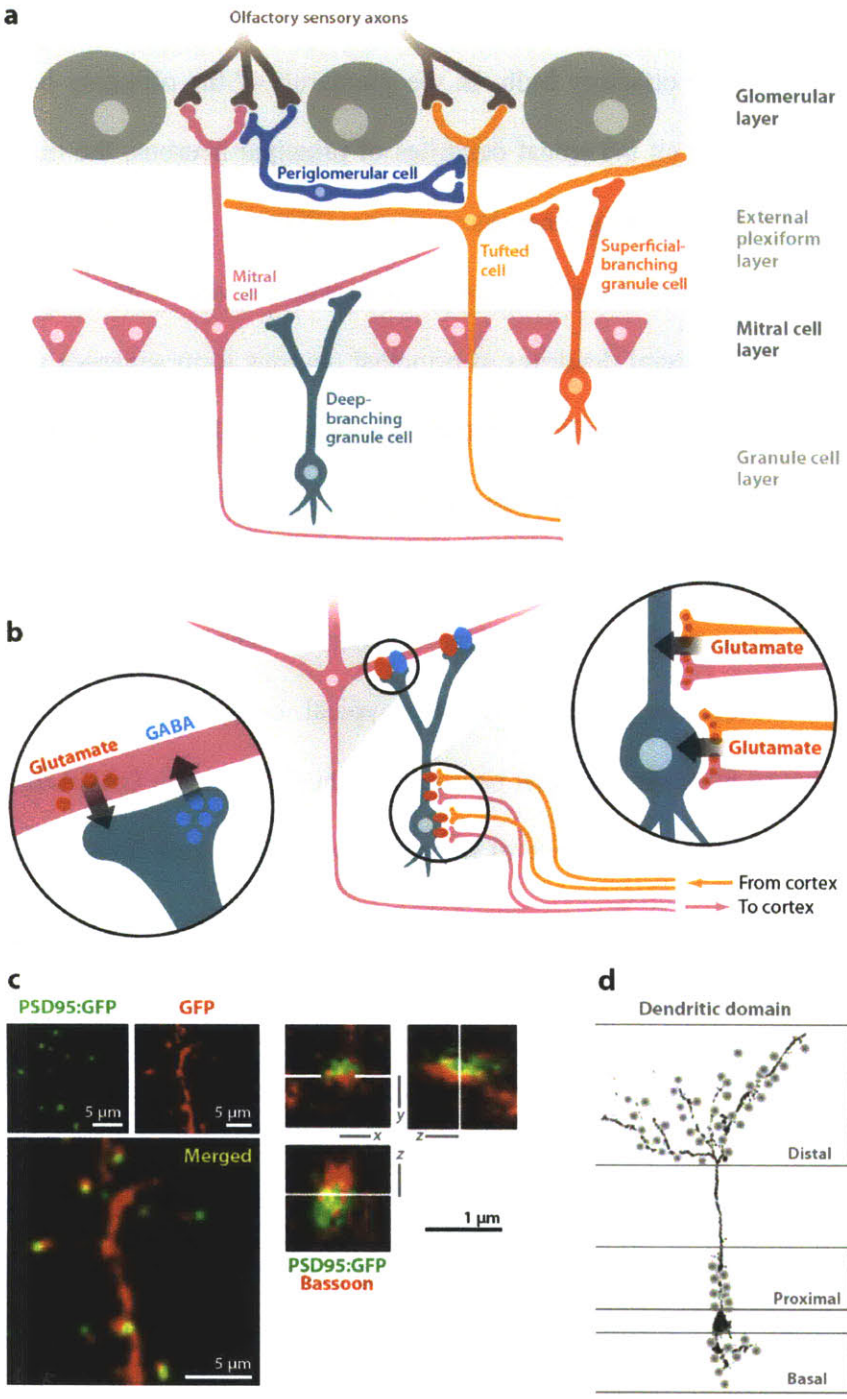
a
Olfactory sensory axons
Periglomerular cell
Tufted cell
Superficial-branching granule cell
Mitral cell
Deep-branching granule cell
Glomerular layer
External plexiform layer
Mitral cell layer
Granule cell layer
b
Glutamate
GABA
Glutamate
Glutamate
From cortex
To cortex
c
PSD95:GFP
GFP
5 µm
5 µm
Merged
5 µm
y
x
z
z
1 µm
PSD95:GFP
Bassoon
d
Dendritic domain
PSD95:GFP
Syp:GFP
Distal
Proximal
Basal
10 µm

**Figure 1. Adult-born olfactory bulb granule cells and their synaptic wiring with the surrounding circuit.**

(*a*) Synaptic organization in the olfactory bulb. In the glomeruli of the olfactory bulb, olfactory sensory axons synapse on the apical dendrites of principal neurons, the mitral and tufted cells, as well as on periglomerular neurons (PGNs), which line these glomeruli. PGNs also form additional synaptic connections with the apical dendrites of principal neurons, whereas the lateral dendrites of principal neurons form synapses with granule cells ($GC_{OB}$). Two independent microcircuits may exist in the olfactory bulb, with $GC_{OB}$ with either deep or superficial dendritic branching

connecting exclusively to mitral or tufted cells, respectively. (*b*) Synaptic connectivity of olfactory bulb granule neurons. $GC_{OB}$ form dendro-dendritic synapses with lateral dendrites of principal neurons in the bulb. These atypical synapses consist of a glutamatergic input synapse from the principal neuron onto the $GC_{OB}$ and a GABAergic output synapse onto the same lateral dendrite of the principal neuron, both located in a single spine. In addition, $GC_{OB}$ receive glutamatergic inputs onto their basal and proximal apical dendrites from centrifugal cortical axons and possibly also from axon collaterals of principal neurons. $GC_{OB}$ are also contacted by GABAergic input synapses from local interneurons in the olfactory bulb as well as cholinergic and monoaminergic inputs. (*c*) Genetic labeling of synapses. *Left*: Progenitors of $GC_{OB}$ were infected in the subventricular zone (SVZ) with retroviral vectors carrying genetic constructs encoding PSD95:GFP, a marker for postsynaptic glutamatergic sites, to generate PSD95:GFP-expressing $GC_{OB}$. PSD95:GFP-positive clusters can be detected by direct visualization of GFP (*shown as green puncta*). The dendritic morphology of the $GC_{OB}$ was revealed by

amplifying the low levels of PSD95:GFP in the cytoplasm (that could not be detected by intrinsic fluorescence) by immunostaining against GFP with a red fluorescent secondary antibody. The merged images of PSD95:GFP positive clusters ( *green*) and dendritic morphology (*red* ) allow investigators to attribute clusters to specific dendritic domains of individual $GC_{OB}$ (scale bar, 5 μm). *Right*: Confocal three-dimensional image showing a PSD95:GFP positive cluster in a new $GC_{OB}$ that is contacted by the presynaptic marker, bassoon (scale bar, 1 μm). (*d* ) Synaptic distribution in the dendritic domains of granule cells. $GC_{OB}$ have a basal dendrite and an apical dendrite, which consist of proximal and distal synaptic domains. The proximal domain is a specialized sector of the unbranched apical dendrite that emerges directly from the soma of $GC_{OB}$, which contains a high density of glutamatergic input

synapses. The branched dendritic segment of the apical dendrite is known as the distal domain. Examples of genetic labeling of synapses in the dendritic domains of granule cells are given for postsynaptic glutamatergic synapses, PSD95:GFP, and for the presynaptic genetic marker, Synaptophysin:GFP (Syp:GFP).

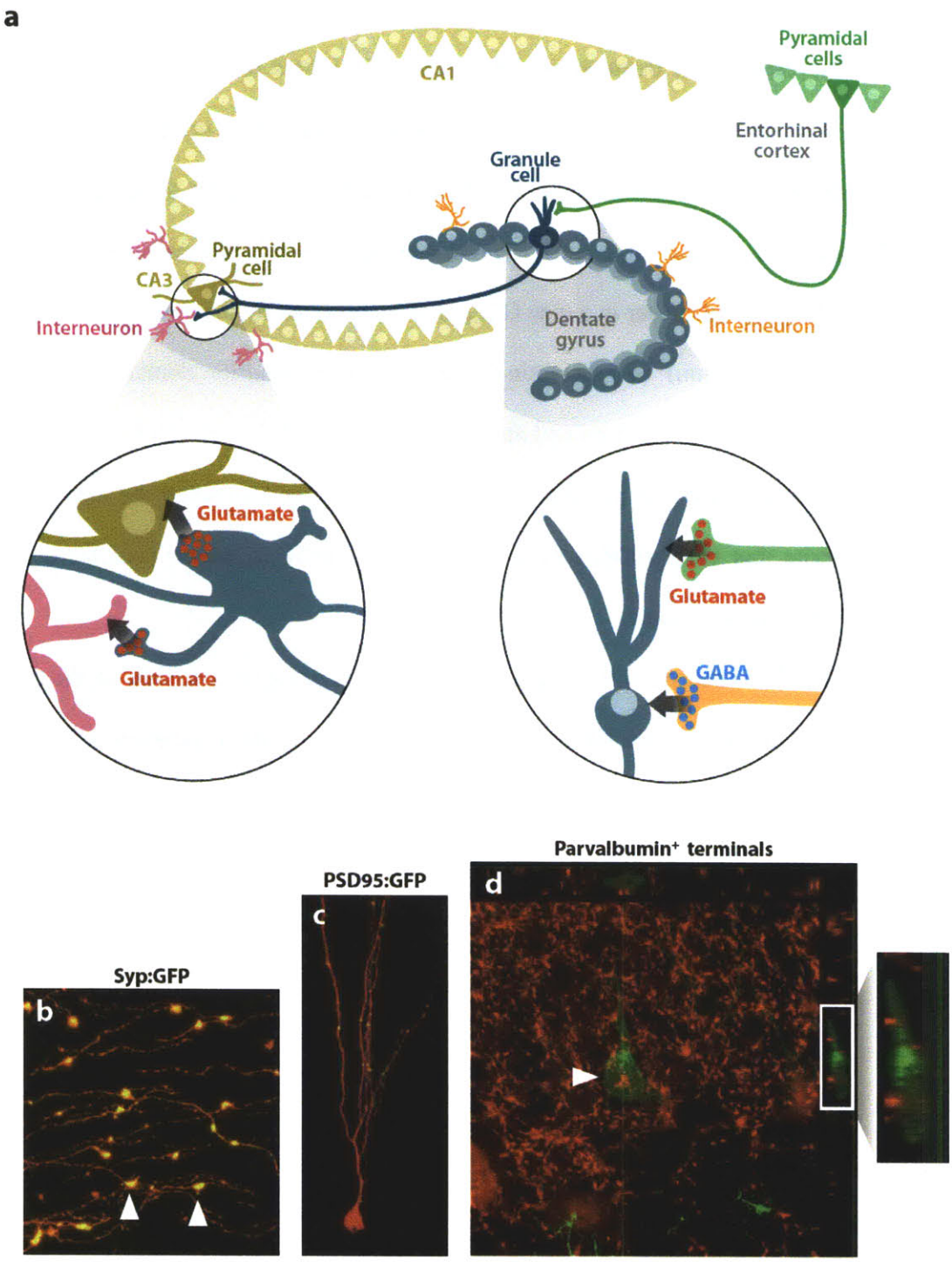
a
CA1
Pyramidal cells
Entorhinal cortex
Granule cell
Pyramidal cell
CA3
Interneuron
Dentate gyrus
Interneuron
Glutamate
Glutamate
Glutamate
GABA
Syp:GFP
b
PSD95:GFP
c
Parvalbumin+ terminals
d

**Figure 2. Adult-born granule cells in the dentate gyrus and their synaptic wiring with the hippocampal and other circuits.**

(*a*) Synaptic organization of dentate granule cells. Adult-born granule cells in the dentate gyrus ($GC_{DG}$) receive excitatory glutamatergic input onto their apical dendrites from projection neurons in the entorhinal cortex and mossy cells in the hippocampus, as well as inhibitory GABAergic input from local interneurons. $GC_{DG}$ project axons solely to the CA3 region of the hippocampus. At the CA3 region, these axons constitute two forms of specialized contact sites: large mossy terminals and en passant boutons. Large mossy terminals are compartmentalized release sites: The central portion of these terminals forms complex interdigitating synapses with proximal dendrites of CA3 pyramidal cells while the emanating filopodia of the terminals synapse on GABAergic interneurons in CA3. En passant boutons are smaller synaptic swellings along the axon collaterals that exclusively contact CA3 interneurons. (*b*) Genetic labeling of output synapses along axon collaterals of dentate granule cells. The release sites from $GC_{DG}$ onto CA3 neurons, at large mossy terminals (*arrowheads*) and en passant boutons on the axons of adult-born $GC_{DG}$, can be visualized by a genetic presynaptic marker, synaptophysin:GFP (Syp:GFP, *yellow*). (*c*) Genetic labeling of input synapses in the apical dendrites of granule cells. Adult-born $GC_{DG}$ develop glutamatergic input sites as visualized by PSD95:GFP (*yellow*) in their apical dendrite during their differentiation. Note the absence of PSD95:GFP-positive sites on the soma. (*d*) Identification of inhibitory innervation on the soma of adult-born dentate granule cells. Parvalbumin-positive inhibitory terminals (*red*) contacting the soma of an adult-born $GC_{DG}$ (*arrowhead*) can be visualized by immunohistochemistry against parvalbumin. *Left*: Confocal image of a GFP-positive

$GC_{DG}$ labeled by retroviral infection of progenitors in the subgranular zone of the dentate gyrus. *Right*: Magnified z-stack cross-section of image on left.

Chapter 1

# Genetically Increased Cell-Intrinsic Excitability Enhances Neuronal Integration into Adult Brain Circuits

The manuscript enclosed in this Chapter has been published in pages 32 – 39 of the 65th issue of the journal *Neuron* dated January 14 2010 and is reproduced with permission from Cell Press.

# Genetically increased cell-intrinsic excitability enhances neuronal integration into adult brain circuits

Chia-Wei Lin*, Shuyin Sim*,
Alice Ainsworth, Masayoshi Okada, Wolfgang Kelsch and Carlos Lois

*These authors contributed equally to this work

## ABSTRACT

New neurons are added to the adult brain throughout life, but only half ultimately integrate into existing circuits. Sensory experience is an important regulator of the selection of new neurons but it remains unknown whether experience provides specific patterns of synaptic input, or simply a minimum level of overall membrane depolarization critical for integration. To investigate this issue, we genetically modified intrinsic electrical properties of adult-generated neurons in the mammalian olfactory bulb. First, we observed that suppressing levels of cell-intrinsic neuronal activity via expression of ESKir2.1 potassium channels decreases, whereas enhancing activity via expression of NaChBac sodium channels increases survival of new neurons. Neither of these modulations affects synaptic formation. Furthermore, even when neurons are induced to fire dramatically altered patterns of action potentials, increased levels of cell-intrinsic activity completely blocks cell death triggered by NMDA receptor deletion. These findings demonstrate that overall levels of cell-intrinsic activity govern survival of new neurons and precise firing patterns are not essential for neuronal integration into existing brain circuits.

*Author Contributions: Chia-Wei Lin and Shuyin Sim designed the experiments, designed and generated retroviral vectors, performed intracranial injections, collected and analyzed cell survival data. Alice Ainsworth and Wolfgang Kelsch assisted with data analysis. Chia-Wei Lin and Masayoshi Okada performed electrophysiological recordings. Chia-Wei Lin, Shuyin Sim and Carlos Lois wrote the manuscript.*

## INTRODUCTION

A striking feature of nervous system development is that many more neurons are produced than are ultimately retained in the mature nervous system (Buss et al., 2006). Neuronal addition persists throughout life in the dentate gyrus of the hippocampus and the olfactory bulb (OB), where there continues to be overproduction and subsequent selection of neurons (Petreanu and Alvarez-Buylla, 2002; Winner et al., 2002; Yamaguchi and Mori, 2005). Unlike during embryonic development, neurons born postnatally are added to functionally mature circuits where their integration is believed to be regulated by sensory input or the behavioral state of the animal (Kee et al., 2007; Petreanu and Alvarez-Buylla, 2002).

It is postulated that the addition of new neurons into the adult brain may be a mechanism for lifelong learning and behavioral adaptation (Aimone et al., 2006; Lledo et al., 2006). Since only half of adult-generated neurons ultimately survive and integrate, it has been hypothesized that only new neurons that form relevant connections are incorporated to achieve fine-tuning of existing neuronal circuits (Aimone et al., 2006; Alonso et al., 2006; Kee et al., 2007; Lledo et al., 2006; Mouret et al., 2008; Wilbrecht et al., 2002). From experiments involving sensory deprivation in the OB and ablation of the NMDA receptor in the dentate gyrus, it is clear that synaptic input is a key regulator of the integration of adult-born neurons (Alonso et al., 2006; Kee et al., 2007; Mouret et al., 2008; Tashiro et al., 2006a; Wilbrecht et al., 2002). This idea is further supported by studies showing a preferential incorporation of adult-generated neurons into active circuits in the dentate gyrus (Kee et al., 2007). In addition, we have recently demonstrated that olfactory deprivation perturbs synaptic development of new neurons in the adult OB and that genetically increasing the intrinsic excitability of individual neurons blocks the changes in synaptic density triggered by sensory deprivation (Kelsch et al., 2009). These observations suggest an interaction between

sensory input and intrinsic neuronal activity in synapse formation, and possibly neuronal survival. However, it is still unclear whether the contribution of synaptic input is mainly to provide a precise pattern of neuronal activity to the new neurons, or merely a minimum level of membrane depolarization necessary for their selection and integration.

The elucidation of the mechanisms regulating the integration of new neurons has important implications both for understanding how neural circuits are constructed, as well as for successful implementation of stem cell-based replacement therapies for brain repair and neurodegenerative diseases. To evaluate the effect of suppressing or elevating electrical activity on the integration of young neurons into the OB, we used retroviral vectors to introduce ion channels into neuronal progenitors in the brains of adult rodents. In the current study, we found that overall levels of activity within a new neuron determined its integration into the circuit irrespective of firing patterns. Moreover, increasing intrinsic activity was sufficient to partially overcome cell death induced by sensory deprivation, and completely rescued neurons deficient in the NMDA receptor. Our observations reveal a rule of neuronal integration that is reliant on overall levels of membrane depolarization rather than on a specific pattern of firing.

## RESULTS

### Expression of the potassium channel ESKir2.1 dampens electrical activity in adult-generated neurons

The vast majority of new neurons in the OB of adult mammals are granule cells (GCs), inhibitory neurons whose progenitors reside in the subventricular zone (SVZ) (Lois and Alvarez-Buylla, 1994). Neuroblasts generated in the SVZ move along the rostral migratory

stream toward the core of the OB and subsequently migrate radially into the granule cell layers. We genetically labeled adult born GCs by injecting retroviral vectors into the SVZ of adult rats. Since retroviral vectors only infect dividing cells, the progenitor cells within the SVZ are labeled but not mature neurons. We later monitored the subsequent integration of new GCs into the OB. The first arriving neuroblasts appeared in the adult rat OB as early as at 5 dpi. By 21 dpi, migrating neuroblasts still in the RMS contributed to 7.4% of the cells in the OB. By 28 dpi, the late arriving neuroblasts contributed to less than 2 percent of total infected cells inside the OB. The low infectivity rate of the retroviruses *in vivo* results in the modification of a very small proportion of GCs (less than 0.01% of all GCs), which appear randomly distributed throughout the bulb, thus negligibly perturbing the rest of the circuit (Kelsch et al., 2008; Kelsch et al., 2007).

To accurately assess neuronal integration, we injected approximate 1:1 titers of mixtures of a virus encoding the channel under study (tagged by GFP) and a virus encoding mCherry, so that mCherry-expressing neurons could be used as age-matched controls. We divided the number of $GFP^+$ and doubly infected ($GFP^+$ and $mCherry^+$) neurons by the number of $mCherry^+$-only neurons to derive a survival ratio and used the raw 7 dpi ratio to normalize subsequent time points. Thus, the 7 dpi ratios are 1 and ratios at other time points are relative to the 7 dpi ratio.

To dampen the excitability of adult-born GCs, we expressed a non-inwardly rectifying variant of the Kir2.1 potassium channel, Kir2.1 E224S (Yang et al., 1995), henceforth referred to as ESKir2.1. Expression of ESKir2.1 resulted in a leak current that reduced the cell's input resistance by ~ 2 fold and set a more negative resting membrane potential, thereby reducing the probability of neuronal spiking by increasing the requirement for synaptic input to achieve firing threshold (Figure 1A-D). Expression of ESKir2.1

hyperpolarized the neuroblasts in the core of the OB as early as at 7 dpi (Figure S1A-H) and did not affect the initial stages of development of new GCs, as ESKir2.1$^+$ GCs successfully migrated into the OB and survived as well as control neurons up till 14 dpi (Figures 1E and S2C,D). This observation argues against the possibility that expression of this ion channel results in non-specific toxic effects in the new neurons.

**Dampening electrical activity inhibits integration of adult-generated neurons into the OB**

By 28 dpi, however, the number of ESKir2.1$^+$ neurons integrated into the OB was reduced by 57±8% (***; $p<0.002$; n = 4 bulbs; Figure 1E and S2E). Interestingly, this timing coincides with a critical period for integration of newly generated GCs in the postnatal OB, between 14 and 28 dpi, during which their survival is most sensitive to olfactory deprivation (Yamaguchi and Mori, 2005). These results demonstrate an important role of neuronal activity in regulating the integration of adult-generated neurons in a cell-autonomous manner. Interestingly, spine density and the frequency of spontaneous excitatory postsynaptic current (sEPSC) were indistinguishable between control and ESKir2.1$^+$ neurons, suggesting that suppression of cell-intrinsic neuronal activity has minimal effects on synaptic development (Figure S1I-L). However, the amplitude of sEPSC was higher for ESKir2.1$^+$ than controls neurons at 28 dpi (Figure S1J). This increase in sEPSC amplitude may reflect the synaptic scaling previously described in activity-deprived neurons (Turrigiano and Nelson, 2004).

**Expression of the voltage-gated sodium channel NaChBac elevates electrical activity in adult-generated neurons**

Recent studies propose that adult neurogenesis serves to facilitate experience-dependent modification of neural circuits for adaptation to environmental changes (Aimone et al., 2006; Wilbrecht et al., 2002). This hypothesis suggests that the timing of synaptic inputs relative to activity in the rest of the circuit, and their source and strength would all be predicted to participate in regulating the integration of new neurons. Alternatively, integration of new neurons may simply be determined by summing overall levels of activity in a neuron during a specific critical period, regardless of its source or timing, and neurons that meet a minimum threshold are retained. To investigate these possibilities, we increased neuronal activity in individual new GCs in the OB in a manner that reduces their dependency on synaptic input for firing, and evaluated the consequences of this manipulation on neuronal integration into the OB.

To disrupt normal firing patterns and increase the occurrence of neuronal firing, such that neuronal spiking would occur with synaptic inputs that are insufficient to evoke action potentials in control neurons, we used the bacterial voltage-gated sodium channel NaChBac. Two key properties of NaChBac allow for this: First, its activation threshold is approximately 15 mV more negative than that of native sodium channels in granule neurons (Kelsch et al., 2007); Second, it inactivates on the order of hundreds of milliseconds, compared to less than 1 ms in mammalian sodium channels (Bean, 2007; Ren et al., 2001). We have previously observed that NaChBac expression in GCs triggers depolarizations approximately 600 ms long (Kelsch et al., 2009). Such long depolarizations are not uncommon in neurons in the mammalian brain. For instance, cholinergic stimulation has been shown to trigger long depolarizations in several neuronal types (Fraser and MacVicar, 1996). Here we examined whether this phenomenon also occurs in newly generated GCs. Application of carbachol, a muscarinic agonist mimicking cholinergic input, induced long

after-depolarization-potentials (ADPs) in adult-born GCs (Figure 2A). These long depolarizations robustly occurred in adult-born GCs during the early (18 dpi) but not late (28 dpi) phases of their integration into the OB (Figure 2A,B). The ADP triggered by carbachol was completely blocked by pre-applying atropine, a muscarinic receptor antagonist (Figures 2A and S2F-H). These findings suggest that physiological stimuli, such as cholinergic innervation, can trigger long membrane depolarizations in adult-born GCs, similar to those induced by NaChBac expression.

We delivered NaChBac to GC precursors in the SVZ using the strategy described for ESKir2.1. To assess the ability of NaChBac to enhance the intrinsic excitability of new GCs, we performed whole cell patch clamp recordings between 14 to 16 dpi, at the beginning of their critical period for survival. At this stage, newly generated GCs expressing NaChBac-EGFP ($NaChBac^+$) have a slow inward current that activates at -41±1.8 mV, which causes neurons to fire spontaneous action potentials significantly more frequently than control neurons and with long plateau potentials lasting on average 608±68 ms (Figure 2D-F). In addition, we have observed that the electrophysiological effects of NaChBac expression on GCs persist throughout the duration of the critical period (Kelsch et al., 2009). Thus, NaChBac expression is sufficient to increase overall levels of neuronal activity in newly generated GCs.

**Increased intrinsic electrical activity enhances the integration of adult-generated neurons into the OB**

We assessed the effect of increasing electrical excitability via NaChBac expression on the integration of adult-born GCs into the OB, and found that up till 14 dpi, $NaChBac^+$ neurons migrated and integrated into the OB at similar levels to control neurons (Figure 2G and

Figure S2A, B). However, beginning at 21 dpi, NaChBac$^+$ neurons integrated into the OB at significantly higher rates than control neurons (21 dpi: 22±6%; **P < 0.002; n = 4 bulbs; 28 dpi: 31±4%; ***p<0.0001; n = 10 bulbs; Figure 2G). This increase in survival persisted for as long as 2 months after infection (56 dpi; 25±3%; **p< 0.0001; n = 6 bulbs). Electrophysiological measurements of sEPSCs in NaChBac$^+$ neurons indicate that they received similar levels of excitatory synaptic input as compared to control neurons, demonstrating that the enhanced survival of NaChBac$^+$ neurons was accompanied by functional integration into the circuit (Figure 3A,B). Furthermore, NaChBac$^+$ neurons were morphologically similar to control neurons, with no changes in the pattern of dendritic arborization or in the linear density of synaptic spines (Figure 3C-G). This observation is consistent with our previous finding that NaChBac does not affect the density of clusters labeled with the synaptic marker PSD95-GFP in OB GCs (Kelsch et al., 2009). These observations illustrate that NaChBac$^+$ neurons are functional, and suggest that strong perturbations of cell-intrinsic neuronal activity via either NaChBac or ESKir2.1 expression have minimal effects on the synaptic development of these neurons.

Our findings suggest that increasing the overall intrinsic level of activity in an adult-born neuron is sufficient to confer a significant survival advantage to that cell, but do not allow us to specify whether adult-generated neurons normally have a requirement for patterns of synaptic input specifically driven by sensory experience in order to integrate into the bulb. Multiple studies have demonstrated that sensory input is crucial for the integration of new neurons into the OB (Alonso et al., 2006; Petreanu and Alvarez-Buylla, 2002), but it remains unclear whether sensory input simply provides a minimum, necessary level of synaptic drive onto new GCs to support survival, or if sensory-driven patterns of synaptic input contain information relevant to the selection of the new GC for integration.

**NaChBac rescues adult-generated neurons from death in a sensory-deprived OB**

To further explore these questions, we tested whether a NaChBac-mediated increase in neuronal activity can substitute for physiological sensory experience in mediating the integration of adult-born neurons into the OB. We co-injected a mixture of retroviruses bilaterally into the SVZ of animals in which we had unilaterally occluded one nostril, a procedure that eliminates sensory input to the ipsilateral bulb. Previous works have demonstrated that 50% of new neurons in the adult ultimately integrate into the normal OBs, whereas nostril occlusion further reduces this proportion to 25% (Winner et al., 2002; Yamaguchi and Mori, 2005). The survival ratio of NaChBac$^+$ neurons compared to control cells in the non-occluded bulb was approximately 1.33, similar to that described above (Figure 2G,H); in contrast, in the occluded bulb this ratio was increased to approximately 1.76 (Figure 2H). Since olfactory deprivation results in approximately 50% decrease in the survival of new GCs, a complete rescue of sensory-dependent GC death by NaChBac in an occluded bulb would result in a survival ratio of 2; thus, a ratio of 1.76 indicates that NaChBac expression provides more than a 75% rescue of GC death resulting from sensory deprivation. This result demonstrates that increased neuronal excitability conferred by NaChBac expression is sufficient to partially substitute for the contribution of sensory-dependent synaptic input in regulating GC integration. This observation parallels our previous data showing that NaChBac expression blocks changes in synaptic density induced by sensory deprivation (Kelsch et al., 2009). Furthermore, this observation suggests that experience-driven synaptic input is not the only mechanism driving the selection of adult-born neurons for integration as corroborated by the finding that 25% of new neurons still

survive in sensory deprived bulbs (Petreanu and Alvarez-Buylla, 2002; Yamaguchi and Mori, 2005).

**NMDA receptor activity is essential for integration of adult-generated neurons in the OB**

Because NaChBac promotes neuronal integration independent of experience-driven synaptic input, it is probable that the mechanism regulating activity-dependent survival is directly tracking the levels of membrane depolarization. The membrane potential of a neuron is constantly modulated by neurotransmitters acting on synaptic receptors, and in the central nervous system, AMPA- and NMDA-receptors (NMDARs) are the major receptors mediating membrane depolarization. Previous studies have suggested that NMDAR activity regulates the survival of adult-born neurons in the dentate gyrus (Tashiro et al., 2006a). The requirement of NMDAR signaling for neuronal survival may depend on the detection of coincident pre- and post-synaptic activity, such as in spike-timing dependent plasticity (Dan and Poo, 2006), or alternatively, the requirement of NMDAR function for new neuron survival may simply reflect the contribution of NMDAR activity to overall levels of neuronal depolarization in new GCs.

To investigate the contribution of NMDAR to new neuron integration, we first sought to confirm the requirement for NMDAR function in the survival of new GCs in the OB. We genetically ablated the essential NR1 subunit to eliminate all NMDAR-mediated input in individual new GCs by sparsely infecting progenitor cells in the SVZ of *NR1* floxed conditional mice ($NR1^{fl/fl}$) with retroviral vectors encoding the Cre recombinase enzyme (Kohara et al., 2007; Tashiro et al., 2006b). Cre-mediated ablation of *NR1* successfully eliminated NMDAR expression since application of NMDA failed to induce any currents in

Cre$^+$ neurons in *NR1*$^{fl/fl}$ mice (Figure 4A-C). By 28 dpi, virtually all NMDAR-deficient neurons were eliminated (Figure 4D,E). In comparison, no change in the survival of EGFP-CRE$^+$ neurons was observed in *NR1*$^{+/+}$ littermates (Figure 4D). This result demonstrates that the NMDAR, whose ablation decreases the survival of new dentate gyrus neurons by only 50% (Tashiro et al., 2006a), is absolutely required for the integration of adult-born GCs in the OB.

**NaChBac expression rescues NMDAR-deficient adult-generated neurons from death**

We next determined whether increasing activity in new GCs via NaChBac expression could substitute for NMDAR function in supporting neuronal integration into the OB. NaChBac and Cre recombinase were simultaneously delivered into *NR1*$^{fl/fl}$ mice, and GC integration was assessed. We found that increasing the excitability of newly generated NMDAR-deficient GCs via NaChBac expression completely rescued their death (Figure 4D,E). The dendritic morphology of NaChBac$^+$ NMDAR-deficient neurons appeared similar to that of control neurons and received AMPAR-mediated synaptic input (Figure S3), indicating that they functionally integrated into the bulb's circuit. These results demonstrate that the requirement for NMDARs in the integration of new GCs most likely reflects the contribution of NMDARs to the overall levels of neuronal activity in the neuron. Furthermore, our data support a model in which activity-dependent integration depends on overall levels of membrane depolarization, irrespective of how this depolarization is achieved.

## DISCUSSION

**An activity threshold for integration of new adult-born neurons into the OB circuit**

To elucidate whether synaptic input regulates survival by providing new neurons with a precise pattern of neuronal activity, or merely a minimal level of membrane depolarization, we used NaChBac, a bacterial voltage-gated sodium channel, to perturb the spiking pattern of new neurons while simultaneously elevating their activity levels. Our results indicate that the integration of new neurons into the OB circuit predominantly depends on their overall levels of membrane depolarization, regardless of the pattern of action potentials generated. Interestingly, tonic cholinergic stimulation, which causes sustained depolarizations in adult-born OB neurons during their early integration (Figures 2A-C and S2), has recently been shown to enhance the survival of new neurons both in the OB and dentate gyrus (Kaneko et al., 2006). Conversely, the removal of cholinergic input into the OB compromises the survival of new neurons (Cooper-Kuhn et al., 2004). Given our findings about depolarization-enhanced integration, the long depolarizations induced by cholinergic stimulation may directly contribute to the improved survival of new neurons observed in previous studies (Kaneko et al., 2006). Interestingly, the long depolarizations induced by cholinergic stimulation occur robustly in young GCs during the critical period of survival at 18 dpi but not after maturation at 28 dpi, indicating a possible role of prolonged cholinergic-induced depolarization specifically in driving survival of new OB granule neurons. General behavioral states, such as running, stress, attentiveness and depression affect neuronal integration of new neurons into adult brains (Gould et al., 1997; Malberg et al., 2000; Mouret et al., 2008; van Praag et al., 1999). Our results suggest that neuromodulators such as acetylcholine may mediate these effects by acting as significant regulators of the level of depolarization of new neurons.

The notion that general membrane depolarization is a determinant of neuronal integration is further supported by our observation that although NMDAR expression is

essential for new neuron integration, NaChBac-mediated depolarization is sufficient to fully rescue NMDAR-deficient neurons from death. Hence, the requirement of NMDAR in new neuron survival may be due to the extended depolarization caused by its slow gating kinetics. Interestingly, recent evidence also indicates that the contribution of NMDAR for synaptic vesicle release in GCs is not directly through the calcium entry through its pore but indirectly through the influx of calcium through voltage-gated calcium channels, which open as a result of the long depolarization induced by NMDAR activity (Isaacson, 2001; Schoppa et al., 1998). Together, our data support a model in which activity-dependent integration depends on overall levels of membrane depolarization, determined, for instance, by monitoring calcium influx through L-type voltage-gated calcium channels (Dolmetsch et al., 2001), rather than specifically on neuronal activity mediated by postsynaptic glutamate receptors.

It is not yet known how activity levels could be monitored in order to determine if a particular cell achieves the minimum threshold of neuronal activity required to survive and successfully integrate into the adult brain. New adult-born neurons could act as integrators that measure and summate levels of activity over a critical period, lasting perhaps on the time scale of days, to compute this life or death decision (McCormick, 2001). This critical period spans a time period sometime between 14 to 28 days after the birth of the neuron, when sensory deprivation or ESKir2.1-mediated suppression of activity has the strongest effect on survival (Yamaguchi and Mori, 2005). Alternatively, instantaneous levels of activity may be continuously evaluated such that neurons that never meet the minimum threshold of activity during the critical period are eliminated.

**Determinants of dendritic morphology of GCs in the OB**

When we introduced ESKir2.1 into GCs in the OB, we observed that although the electrical properties of these neurons were altered significantly, their dendritic structures remained unchanged. This is unexpected because overexpression of Kir2.1 in neurons has been previously shown to alter the morphology of axons, in transfected retinal neurons in zebrafish (Hua and Smith, 2004), as well as dendrites, in transfected rat hippocampal neurons *in vitro* (Burrone et al., 2002). Two non-mutually exclusive explanations could account for our findings. First, in previous experiments, Kir2.1 channels were expressed in excitatory neurons (Burrone et al., 2002; Hua and Smith, 2004), whereas here we specifically target inhibitory interneurons. The plasticity responses of excitatory and inhibitory neurons differ in many respects (Bi and Poo, 1998), and it is plausible that electrical silencing by Kir2.1 channels affects the morphology of excitatory, but not inhibitory neurons. Next, gene delivery methods used in previous work induce much higher levels of Kir2.1 expression than what we report here with oncoretroviral delivery. For instance, calcium-phosphate transfection of Kir2.1 into cultured hippocampal neurons lowers the neurons' input resistance from 166+/-11 to 63+/-25 MΩ, which corresponds to a 10,000 pS increase of Kir2.1 conductance (Burrone et al., 2002). In contrast, our oncoretroviral vector delivery of ESkir2.1 results in expression levels that only introduces 600 pS of resting leak conductance and lowers the input resistance of GCs from 1147+/-59 to 655+/-76 MΩ, even though neuronal firing is largely eliminated. Thus, it is possible that the changes in neuronal morphology previously reported were not solely due to reduction of neuronal excitability by Kir2.1 activity, but to additional effects resulting from very high levels of expression.

Reduction of sensory input by olfactory deprivation has been shown to modify synaptic structure of GCs (Saghatelyan et al., 2005). We have recently confirmed this

observation using genetic labeling of postsynaptic glutamatergic densities with the PSD95-GFP marker (Kelsch et al., 2009). In addition, we observed that whereas NaChBac did not affect the density of PSD95-GFP synapses in normal conditions, it blocked the synaptic changes triggered by olfactory deprivation (Kelsch et al., 2009). These observations suggest an interaction between sensory input and intrinsic membrane excitability to achieve a minimal level of neuronal activity necessary for the normal development of synapses in GCs. Our current results indicate that this principle also extends to neuronal survival, since there seems to be a minimum threshold of neuronal activity required for the integration of young GCs into the OB. This threshold level of activity can similarly be provided by a combination of synaptic input and intrinsic membrane excitability. Our experiments indicate that the elevation of intrinsic excitability via NaChBac expression is sufficient to counteract the reduction of sensory input. Reaching this minimal level of activity both rescues young GCs from death and allows them to acquire normal synaptic organization in an odor-deprived OB.

**Determinants of overall activity level in new neurons**

What drives overall activity levels, and hence survival of new adult-born neurons during the critical period? One feature of the critical period is that it coincides with the onset of synapse formation in GCs, and this has led previous studies to primarily focus on the role of phasic synaptic input, as regulated by sensory experience, in new neuron survival. In addition, during this critical period the intrinsic conductance (e.g. A-type potassium channels, voltage-gated sodium channels) of new neurons undergo major changes as the neurons mature. Our findings show that in addition to synaptic input, membrane conductance, as determined by the repertoire of ion channels expressed by new neurons, may play a pivotal role in regulating integration and survival. Variability in membrane conductance between neurons of the same

type has been shown to be significant (Marder and Goaillard, 2006), and fluctuations in the intrinsic excitability of young neurons could result in differing levels of synaptic input required for their survival. In addition, the intrinsic excitability of OB neurons is strongly modulated by centrifugal innervation originating from other parts of the brain. In particular, cholinergic stimulation induces long-lasting depolarizations in GCs, which facilitate persisting firing modes (Figure S2 and Pressler et al., 2007). These phenomena could account for the observation that cells rendered hyperexcitable by NaChBac expression are able to survive with reduced levels of synaptic input resulting from olfactory deprivation or NMDAR ablation. In this manner, the overall level of activity, as determined by the combination of synaptic inputs received and intrinsic membrane properties, drives integration of new neurons into a circuit.

**ACKNOWLEDGEMENTS**

We thank Alberto Stolfi and Drew Friedman for help with engineering of the viral constructs, David Clapham for providing us with NaChBac cDNA, Susumu Tonegawa for providing conditional NR1 mice, Benjamin Scott for help with two-photon imaging, and Leopoldo Petreanu, Sacha Nelson, Suzanne Paradis and Elizabeth Hong for comments on the manuscript. This work was supported by an NIDCD RO1 grant to C.L., an M.I.T. Singleton and Chyn Duog Shiah Memorial fellowships to C.W.L., and a Newton postdoctoral fellowship to W.K.

## REFERENCES


Aimone, J.B., Wiles, J., and Gage, F.H. (2006). Potential role for adult neurogenesis in the encoding of time in new memories. Nat Neurosci *9*, 723-727.

Alonso, M., Viollet, C., Gabellec, M.M., Meas-Yedid, V., Olivo-Marin, J.C., and Lledo, P.M. (2006). Olfactory discrimination learning increases the survival of adult-born neurons in the olfactory bulb. J Neurosci *26*, 10508-10513.

Bean, B.P. (2007). The action potential in mammalian central neurons. Nat Rev Neurosci *8*, 451-465.

Bi, G.Q., and Poo, M.M. (1998). Synaptic modifications in cultured hippocampal neurons: dependence on spike timing, synaptic strength, and postsynaptic cell type. J Neurosci *18*, 10464-10472.

Burrone, J., O'Byrne, M., and Murthy, V.N. (2002). Multiple forms of synaptic plasticity triggered by selective suppression of activity in individual neurons. Nature *420*, 414-418.

Buss, R.R., Sun, W., and Oppenheim, R.W. (2006). Adaptive roles of programmed cell death during nervous system development. Annu Rev Neurosci *29*, 1-35.

Cooper-Kuhn, C.M., Winkler, J., and Kuhn, H.G. (2004). Decreased neurogenesis after cholinergic forebrain lesion in the adult rat. J Neurosci Res *77*, 155-165.

Dan, Y., and Poo, M.M. (2006). Spike timing-dependent plasticity: from synapse to perception. Physiol Rev *86*, 1033-1048.

Dolmetsch, R.E., Pajvani, U., Fife, K., Spotts, J.M., and Greenberg, M.E. (2001). Signaling to the nucleus by an L-type calcium channel-calmodulin complex through the MAP kinase pathway. Science *294*, 333-339.

Fraser, D.D., and MacVicar, B.A. (1996). Cholinergic-dependent plateau potential in hippocampal CA1 pyramidal neurons. J Neurosci *16*, 4113-4128.

Gould, E., McEwen, B.S., Tanapat, P., Galea, L.A., and Fuchs, E. (1997). Neurogenesis in the dentate gyrus of the adult tree shrew is regulated by psychosocial stress and NMDA receptor activation. J Neurosci *17*, 2492-2498.

Hua, J.Y., and Smith, S.J. (2004). Neural activity and the dynamics of central nervous system development. Nat Neurosci *7*, 327-332.

Isaacson, J.S. (2001). Mechanisms governing dendritic gamma-aminobutyric acid (GABA) release in the rat olfactory bulb. Proc Natl Acad Sci U S A *98*, 337-342.

Kaneko, N., Okano, H., and Sawamoto, K. (2006). Role of the cholinergic system in regulating survival of newborn neurons in the adult mouse dentate gyrus and olfactory bulb. Genes Cells *11*, 1145-1159.

Kee, N., Teixeira, C.M., Wang, A.H., and Frankland, P.W. (2007). Preferential incorporation of adult-generated granule cells into spatial memory networks in the dentate gyrus. Nat Neurosci *10*, 355-362.

Kelsch, W., Lin, C.W., and Lois, C. (2008). Sequential development of synapses in dendritic domains during adult neurogenesis. Proc Natl Acad Sci U S A *105*, 16803-16808.

Kelsch, W., Lin, C.W., Mosley, C.P., and Lois, C. (2009). A critical period for activity-dependent synaptic development during olfactory bulb adult neurogenesis. J Neurosci *29*, 11852-11858.

Kelsch, W., Mosley, C.P., Lin, C.W., and Lois, C. (2007). Distinct mammalian precursors are committed to generate neurons with defined dendritic projection patterns. PLoS Biol *5*, e300.

Kohara, K., Yasuda, H., Huang, Y., Adachi, N., Sohya, K., and Tsumoto, T. (2007). A local reduction in cortical GABAergic synapses after a loss of endogenous brain-derived

neurotrophic factor, as revealed by single-cell gene knock-out method. J Neurosci *27*, 7234-7244.
Lledo, P.M., Alonso, M., and Grubb, M.S. (2006). Adult neurogenesis and functional plasticity in neuronal circuits. Nat Rev Neurosci *7*, 179-193.
Lois, C., and Alvarez-Buylla, A. (1994). Long-distance neuronal migration in the adult mammalian brain. Science *264*, 1145-1148.
Malberg, J.E., Eisch, A.J., Nestler, E.J., and Duman, R.S. (2000). Chronic antidepressant treatment increases neurogenesis in adult rat hippocampus. J Neurosci *20*, 9104-9110.
Marder, E., and Goaillard, J.M. (2006). Variability, compensation and homeostasis in neuron and network function. Nat Rev Neurosci *7*, 563-574.
McCormick, D.A. (2001). Brain calculus: neural integration and persistent activity. Nat Neurosci *4*, 113-114.
Mouret, A., Gheusi, G., Gabellec, M.M., de Chaumont, F., Olivo-Marin, J.C., and Lledo, P.M. (2008). Learning and survival of newly generated neurons: when time matters. J Neurosci *28*, 11511-11516.
Petreanu, L., and Alvarez-Buylla, A. (2002). Maturation and death of adult-born olfactory bulb granule neurons: role of olfaction. J Neurosci *22*, 6106-6113.
Pressler, R.T., Inoue, T., and Strowbridge, B.W. (2007). Muscarinic receptor activation modulates granule cell excitability and potentiates inhibition onto mitral cells in the rat olfactory bulb. J Neurosci *27*, 10969-10981.
Ren, D., Navarro, B., Xu, H., Yue, L., Shi, Q., and Clapham, D.E. (2001). A prokaryotic voltage-gated sodium channel. Science *294*, 2372-2375.
Saghatelyan, A., Roux, P., Migliore, M., Rochefort, C., Desmaisons, D., Charneau, P., Shepherd, G.M., and Lledo, P.M. (2005). Activity-dependent adjustments of the inhibitory network in the olfactory bulb following early postnatal deprivation. Neuron *46*, 103-116.
Schoppa, N.E., Kinzie, J.M., Sahara, Y., Segerson, T.P., and Westbrook, G.L. (1998). Dendrodendritic inhibition in the olfactory bulb is driven by NMDA receptors. J Neurosci *18*, 6790-6802.
Tashiro, A., Sandler, V.M., Toni, N., Zhao, C., and Gage, F.H. (2006a). NMDA-receptor-mediated, cell-specific integration of new neurons in adult dentate gyrus. Nature *442*, 929-933.
Tashiro, A., Zhao, C., and Gage, F.H. (2006b). Retrovirus-mediated single-cell gene knockout technique in adult newborn neurons in vivo. Nat Protoc *1*, 3049-3055.
Turrigiano, G.G., and Nelson, S.B. (2004). Homeostatic plasticity in the developing nervous system. Nat Rev Neurosci *5*, 97-107.
van Praag, H., Kempermann, G., and Gage, F.H. (1999). Running increases cell proliferation and neurogenesis in the adult mouse dentate gyrus. Nat Neurosci *2*, 266-270.
Wilbrecht, L., Crionas, A., and Nottebohm, F. (2002). Experience affects recruitment of new neurons but not adult neuron number. J Neurosci *22*, 825-831.
Winner, B., Cooper-Kuhn, C.M., Aigner, R., Winkler, J., and Kuhn, H.G. (2002). Long-term survival and cell death of newly generated neurons in the adult rat olfactory bulb. Eur J Neurosci *16*, 1681-1689.
Yamaguchi, M., and Mori, K. (2005). Critical period for sensory experience-dependent survival of newly generated granule cells in the adult mouse olfactory bulb. Proc Natl Acad Sci U S A *102*, 9697-9702.
Yang, J., Jan, Y.N., and Jan, L.Y. (1995). Control of rectification and permeation by residues in two distinct domains in an inward rectifier K+ channel. Neuron *14*, 1047-1054.

## Main Figures

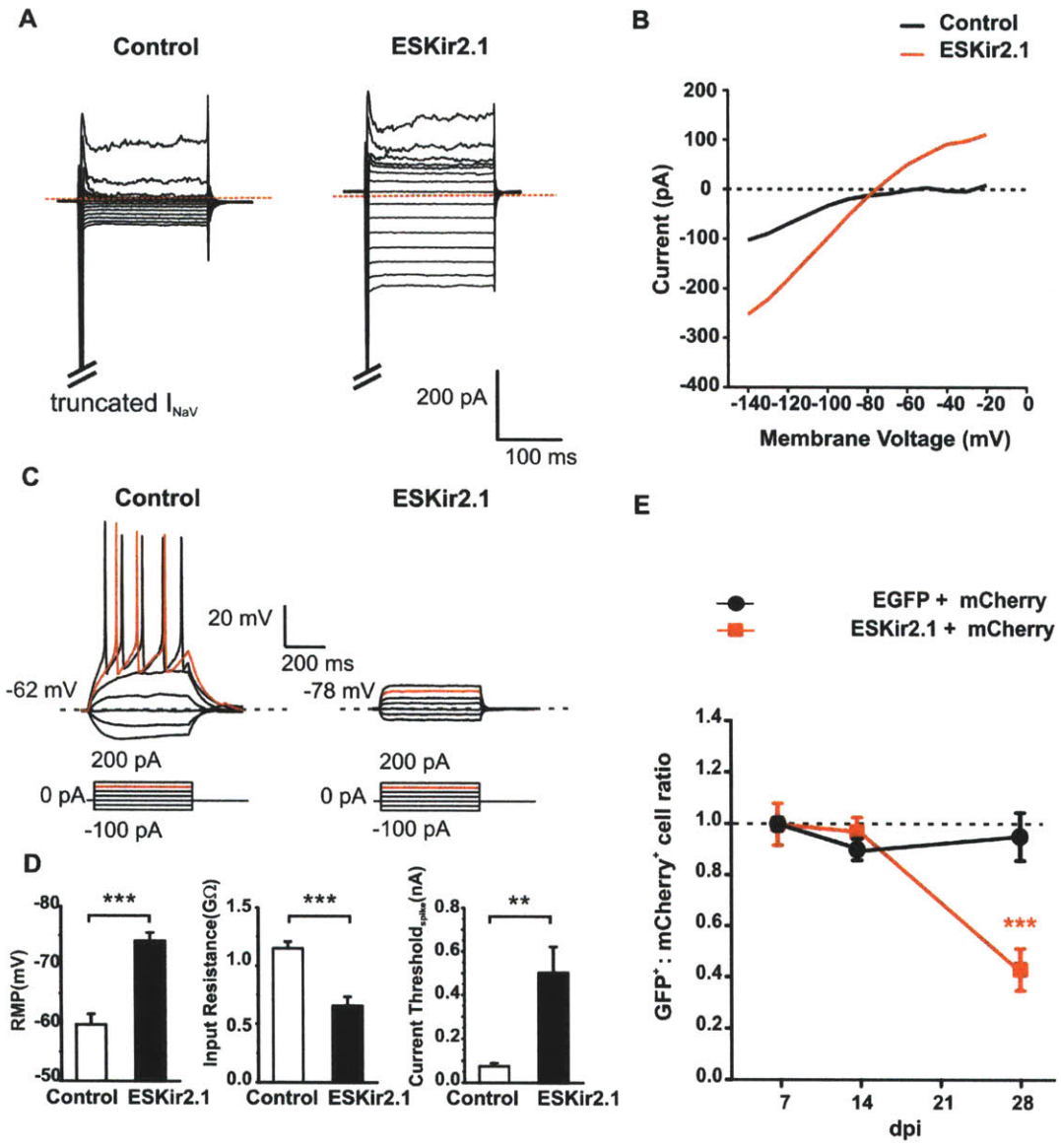


**Figure 1. Decreased intrinsic neuronal activity via ESKir2.1 expression compromises the survival and integration of adult-generated neurons**

(A) Current-voltage relationship in control (mCherry$^+$) and ESKir2.1$^+$ neurons. Neurons were clamped at -70 mV and stepwise voltage was applied from -140 to 0 mV.

(B) ESKir2.1$^+$ neurons displayed larger steady-state leak currents than control neurons.

(C) The amount of current sufficient to trigger action potentials in control neurons (left) was below the threshold necessary to elicit action potentials in new neurons expressing ESKir2.1 (right).

(D) Relative to control neurons at 16-18 dpi, ESKir2.1 expression hyperpolarized neurons by 14±2.4 mV (left, ***$p < 0.000003$; $n = 13$ neurons), decreased their input resistance by 492±100.3 MΩ (center, ***$p < 0.0002$; $n = 11$ neurons), and increased the minimal amount of current required to reach spiking threshold by 0.427±0.13 nA (right, **$p < 0.004$; $n = 10$ neurons).

(E) Normalized survival ratios (Number of $EGFP^+$ cells, including double-labeled cells, divided by the number of singly labeled $mCherry^+$ cells, normalized to the 7 dpi value) of ESKir2.1/$hrGFP^+$ and $EGFP^+$ neurons. By 28 dpi, ESKir2.1$^+$ neurons survived significantly less well than control neurons (red line; -56±12%; $n = 4$ bulbs each group; **$p < 0.002$) while EGFP did not have an effect (black line; $p < 0.636$; $n = 4$ bulbs).

Two-tailed t-test used for statistical analysis. Error bars represent SEM.

See also Figure S1.

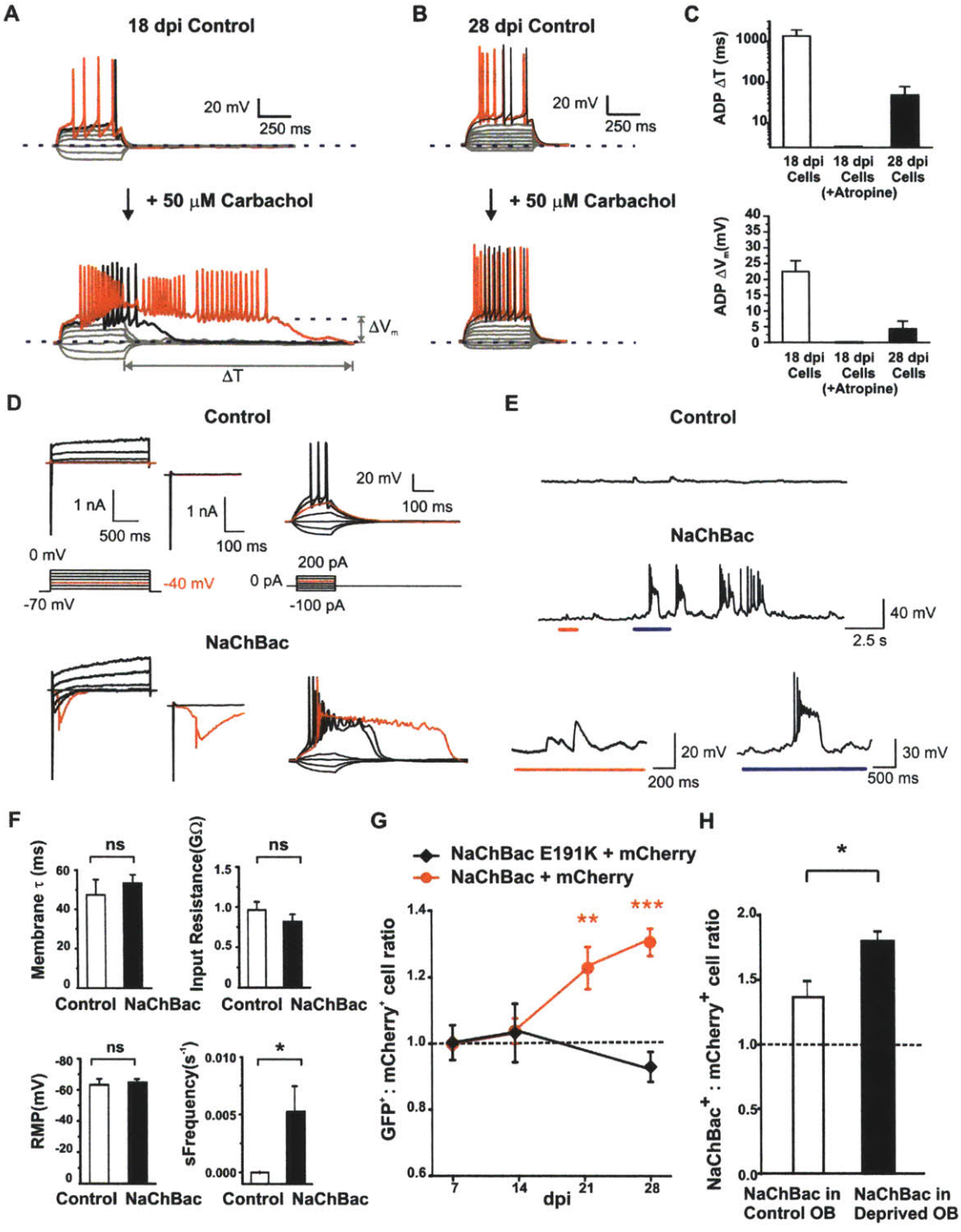


**Figure 2. Increased intrinsic neuronal activity via NaChBac expression enhances the survival of adult-generated neurons.**

(A) Carbachol induced a long-lasting after-depolarization-potential (ADP) in 18 dpi GCs. Additionally, carbachol increased spike numbers upon suprathreshold stimulation.

(B) Carbachol enhanced membrane excitability of 28 dpi GCs by increasing spike numbers upon suprathreshold stimulation, but did not induce the long ADP observed at 18 dpi.

(C) (Upper panel) The after-depolarization-potential (ADP) induced by carbachol was much longer in 18 dpi than in 28 dpi neurons. (Lower panel) The amplitude of ADP induced by carbachol was significantly larger in 18 dpi than in 28 dpi neurons.

(D) (Upper left and center) At 18 dpi, new control neurons ($mCherry^+$) recorded in voltage-clamp mode displayed > 2 nA of voltage-sensitive sodium inward current at -10 mV, but none at -40 mV (red trace). In contrast, $NaChBac^+$ neurons (red trace, lower left and center) had a 762±119 pA slow inward current opening at -43±2.1 mV (n = 6 neurons) and >2 nA of inward current at -20 mV. In current-clamp mode (right), a 200 ms pulse of positive 150 pA current injection generated repetitive action potentials in control neurons (upper right) whereas repetitive action potentials with sustained depolarization (608±68 ms, n = 6 neurons) were induced in $NaChBac^+$ neurons (red trace, lower right).

(E) In current-clamp mode, control neurons (top trace) did not fire action potentials, while NaChBac expression resulted in spontaneous, repetitive firing at resting membrane potential (middle trace). A closer look at the NaChBac trace (bottom left) shows that $NaChBac^+$ neurons received functional synaptic inputs as indicated by frequent spontaneous synaptic events. These neurons fired action potentials mediated by

endogenous sodium channels riding atop NaChBac-mediated depolarization (bottom right).

(F) All passive electrical properties in NaChBac$^+$ neurons remained similar to control neurons except for a significantly higher rate of spontaneous firing (NaChBac, 0.02±0.007 Hz; Control, 0.004±0.004 Hz; *p <0.01; Mann-Whitney test; n = 6 neurons in each group).

(G) Cell survival ratios of neurons with increased intrinsic excitability. NaChBac$^+$ neurons survived significantly better than control neurons at 21 dpi (red line; 22±6%; *n* = 4 bulbs; **p < 0.001) and 28 dpi (31±4%; n = 10 bulbs; ***p < 0.0001). The non-conducting mutant NaChBac E191K (black line) did not alter survival.

(H) NaChBac increased the relative survival of adult-generated neurons by a significantly larger factor in the sensory-deprived compared to the non-deprived OB (42±14%; *p <0.05; n = 4 deprived bulbs, n = 4 control bulbs; paired sample t-test).

Two-tailed t-test used for statistical analysis. Error bars represent SEM.

See also Figure S2.

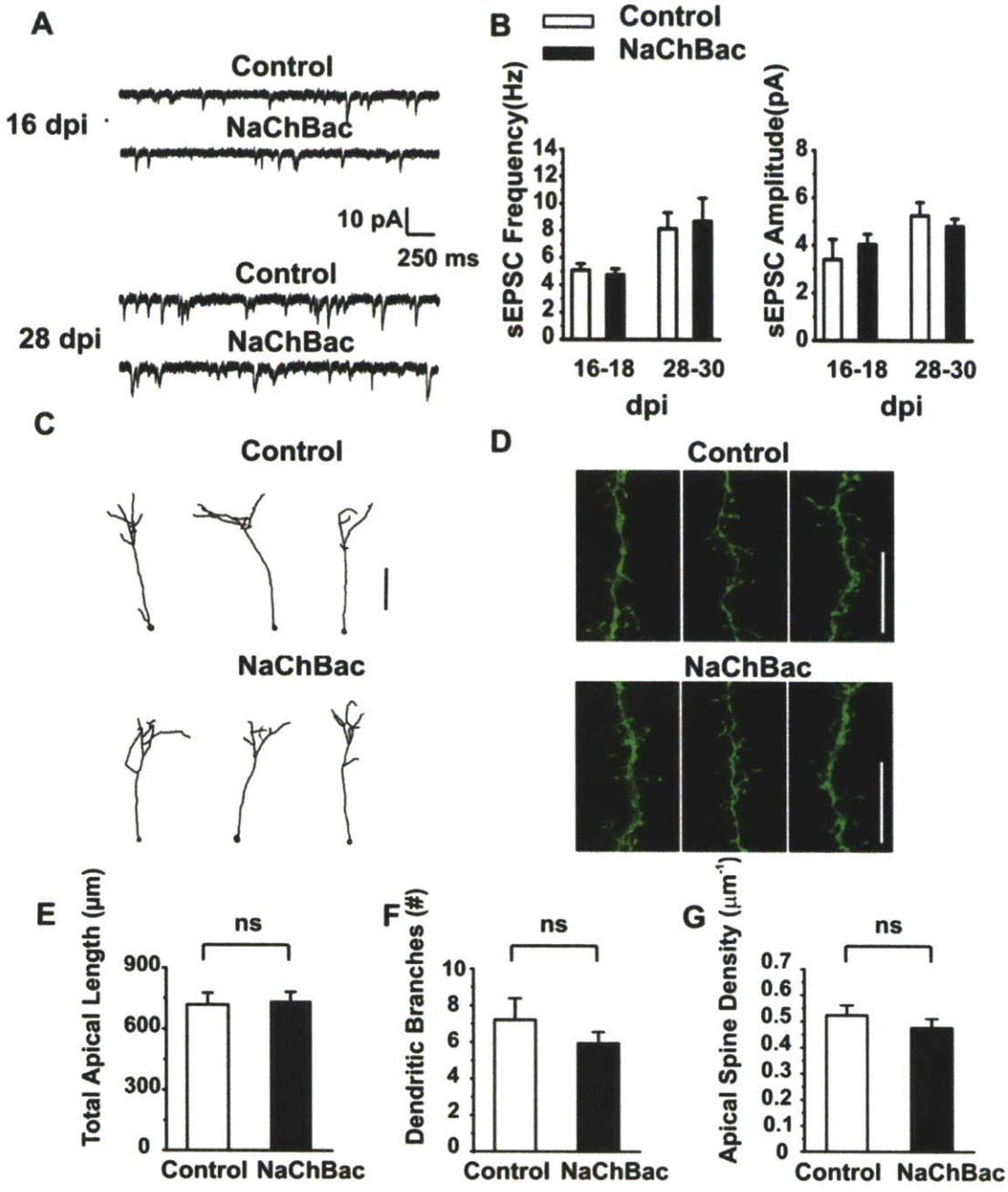


**Figure 3. NaChBac$^+$ neurons receive normal synaptic input and display identical morphological characteristics as wild-type neurons**

(A) Spontaneous excitatory postsynaptic current (sEPSC) was recorded in NaChBac$^+$ or mCherry$^+$ neurons at 16 and 28 dpi.

(B) NaChBac$^+$ neurons had similar sEPSC frequency and amplitude to control neurons in both the early (16-18 dpi) and late phase (28-30 dpi) of the critical period for survival.

(C) 3-dimensional Neurolucida reconstructions of representative granule neurons. Scale bar represents 100 μm.

(D) Confocal images showing representative dendrite sections. Scale bar represents 20 μm.

(E-G) NaChBac$^+$ neurons in the OB did not display altered apical length ($p < 0.78$; n = 20-25 neurons per group) (C), dendritic branching ($p < 0.39$; n = 14-16 neurons per group) (D) or apical spine density ($p < 0.33$; n = 8-10 neurons per group) (E).

Two-tailed t-test used for statistical analysis. Error bars represent SEM.

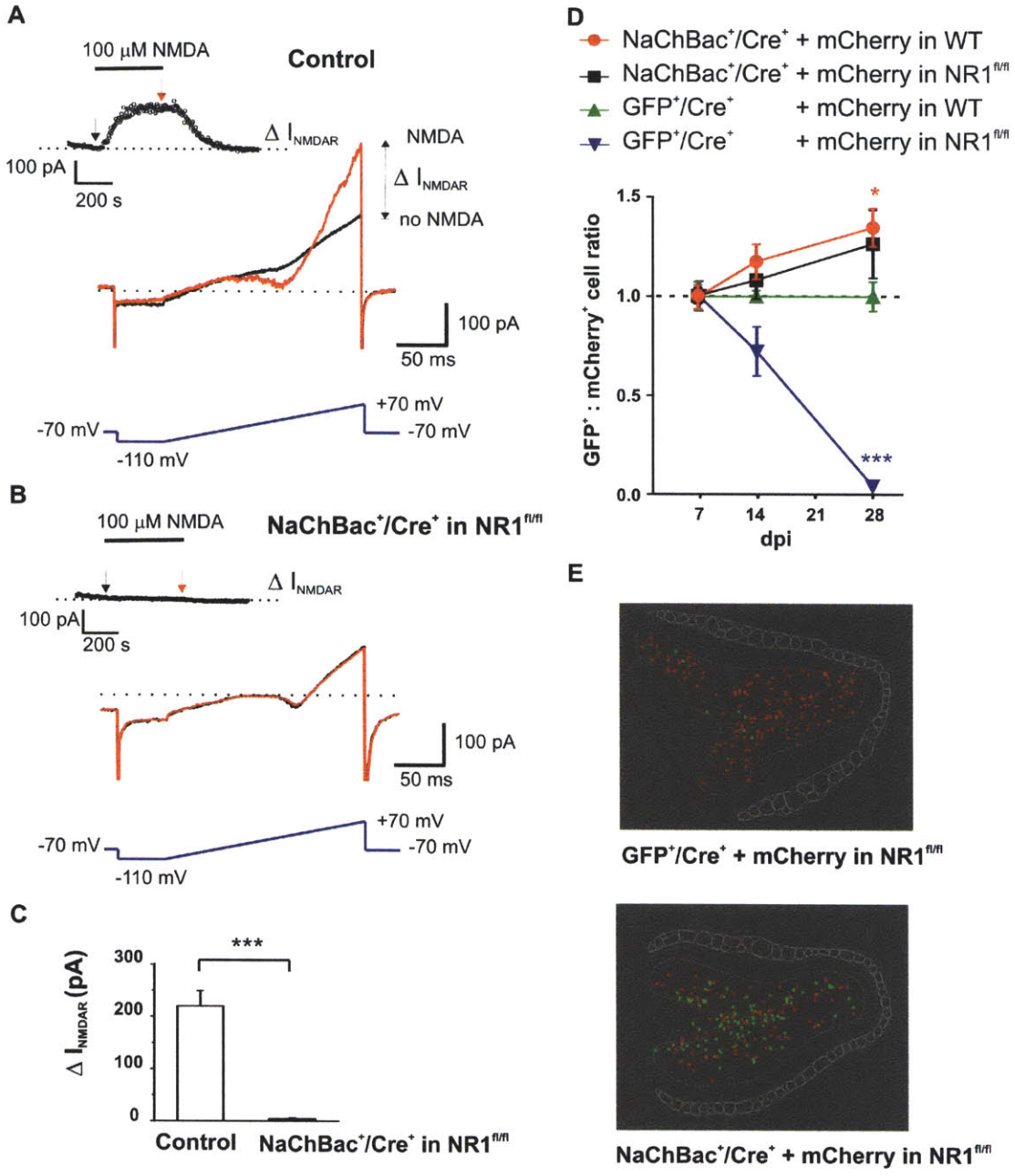


**Figure 4. Increased intrinsic neuronal activity protects NMDAR-deficient neurons from death.**

(A) Application of 100 μM NMDA activated NMDAR-mediated currents measured at +70 mV in a single control neuron ($mCherry^+$) at 18 dpi (inset). The voltage ramp

protocol, from -110 to +70 mV, performed before (black arrow) and during NMDA application (red arrow) showed characteristics of outward-rectifying NMDA currents (red trace) evoked by 1 mM $Mg^{2+}$ present in bath solution.

(B) Expression of the NaChBac-Cre construct completely eliminated NMDAR-mediated currents as examined by application of 100 μM NMDA (inset). The I-V curve remained unchanged before (black trace) and after (red trace) NMDA application.

(C) 100 μM NMDA application elicited 220±29 pA NMDAR-mediated current in 18 dpi control neurons but none in neurons expressing the NaChBac-Cre construct (n = 4 neurons in each group).

(D) Survival rates of control (EGFP/Cre in WT), $NR1^{-/-}$ (EGFP/Cre in $NR1^{fl/fl}$), $NaChBac^{+}$ (NaChBac/Cre in WT) and $NR1^{-/-}$ $NaChBac^{+}$ neurons (NaChBac/Cre in $NR1^{fl/fl}$) in the OB. As expected, $NaChBac^{+}$ neurons survived significantly better than control at 28 dpi in wild-type OBs (red circles; 34.64±12.17%; *p <0.05; n = 5 bulbs). NMDAR-deficient neurons were completely eliminated by 28 dpi (blue triangles; -96.3±0.1%; ***p <0.0001; n = 3 bulbs) but survived as well as control neurons when they expressed NaChBac (black squares; p <0.1290; n = 5 bulbs).

(E) Neurolucida trace images showing representative distributions of $EGFP^{+}$ and $mCherry^{+}$ cells within representative OB sections at 28dpi.

Two-tailed t-test used for statistical analysis. Error bars represent SEM. See also Figure S3.

## Supplemental Figures

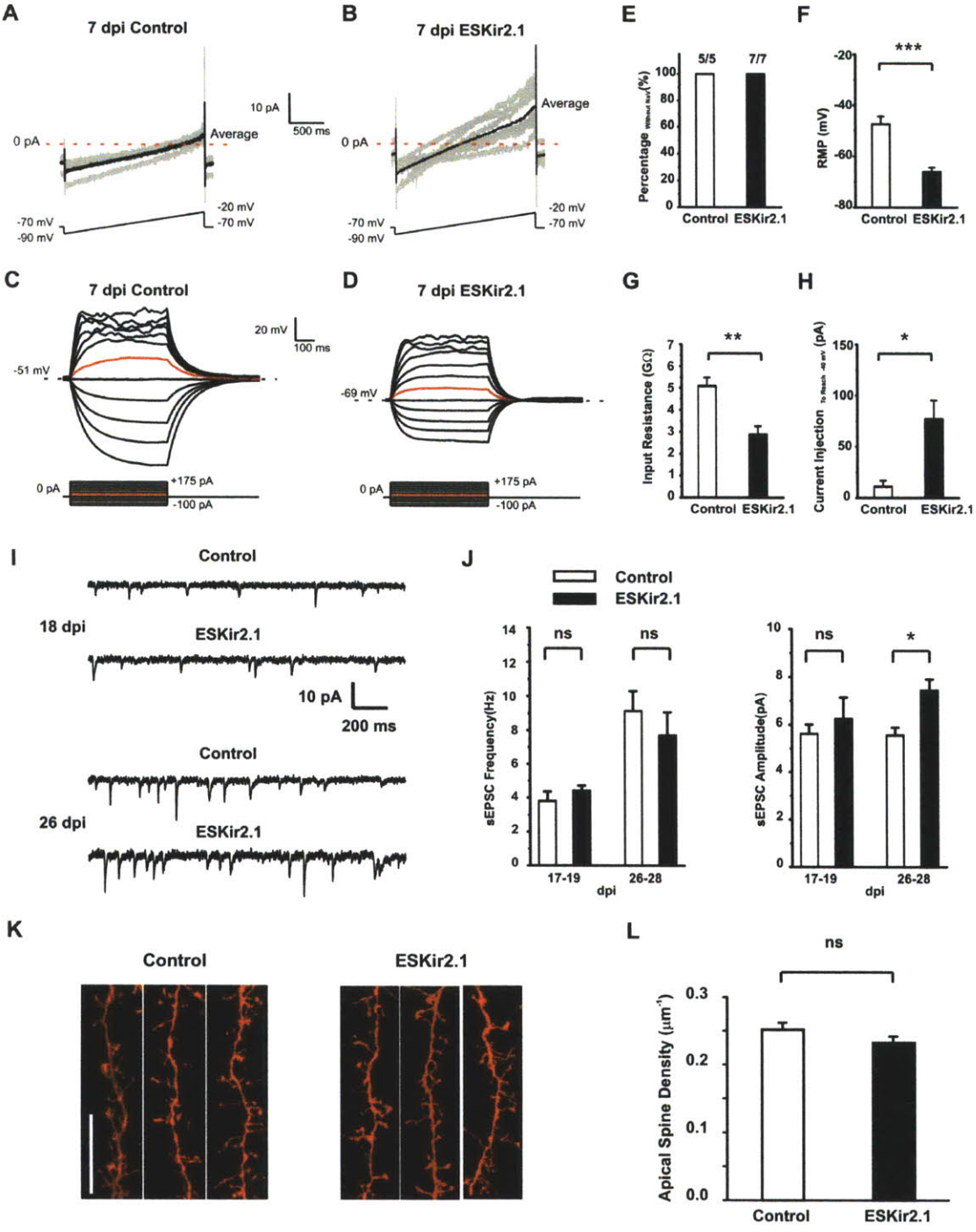

**Figure S1. Electrophysiological properties and spine density of ESKir2.1$^+$ neurons**

(A and B) Leak currents in 7 dpi neuroblasts measured by sweeping the membrane voltage from -90 to -20 mV at a rate of 35 mV/s. Control neuroblasts (A) had significantly lower levels of linear leak currents than ESKir2.1$^+$ neuroblasts (B).

(C and D) Representative traces showing membrane potential changes in response to current injection in control (C) and ESKir2.1$^+$ neuroblasts (D). ESKir2.1$^+$ neuroblasts were hyperpolarized and required larger current injection to depolarize to levels of membrane potential similar to those of control neuroblasts.

(E—G) At 7 dpi, neither control nor ESKir2.1$^+$ neuroblasts had voltage-gated sodium currents. ESKir2.1$^+$ neuroblasts were more hyperpolarized (F) and had lower input resistances (G) than control neuroblasts.

(H) ESKir2.1$^+$ neuroblasts required 70 pA more of current injection than control neuroblasts to reach a membrane potential of -40 mV at 7 dpi.

(I) Spontaneous excitatory postsynaptic current (sEPSC) in ESKir2.1$^+$ or mCherry$^+$ neurons at 18 and 26 dpi.

(J) In the early phases of maturation (17-19 dpi) the frequency and amplitude of sEPSCs were similar for control and ESKir2.1 neurons (n = 7-9 neurons in each group). In the late phase of maturation (26-28 dpi) the frequency of sEPSCs was similar for control and ESKir2.1$^+$ neurons, but the amplitude of sEPSCS was significantly increased in ESKir2.1$^+$ neurons. (26-28 dpi; n = 8-9 neurons in each group; *$p$=0.0056).

(K) Confocal images of representative apical dendrites of ESKir2.1$^{+}$ and control neurons at 28 dpi. Scale bar represents 20 μm.

(L) The density of spines in the apical dendrites was similar for control and ESKir2.1$^{+}$ neurons (n = 21-22 neurons in each group).

Two-tailed *t*-test used for statistical analysis. Error bars indicate SEM.

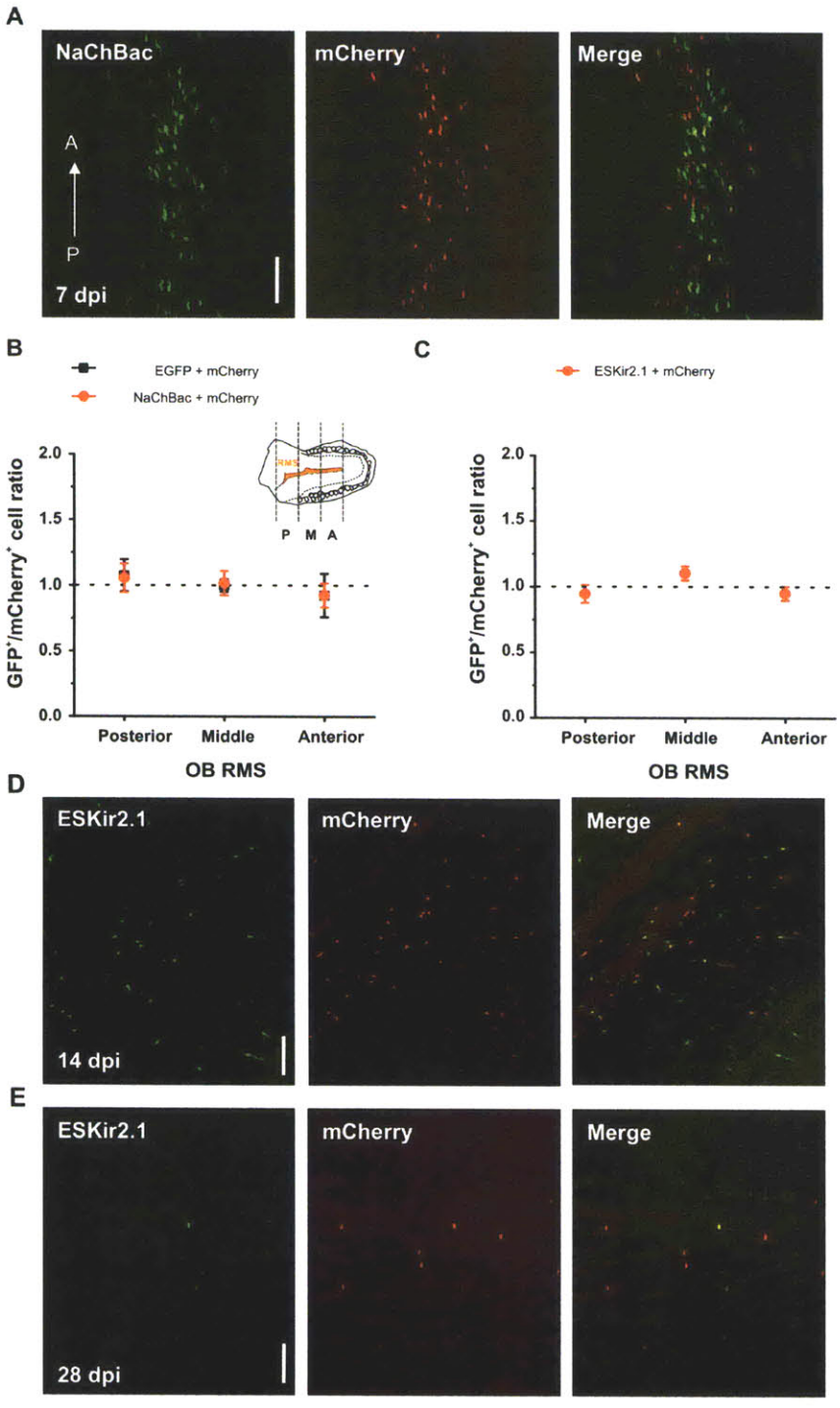
A
NaChBac
mCherry
Merge
A
P
7 dpi
B
EGFP + mCherry
NaChBac + mCherry
GFP+/mCherry+ cell ratio
2.0
1.5
1.0
0.5
0.0
RMS
P M A
Posterior
Middle
Anterior
OB RMS
C
ESKir2.1 + mCherry
GFP+/mCherry+ cell ratio
2.0
1.5
1.0
0.5
0.0
Posterior
Middle
Anterior
OB RMS
D
ESKir2.1
mCherry
Merge
14 dpi
E
ESKir2.1
mCherry
Merge
28 dpi

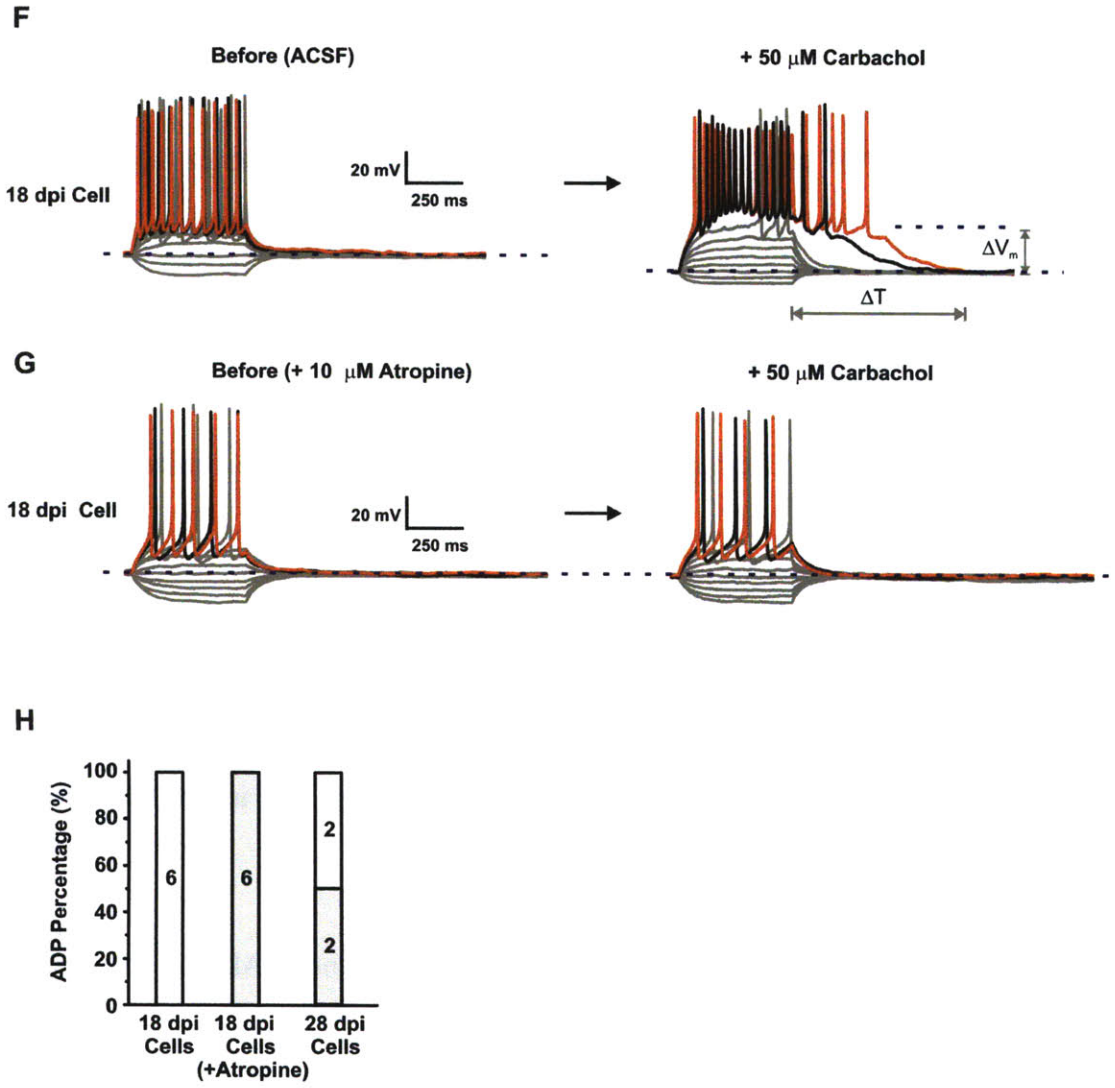


**Figure S2. Expression of either ESKir2.1 or NaChBac does not alter the distribution of migrating neuroblasts within the rostral migratory stream (RMS), and the muscarinic agonist carbachol induces long depolarizations in adult-born GCs**

(A) Confocal images showing the distribution of migrating NaChBac$^+$ and mCherry$^+$ neuroblasts in the RMS within the OB at 7 dpi. "A" and "P" indicate the anterior and posterior sections of the bulb, respectively. Scale bar represents 100 μm.

(B) $EGFP^+/mCherry^+$ cell ratios in the posterior, middle, and anterior portions of the RMS remain unchanged by expression of NaChBac at 7 dpi (n = 6-12 bulb sections in each group). "A", "M" and "P" indicate the anterior, middle and posterior regions of the bulb, respectively. The regions are defined as three equal parts that divide the entire population of migrating neuroblasts in horizontal OB sections at 7 dpi when >99% of neuroblasts are located within the RMS (inset diagram).

(C) Expression of ESKir2.1 did not change the migration pattern of neuroblasts at 7 dpi (n = 14 bulb sections).

(D) Images showing the distribution of $ESKir2.1^+$ and $mCherry^+$ cells within the OB at 14 dpi. Scale bar represents 250 μm.

(E) Images showing the distribution of $ESKir2.1^+$ and $mCherry^+$ cells in the OB at 28 dpi. Scale bar represents 100 μm.

(F) Carbachol induced a long-lasting after-depolarization-potential (ADP) in 18 dpi GCs and increased spike numbers upon suprathreshold stimulation.

(G) Application of 10 mM atropine, a muscarinic receptor antagonist, prevented the depolarizing action of carbachol in 18 dpi cells.

(H) All cells studied at 18 dpi had ADPs triggered by carbachol, which was blocked by atropine. In contrast, carbachol exposure only induced ADPs in 50% of the cells at 28 dpi.

Two-tailed *t*-test used for statistical analysis. Error bars indicate SEM.

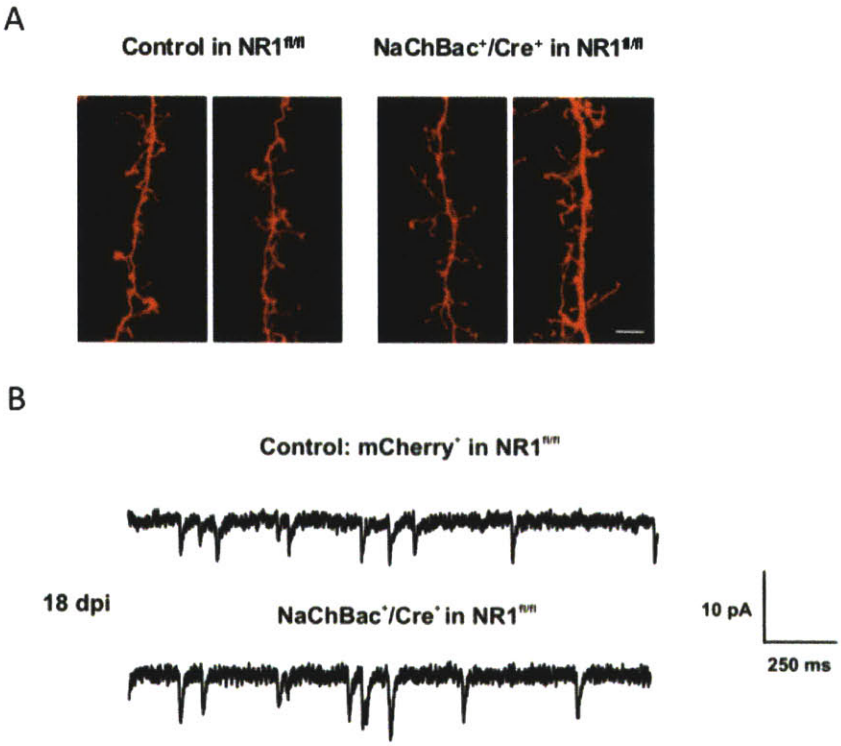


**Figure S3. NMDAR-deficient neurons rescued by up-regulating intrinsic electrical activity develop a similar morphology to control neurons and receive AMPAR-mediated synaptic input.**

(A) Confocal images of representative apical dendrites at 28 dpi, of $NR1^{-/-}$ neurons that express NaChBac and of control neurons. Scale bar represents 20 μm.

(B) Representative electrophysiological recording trace showing that $NR1^{-/-}$ neurons expressing NaChBac receive AMPAR-mediated synaptic input.

## Supplemental experimental procedures

### Retroviral constructs

The cDNA for NaChBac was obtained from David Clapham (HHMI, Children's Hospital, Harvard Medical School, Boston). NaChBac E191K and Kir2.1 E224S (ESKir2.1) were generated by PCR based on previously published sequences (Taglialatela et al., 1995; Yang et al., 1995; Yue et al., 2002). Retroviral vectors were derived from a Moloney leukemia virus with an internal promoter derived from the Rous sarcoma virus (Molar) (Kelsch et al., 2007). Retroviral particles were produced and stored as previously described (Lois et al., 2002). The viral titers were approximately $10^6$ infectious units/μl. Viral constructs were generated as follows. NaChBac-EGFP: the stop codon of NaChBac was eliminated by PCR and fused in frame to the cDNA of EGFP (Kelsch et al., 2009). NaChBac-Cre: the stop codon of the NaChBac-EGFP fusion was eliminated by PCR, and linked by a foot-and-mouth disease (FMDV) virus 2A sequence to the cDNA of Cre. ESKir2.1-hrGFP: the cDNA of ESKir2.1 was cloned downstream from the encephalomyelocarditis (EMC) virus internal ribosomal entry site (IRES), and the IRES-ESKir2.1 cassette was subcloned downstream from the humanized recombinant GFP (hrGFP) cDNA. PalmEGFP-NaChBac: the palmitoylation sequence from the GAP43 gene was first added to the N-terminus of EGFP. The stop codon of the palmitoylated version of EGFP was eliminated by PCR and linked by a FMDV 2A picornavirus sequence to the cDNA of NaChBac. PalmEGFP-IRESKir2.1: the IRES ESKir2.1 cassette was subcloned downstream from palmitoylated EGFP.

**Retroviral injection into animals**

8-week old female Sprague-Dawley rats (Charles River and Taconic) and 'floxed' NMDA-receptor subunit 1 mice (Tsien et al., 1996) were stereotaxically injected with 1 μl/hemisphere and 0.5 μl/hemisphere of retroviral vectors respectively, after anesthesia with ketamine/xylazine solution. The stereotaxic coordinates were 1.2 mm anterior from bregma, 1.6 mm lateral from the midline, and 3.1 mm ventral from the brain surface in rats (Kelsch et al., 2009), and 1.0 mm anterior, 1.0 mm lateral and 2.3 mm ventral in mice.

**Histology**

Rats were over-anesthetized with isofluorane (Baxter), while mice were given an overdose of avertin, before they were perfused intracardially, first with phosphate buffer saline (PBS) and then with 3% paraformaldehyde (PFA). The bulbs were incubated with 3% PFA overnight, and cut horizontally with a Leica vibratome into 45 μm sections. For immunocytochemistry, the sections were first blocked with blocking solution containing bovine serum albumin (3 mg/ ml PBS), and 0.25% Triton X-100 in PBS, and incubated overnight with a polyclonal rabbit anti-GFP antibody (Chemicon; AB3080) diluted 1:3000 in blocking solution. Sections were washed 4 times in PBS, for 15 min each time, before a 2-hour incubation at room temperature with Alexa Fluor® 488 or 555 goat anti-rabbit secondary antibody (Molecular Probes, catalog A11008) diluted 1:700 in blocking solution. The sections were washed 4 times in PBS, for 15 min each time, before mounting on slides with mounting medium (Gel Mount™; Sigma).

**Survival ratio analysis**

Two viruses were mixed at an approximate 1:1 ratio for survival analysis. One of the viruses carried the construct encoding mCherry, while the other carried one of a range of constructs: hrGFP linked to ESKir2.1 by an EMC IRES, EGFP alone, NaChBac or NaChBac E191K fused to EGFP (NaChBac-EGFP or NaChBacE191K-EGFP), and Cre Recombinase linked with the 2A linker to EGFP, NaChBac-EGFP or NaChBacE191K-EGFP (NaChBac-Cre or NaChBacE191K-Cre). Fluorescently labeled cells were quantified with the aid of the Neurolucida software (MicroBright Field Inc.). The survival ratio is defined as the total number of EGFP-positive cells (including double-labeled cells) divided by of the number of singly labeled mCherry-expressing cells. The ratio of $EGFP^+$ to $mCherry^+$ neurons at 7 days post infection (dpi) was used to normalize all data at subsequent time points for comparison, hence ratios at all subsequent time points were relative to the 7 dpi ratio. Three to 7 entire sections per olfactory bulb were analyzed to collect at least 400 counted cells in each bulb. The mean survival ratio from each bulb was treated as a single sample.

**Morphological analysis**

Viruses carrying constructs for palmitoylated EGFP connected by a FMDV 2A linker to either NaChBac or NaChBacE191K were injected separately into each SVZ in a single animal. Coronal sections 350 μm-thick were made of each olfactory bulb. The labeled neurons were imaged with a two-photon microscope (Sutter Instruments) with a 60X objective lens. Serial reconstruction and dendrite analysis was performed with the Neurolucida software by a blinded second experimenter. Confocal image stacks were taken with an Olympus Fluoview laser confocal microscope (Olympus) with a 60X objective lens, a zoom of 1.5 and at z-intervals of 0.5 μm.

**Nostril occlusion**

The outer edges of one nostril were cauterized with a high temperature cautery tip (Bovie Aaron Change-A-Tip™) and pinched with forceps to seal together. 500 µl of tissue adhesive (Vetbond™ , 3M) was dispensed onto the outer surface of the cauterized nostril as an additional seal. The effectiveness of nostril occlusion was examined 10 days after the surgery after recuperation of the cauterization wound.

**Electrophysiological recordings**

Animals were given an overdose of ketamine/xylazine then perfused intracardially with ice-cold slicing solution containing (in mM): 212 sucrose, 3 KCl, 1.25 $NaH_2PO_4$, 26 $NaHCO_3$, 7 $MgCl_2$, 10 glucose (308 mOsm, and pH 7.3). Bulbs were incubated in ice-cold cutting solution and cut horizontally into 350 µm slices with a Leica microtome at a speed of 0.08 mm/s. Slices were incubated for 30 min at 35°C, for recovery, in carbogenated recording solution containing (in mM): 125 NaCl, 2.5 KCl, 1.25 $NaH_2PO_4$, 26 $NaHCO_3$, 1 $MgCl_2$, 2 CaCl2, 20 glucose (312 mOsm, and pH 7.3). Fluorescent-guided whole-cell patch clamp recordings were performed with a MultiClamp 700B amplifier (Axon Instruments). The pipette solution contained (in mM): 2 NaCl, 4 KCl, 130 K-gluconate, 10 HEPES, 0.2 EGTA, 4 Mg-ATP, 0.3 Tris-GTP, 14 Tris-phosphocreatine (pH 7.3). Successful patching onto the target cell was confirmed by identifying a fragment of fluorescent membrane trapped inside the pipette tip during or after the recording. Pipette resistance ranged from 5 to 8 MΩ, and the pipette access resistance was always less than 16 MΩ after series resistance compensation. The junction potential was not corrected throughout the study. For spontaneous EPSC (sEPSC) recording, the neuron was held at -77 mV and synaptic events were collected at 25°C. sEPSC contributed to the majority of spontaneous events because

~98% of events could be blocked by 100 μM D, L-AP-5 and 20 μM NBQX (Sigma) at the end of the recording. Inhibitory blockers such as bicuculline were not included during sEPSC recording because they triggered frequent EPSC bursting input in granule neurons, which precluded further analysis. NMDAR-mediated current was recorded with pipette solution containing (in mM): 125 Cs-Methanesulfonate, 4 CsCl, 0.2 Cs-EGTA, 2 NaCl, 10 HEPES, 4 Mg-ATP, 0.3 Na-GTP, 10 Tris-phosphocreatine, 5 QX-314, and examined by applying 100 μM NMDA in recording bath solution containing (in μM): 1 TTX, 10 NBQX, 5 Glycine, 20 BMI. It was necessary to record as late as 18 dpi since all control granule cells received NMDAR-mediated current by then. NMDAR elimination by Cre recombinase in $NR1^{fl/fl}$ mice was verified by patch clamp recordings only on neurons expressing both Cre recombinase and NaChBac-EGFP since the number of neurons expressing both Cre recombinase and EGFP was dramatically reduced by 18 dpi and too few surviving neurons remained for recording.

**Analysis of electrophysiological data**

Data was acquired and analyzed with pClamp9 software (Axon Instruments), and sEPSCs were analyzed with Mini Analysis Program (Synaptosoft Inc.). Only morphologically mature granule neurons with at least 800 pA of TTX-sensitive sodium current measured at -20 mV, and resting membrane potential more negative than -55 mV, were included in the 14 dpi and 28 dpi analyses.

**Statistical analysis**

The Mann-Whitney test was used for comparing the frequency of spontaneous firing in $NaChBac^+$ and control neurons at resting membrane potential to determine statistical significance (Figure 2C). To analyze survival rates in sensory-deprived versus control bulbs, the paired Student's *t*-test was used since these were paired bulbs of the same animal (Figure 2E). All other data was analyzed with the two-sample two-tailed Student's *t*-test in OriginPro 8 (Origin Lab Corporation). Data was reported as mean ± SEM.

**Supplemental References**

Kelsch, W., Lin, C.W., and Lois, C. (2008). Sequential development of synapses in dendritic domains during adult neurogenesis. Proc Natl Acad Sci U S A 105, 16803-16808.
Kelsch, W., Lin, C.W., Mosley, C.P., and Lois, C. (2009). A critical period for activity-dependent synaptic development during olfactory bulb adult neurogenesis. J Neurosci 29, 11852-11858.
Kelsch, W., Mosley, C.P., Lin, C.W., and Lois, C. (2007). Distinct mammalian precursors are committed to generate neurons with defined dendritic projection patterns. PLoS Biol 5, e300.
Lois, C., Hong, E.J., Pease, S., Brown, E.J., and Baltimore, D. (2002). Germline transmission and tissue-specific expression of transgenes delivered by lentiviral vectors. Science 295, 868-872.
Taglialatela, M., Ficker, E., Wible, B.A., and Brown, A.M. (1995). C-terminus determinants for Mg2+ and polyamine block of the inward rectifier K+ channel IRK1. EMBO J 14, 5532-5541.
Tsien, J.Z., Huerta, P.T., and Tonegawa, S. (1996). The essential role of hippocampal CA1 NMDA receptor-dependent synaptic plasticity in spatial memory. Cell 87, 1327-1338.
Yang, J., Jan, Y.N., and Jan, L.Y. (1995). Control of rectification and permeation by residues in two distinct domains in an inward rectifier K+ channel. Neuron 14, 1047-1054.
Yue, L., Navarro, B., Ren, D., Ramos, A., and Clapham, D.E. (2002). The cation selectivity filter of the bacterial sodium channel, NaChBac. J Gen Physiol 120, 845-853

Chapter 2

# Activity-dependent Connectivity of New Neurons in the Adult Dentate Gyrus is regulated by Npas4

# Activity-dependent Connectivity of New Neurons in the Adult Dentate Gyrus is regulated by Npas4

Shuyin Sim, Chia-Wei Lin, Yingxi Lin and Carlos Lois

## ABSTRACT

Electrical activity regulates the manner in which neurons form connections to each other. However, it remains unclear whether increased single-cell activity is sufficient to induce changes in synaptic connectivity of that neuron or if a global increase in activity of the circuit is necessary. To address this question, we genetically increased neuronal excitability of individual adult-born neurons in vivo in the dentate gyrus via expression of a voltage-gated bacterial sodium channel. We observed that an increase in excitability of new neurons in an otherwise unperturbed circuit leads to changes in both their input and axonal synapses. Furthermore, the activity-dependent transcription factor Npas4 is necessary for the changes in these neurons' input synapses, but is not involved in changes to their axonal synapses. Our results reveal that an increase in cell-intrinsic activity is sufficient to alter a neuron's synaptic connectivity with the hippocampal circuit, and that Npas4 is required for activity-dependent changes in input synapses.

*Author Contributions: Shuyin Sim designed the experiments, designed and generated retroviral vectors, performed intracranial injections, collected and analyzed the data. Chia-Wei Lin performed electrophysiological recordings. Shuyin Sim, Yingxi Lin and Carlos Lois wrote the manuscript.*

## INTRODUCTION

The manner in which adult-born neurons are incorporated into the DG is likely to be important in shaping new memory traces during adult life. It is thought that the addition of new neurons to the adult dentate gyrus (DG) of the hippocampus serves as a substrate for experience-dependent learning and memory throughout life (Aimone et al., 2006). The ablation of new neurons in the DG results in deficits in hippocampal-dependent processes such as spatial memory (Imayoshi et al., 2008). These neurons are generated in significant numbers – new granule cells (GCs) generated in a month constitute about 6% of the total number of cells in the DG in adult rodents (Cameron and McKay, 2001). Furthermore, new neurons display enhanced synaptic plasticity (Schmidt-Hieber et al., 2004), and are functionally integrated into the existing circuitry (Jessberger and Kempermann, 2003).

It is known that integration of neurons into circuits is affected by activity. Not only is the production and subsequent survival of GCs in the DG sensitive to activity (Kee et al., 2007; Kempermann et al., 1997; Tashiro et al., 2006; van Praag et al., 1999), but their wiring in the DG circuit is also activity-dependent. *In vitro*, the size of large mossy terminals (LMTs) on the axons of DG GCs is affected by changes in spiking activity (Galimberti et al., 2006), while *in vivo*, experimentally induced seizures profoundly alter the connections made by adult-born GCs to the DG circuit (Parent et al., 1997). After seizures, there are several changes in the synapses, including increased number of large spines and the persistence of basal dendrites (Jessberger et al., 2007).

Understanding the factors underlying activity-dependent connectivity in adult-born neurons is important not only to understand the basis of lifelong learning and the pathologic basis of epilepsy, but also to develop neuronal replacement therapies for neurodegenerative diseases. In a seizure, or in learning paradigms used to stimulate activity in the DG, general

levels of activity in the brain are increased, so it is unclear if the observed changes in connectivity result directly from the increased activity of an individual new neuron, indirectly via elevated activity of other neurons in the circuit in which the new neurons are embedded, or a combination of both. To investigate how the level of neuronal activity of a single developing neuron affects its integration into an unperturbed circuit, we genetically increased excitability in individual GCs by introducing the voltage-gated sodium channel NaChBac via oncoretroviruses into neuronal progenitors in the DG. We then examined the genetic basis for these alterations by deleting genes in individual neurons via retroviral delivery of Cre Recombinase into new neurons in conditional knockout mice. Our experiments reveal that elevation of neuronal excitability of individual new neurons is sufficient to induce some of the changes in synaptic connectivity that have been observed in seizures, such as aberrant localization of synapses within the DG and enlarged spines. Cell-autonomous increased neuronal activity leads to both input and output connectivity alterations that increase inhibition on the hyperexcitable neuron and dampen its excitatory influence on its downstream targets. The transcription factor Npas4 is required for the activity-induced changes in synaptic inputs to these neurons, but not for changes to output synapses in their axons. These observations indicate that cell-autonomous increases in excitability can effect profound changes in neuronal connectivity and that separate genetic programs regulate activity-dependent changes in input and output synapses.

## RESULTS

### Expression of NaChBac in adult-born DG granule cells elevates neuronal excitability

Changes in brain activity, such as those triggered by seizures or behavior, affect the connectivity of new neurons born in the adult DG (Kron et al., 2010). These changes in

connectivity could be due to the increased activity of the new neurons, or of the circuit in which the neurons are embedded, or a combination of both. To isolate the contribution of elevated activity in new neurons, we increased the activity of individual new neurons cell autonomously with the ion channel NaChBac. NaChBac is a bacterial voltage-gated sodium channel that has both a more negative activation threshold than native sodium channels in GCs (approximately 15mV more negative) and a longer time to inactivation (hundreds of milliseconds compared to less than 1 ms in mammalian sodium channels) (Bean, 2007; Ren et al., 2001). Because of its unique electrical properties, NaChBac was previously used to induce hyperexcitability in Drosophila pacemaker neurons (Nitabach et al., 2006). More recently, we took advantage of NaChBac-induced depolarization to demonstrate that precise firing patterns are not essential for integration of adult-born granule neurons into the olfactory bulb (Kelsch et al., 2009; Lin et al., 2010).

To investigate whether cell-autonomous increases in excitability are sufficient to alter neuronal connectivity in adult-born DG granule neurons, we used oncoretroviruses to introduce NaChBac into individual GCs in adult mice. Because this class of retroviruses cannot transport their genetic material across the intact nuclear envelopes of non-dividing cells (Lewis and Emerman, 1994), they selectively infect dividing cells in the hilus region of the DG, labeling and effectively birthdating new GCs. We used a titer of oncoretrovirus that sparsely labeled GCs in the DG, thus keeping the vast majority of the circuit unaltered. We performed patch clamp electrophysiological recordings of labeled GCs at 17 days post infection (dpi) and found that a level of current injection (15pA) that does not induce spiking in control GCs triggers action potentials and prolonged depolarization in NaChBac-positive GCs of the same developmental stage (Figure 1A, red trace). These results confirm that

expression of NaChBac in new DG GCs increases their excitability in a cell-autonomous manner.

**NaChBac-induced excitability results in additional GABAergic input to the cell body**

In many circuits, surrounding neurons react to individual neurons' activity in order to keep circuit activity within a range that prevents disruption of function (Jakubs et al., 2006; Turrigiano and Nelson, 2004). DG GCs only start receiving glutamatergic input late in development, around 21 days post-birth, but receive GABAergic input much earlier. These cells first receive extrasynaptic input by ambient GABA starting 3 days after they are generated, followed by GABA-mediated synaptic inputs as early as 7 days after their birth (Ge et al., 2006). For this reason, we hypothesized that when hyperexcitable adult-born GCs are introduced into the DG circuit, one of the earliest responses of the surrounding circuit would be to alter the GABAergic input targeted to NaChBac$^+$ neurons. To test this hypothesis, we performed immunostaining against the vesicular GABA transporter (VGAT), which is present in the vast majority of the presynaptic terminals of inhibitory interneurons (Chaudhry et al., 1998). We quantified VGAT$^+$ puncta on cell bodies, as this measurement was more reliable than counting the number of contacts on dendrites.

At 9 dpi there was no significant difference in the density of VGAT$^+$ contacts with the soma of either control or NaChBac$^+$ neurons. However by 13 dpi there were significantly more VGAT$^+$ contacts on the soma of NaChBac$^+$ neurons compared to neurons expressing NaChBac E191K, a nonconducting variant of NaChBac (Yue et al., 2002), and this effect persisted till at least 28 dpi (Figure 1B). Parvalbumin$^+$ cells are a subset of inhibitory interneurons that preferentially synapse onto the cell bodies of DG granule neurons (Freund

and Buzsaki, 1996) while GAD65 is an isoform of glutamic acid decarboxylase (GAD), an enzyme present in a large proportion of inhibitory interneurons (Erlander and Tobin, 1991). We confirmed the trend of increased GABAergic contact in NaChBac$^+$ neurons using parvalbumin and GAD65 immunolabeling (Figures 1C and S1A). To verify if our observations regarding perisomatic GABAergic contact corresponded to a functional increase in inhibitory input, we performed electrophysiological recordings to measure spontaneous inhibitory postsynaptic potentials (sIPSCs) of individual neurons. We co-injected a mixture of retroviruses, one carrying the construct for NaChBac fused to GFP and the other carrying the construct for mCherry, into the DG and recorded from control neurons (mCherry-only) and NaChBac$^+$ neurons in the same DG at 17 dpi. mCherry was used to label control neurons since these cells would appear red and could be easily distinguished from the GFP-expressing NaChBac$^+$ neurons. Indeed, there was an increase in both the frequency and amplitude of sIPSCs received by NaChBac$^+$ GCs relative to control GCs (Figure 1D). These results indicate that individual adult-born DG GCs with elevated neuronal excitability receive more GABAergic inputs than age-matched wild-type GCs.

GABAergic innervation to adult-born GCs is initially depolarizing due to high levels of expression of the $K^+/Cl^-/Na^+$ co-transporter NKCC1 relative to the $K^+/Cl^-$ co-transporter KCC2 (Clayton et al., 1998; Plotkin et al., 1997). The subsequent upregulation of KCC2 as cells mature lowers the intracellular concentration of $Cl^-$ and eventually makes the GABA reversal potential more negative than the resting membrane potential, rendering GABAergic innervation hyperpolarizing (Rivera et al., 1999; Wang et al., 2002). This switch from depolarizing to hyperpolarizing GABAergic inputs occurs after 14 dpi in adult-born GCs (Ge et al., 2006). The increase in inhibitory input to NaChBac$^+$ GCs occurs by 13 dpi (Figure 1B). At 13 dpi, we also observed an increase in the number of KCC2-positive NaChBac$^+$ GCs

compared to controls (Figure S1B). The increase in the percentage of $KCC2^+$ cells induced by NaChBac expression suggests a premature reduction in $Cl^-$ concentration, which would in turn result in an earlier switch to inhibition by GABA. This accelerated maturation could enable the increase in GABAergic input to dampen the hyperexcitable neurons earlier in development. PSA-NCAM (polysialylated neural cell adhesion molecule), a marker for immature neurons (Seki and Arai, 1993), is also downregulated earlier in $NaChBac^+$ GCs compared to control neurons (Figure 1E).

Our results indicate that NaChBac activity impacts the early integration of DG GCs into the circuit. From an early developmental stage, hyperexcitable GCs start receiving more GABAergic input from surrounding interneurons. In addition, cell-autonomous hyperexcitability speeds up development of newly born GCs, suggesting that the accelerated maturation seen after seizures is at least partly due to increased intrinsic activity of individual new neurons (Overstreet-Wadiche et al., 2006).

**Increased excitability leads to changes in excitatory glutamatergic input**

Having discovered that NaChBac-induced hyperexcitability induces marked changes in neuronal development and an increase in inhibitory inputs early on, we proceeded to study how NaChBac affects the next phase of development of these GCs, when they start to form excitatory input synapses. DG GCs normally begin receiving excitatory inputs, via spines along their apical dendrites, from around 21 days post-birth, and the apical dendrites acquire mature morphology by around 28 days. In order to examine the changes in excitatory input received by a neuron rendered hyperexcitable by NaChBac, we infected neural progenitors in the DG with a bicistronic retroviral vector that expresses both palmitoylated EGFP (PalmG)

and NaChBac. PalmG is localized into the membranes of infected neurons, allowing us to visualize the full fine morphology of the neurons, including dendritic spines.

Using the bicistronic palmG: NaChBac construct, it was immediately apparent that NaChBac$^+$ GCs exhibited some connectivity changes that were similar to those observed in immature neurons after seizure manipulations. DG GCs migrate a small distance, about 5-10 μm, from the hilar border in the DG where neural progenitors reside, to the granule layer of the GC where they settle and integrate into the DG circuit. Seizures induce the ectopic migration of GCs either to the outer third of the granule cell layer or the hilar region (Jessberger et al., 2009; Parent et al., 1997). The vast majority of NaChBac$^+$ neurons had cell bodies correctly localized within the granule layer of the DG. We observed no NaChBac$^+$ neurons in the outer third of the granule cell layer, but found occasional neurons in the hilar region (Figure S2A), while no wildtype neurons were ever found there. The morphology of these ectopic neurons was similar to their counterparts in the granule cell layer. They were polarized, and had dendrites extending in the opposite direction of their axon. The neurons were entirely in the hilus and their dendrites were also located solely in the hilus instead of the molecular layer. Due to the location of their dendrites, the connectivity of these neurons is likely to be perturbed. As mentioned above, NaChBac activity induces premature downregulation of PSA-NCAM, which has been implicated in neuronal migration either through its role in decreasing cell-cell adhesion (Johnson et al., 2005) or in sensing growth factor gradients (Muller et al., 2000). It is possible that the downregulation of PSA-NCAM is responsible for the ectopic location of some of these NaChBac$^+$ neurons. In addition to cells found in the hilus, we also observed that cell bodies of NaChBac-positive GCs reside closer to the hilar border than wildtype controls at 28 dpi (Figure S2B). This observation suggests

accelerated halting of the GCs within the granule cell layer that could have resulted from the premature downregulation of PSA-NCAM by NaChBac (Figure 1E).

Mature GCs in the DG display apical dendrites that branch into the molecular layer of the DG. During their development, newly generated GCs in the adult DG transiently display basal dendrites extending into the hilus, which disappear by 4 or 5 days after the neuron's birth (Shapiro and Ribak, 2006). The presence of spiny basal dendrites emanating from the cell bodies of fully mature GCs and extending into the hilus is one of the hallmarks of seizure-related changes in the DG (Jessberger et al., 2007; Shapiro and Ribak, 2006). About 20% of NaChBac$^+$ neurons displayed these aberrant basal dendrites while control neurons expressing the E191K non-conducting channel never did (Figure S2C and D). The persistence of basal dendrites beyond that time suggests that hyperexcitable neurons receive additional synaptic inputs to their cell bodies and this input is likely to be excitatory (Ribak et al., 2000; Thind et al., 2008).

Increase in neuronal activity via seizures also affects the formation of apical dendrites and their synapses. When we examined the morphology of NaChBac$^+$ GCs in the granule layers, we observed that they had shorter apical dendrites on average (Figure 2A). In addition, the density of protrusions on apical dendrites of NaChBac$^+$ neurons was half of the spine density of control neurons expressing the pore-dead NaChBac E191K channel at 28 dpi (Figure 2B). There was an increase in spine density from 28 to 42 dpi for control neurons (Figure 2B far right panel) but no further change for NaChBac$^+$ neurons. The average spine size at 28 dpi of NaChBac$^+$ neurons was twice of that of NaChBac E191$^+$ neurons (Figure 2C, far right panel). Interestingly, the increase in spine size of NaChBac$^+$ neurons resembles the increased proportion of mushroom spines observed in GCs after seizure (Jessberger et al., 2007).

To investigate whether the large protrusions on NaChBac$^+$ neurons' apical dendrites were indeed synaptic spines, we infected new DG GCs with GFP constructs fused to PSD95, a scaffolding protein selectively localized to the postsynaptic density of glutamatergic input synapses (Kelsch et al., 2008). Control neurons were infected with a virus expressing only the PSD95-GFP fusion while hyperexcitable neurons were infected with PSD95-GFP:NaChBac, a bicistronic construct encoding both GFP-tagged PSD95 and NaChBac. We performed immunocytochemistry against the diffuse, unclustered GFP that filled the cytoplasm with a red secondary antibody to visualize the dendritic morphology, while PSD95-positive clusters were identified by the direct green fluorescence from GFP. All protrusions present on the dendrites of labeled neurons expressed GFP:PSD-95 (Figure 2C, left panels), confirming that the larger protrusions in NaChBac$^+$ cells are postsynaptic sites. Furthermore, larger protrusions exhibited larger GFP:PSD-95$^+$ clusters, suggesting that any observed change in spine size could possibly indicate larger postsynaptic densities and, in effect, larger synapses.

The morphological alterations we report here suggest that NaChBac$^+$ neurons experience an overall decrease in the number of excitatory inputs to NaChBac$^+$ neurons. However, although fewer in number, each individual spine in NaChBac$^+$ neurons was larger on average than those of control neurons. To examine how these morphological changes translated into functional differences, we measured the spontaneous EPSCs (sEPSCs) of individual NaChBac$^+$ neurons by electrophysiological recording and found that overall frequency of sEPSCs is significantly reduced in NaChBac$^+$ neurons (Figure 2D bottom panel, left), whereas the average amplitude of sEPSCs was increased (Figure 2D bottom panel, middle). These results are consistent with NaChBac$^+$ neurons having fewer but larger synapses. Since the frequency and amplitude of sEPSCs in NaChBac$^+$ neurons changed in

opposing directions, in order to find out what the resultant current was, we calculated the overall excitatory current received by the neurons by multiplying average frequency by average area under each spike, for each neuron. The overall excitatory current received by $NaChBac^+$ neurons was not significantly different from that received by controls (Figure 2D, bottom panel, right).

**Elevated excitability leads to changes in excitatory outputs at CA3**

To quantify the changes in outputs of NaChBac-expressing DG granule cells, we examined the morphology of presynaptic terminals on their axons in the CA3 region, where their main output is.

The axons of DG granule cells synapse on multiple targets on CA3, both on excitatory pyramidal cells and inhibitory interneurons. The axon collaterals of dentate GCs form specialized presynaptic sites called large mossy fiber terminals (LMT). LMTs measure between 3 to 8 μm in their greatest dimension, and form complex interdigitating connections with CA3 pyramidal cells. DG axons also have two other types of smaller output synapses that contact inhibitory neurons at CA3 called *en passant* boutons and filopodial terminals (Acsady et al., 1998). *En passant* boutons are varicosities 0.5 to 2 μm in diameter distributed along the axons of GCs, and filopodial terminals are thin protrusions emanating from the LMT. We focused on the effects of hyperexcitability on LMTs because due to their characteristic morphology, these presynaptic sites can be unambiguously identified by membrane-bound GFP labeling. Expression of NaChBac decreased the overall density of presynaptic terminals present on the axons of adult-born dentate granule cells at CA3 (Figure 3B), which suggests that the hyperexcitable neurons downregulated their overall output to

CA3. We observed that the overall density of LMTs in the axons of NaChBac$^+$ neurons was significantly decreased in comparison with control neurons (Figure 3A and C). The proportion of total presynaptic sites that are LMTs is also significantly reduced in NaChBac$^+$ neurons (Figure 3D). These observations indicate that the output from hyperexcitable NaChBac$^+$ DG GCs onto CA3 is significantly decreased.

In order to confirm we were quantifying actual presynaptic sites in our measurements, we injected adult mice with retroviral vectors expressing Synaptophysin-GFP, a protein selectively localized to presynaptic neurotransmitter vesicles (Wiedenmann and Franke, 1985). Neurons were infected with a bicistronic virus encoding both Synaptophysin-GFP and NaChBac to visualize the presynaptic sites on axons of hyperexcitable cells. Cells in a separate DG infected with a virus encoding Synaptophysin-GFP were used as controls. Using a red fluorescent secondary antibody against the diffuse, unclustered GFP that filled the cytoplasm, we were able to visualize the full morphology of the axons at CA3, as well as determine the location of synaptophysin-positive presynaptic sites, which showed up as green GFP-positive clusters. All structures resembling presynaptic terminals as labeled by PalmGFP were positive for GFP:synaptophysin both in wildtype neurons and those expressing NaChBac (Figure 3E). This confirms that the structures we quantified corresponded to presynaptic terminals on the axons of these adult-born GCs.

Our observations of output connectivity at CA3 indicate that an increase in intrinsic excitability in adult-born GCs leads to a decrease in excitatory output at CA3. This change could help ensure that the addition of some hyperexcitable neurons does not result in increased excitation in the hippocampal circuits.

**Activity-induced changes in input connectivity are dependent on cell-autonomous Npas4 signaling**

Two of our observations in NaChBac$^+$ neurons led us to hypothesize that the early increase of GABAergic synapses triggered by hyperexcitability could be related to the later changes in synaptic connectivity observed in dendrites and axons. First, one of the earliest changes observed in the development of NaChBac$^+$ neurons was the increase in perisomatic GABAergic inputs before 13 dpi (Figure 1B). The overall current of sIPSCs received by NaChBac$^+$ neurons was 10 times that of controls at 17dpi (Figure 1D bottom panel, right). An alteration of this magnitude so early in neuronal development could have a significant impact on subsequent integration. Second, the premature upregulation of KCC2 (Figure S1B) suggests that the action of GABA could be hyperpolarizing earlier in the maturation of NaChBac$^+$ neurons. Rendering GABA hyperpolarizing on immature neurons by altering chloride concentration is known to affect the dendritic development of adult-born GCs in the DG (Ge et al., 2006).

BDNF (brain-derived neurotrophic factor) was a likely candidate underlying the increase of inhibition in NaChBac$^+$ neurons, because it is regulated by activity (Ballarin et al., 1991) and known to directly regulate the formation of GABAergic inputs (Huang et al., 1999; Marty et al., 2000; Rutherford et al., 1997; Seil and Drake-Baumann, 2000) as well as dendritic growth (Xu et al., 2000).

In order to study the effects of expressing NaChBac in the absence of BDNF, we expressed Cre Recombinase, NaChBac and a fluorescent protein in individual neurons in the DG of BDNF conditional knockout mice. The expression level of a tricistronic vector containing the 3 abovementioned genes was too low for visualization of the labeled neurons.

In order to achieve stronger expression of fluorescent proteins, we injected a mixture of viruses into the DG of BDNF conditional knockout mice. The first virus carried a bicistronic construct expressing GFP and Cre Recombinase, and the 2nd virus carried an invertible cassette with a bicistronic construct encoding both palmitoylated mCherry and NaChBac. The invertible cassette is in the reverse 3' to 5' orientation with respect to the retroviral promoter except in the presence of Cre Recombinase when it flips to the correct 5' to 3' orientation and expresses both mCherry and NaChBac. In this manner, the presence of Cre leads to the expression of mCherry and NaChBac, and simultaneously, to the deletion of the BDNF locus in individual GCs in the BDNF conditional knockout mice. The palmitolyated mCherry protein localizes to the membranes of such neurons, enabling the identification of fine structural features such as synaptic spines. In this experiment we used the same dual virus strategy in both wildtype mice and conditional knockout mice and compared results between them.

Surprisingly, the morphological alterations as well as changes in the frequency and amplitude of sIPSCs triggered by NaChBac were identical in neurons expressing or lacking BDNF. This observation suggests that BDNF does not contribute to any of the changes in connectivity triggered by NaChBac activity. Accordingly, we shifted our attention to another candidate gene, Npas4, a transcription factor involved in the activity-dependent regulation of inhibitory synapses in hippocampal neurons (Lin et al., 2008). We hypothesized that the increased inhibition observed in hyperexcitable new DG GCs could be due to the expression of Npas4. To study the involvement of Npas4 in connectivity changes triggered by hyperexcitability, we used the same strategy described for BDNF, but with Npas4 conditional knockout mice.

As described above, expression of NaChBac in wildtype adult mice results in an increase in $VGAT^+$ perisomatic inhibitory terminals on new DG GCs (Figure 1B). In contrast, the deletion of Npas4 in individual hyperexcitable new GCs blocked the increase in VGAT terminals triggered by NaChBac both at 17 and 28 dpi (Figure 4A). Knocking out Npas4 alone in DG GCs, using a virus carrying a GFP-Cre Recombinase construct, has no effect on the number of $VGAT^+$ puncta at 17 dpi and leads to a very small increase at 28 dpi (Figure 4A). Furthermore, Npas4 signaling within individual adult-born neurons in the DG is necessary to trigger the changes in dendritic morphology induced by $NaChBac^+$ neurons (Figures 4B, D and E). Deletion of Npas4 in new GCs blocked the changes caused by NaChBac expression in dendritic length, spine density and size. Dendritic length and spine density in $NaChBac^+Npas4^-$ neurons are indistinguishable from those of control neurons expressing the pore-dead version of NaChBac (Figures 4B, D and S3A).

Interestingly, Npas4 was not required for activity-dependent changes in the output synapses, because $NaChBac^+$ $Npas4^-$ neurons still exhibited a dramatic reduction in density of large mossy terminals at CA3 (Figure 4C). Knocking out Npas4 alone has no effect on either dendritic or axonal synapses (Figures 4B-4E). These results demonstrate that Npas4 signaling specifically regulates activity-dependent formation of inputs to DG GCs.

## DISCUSSION

### Increase in electrical activity of a single new neuron is sufficient to induce changes in connectivity

Global manipulations of brain activity via seizures or learning paradigms have demonstrated the influence of neuronal activity on the integration and connectivity of adult-born neurons in

the DG (Kee et al., 2007; Kron et al., 2010). However, it is unclear whether these connectivity changes resulted directly from cell-autonomous increased firing of new neurons, indirectly through the elevated activity in the surrounding circuit, or from a combination of both. Here, we genetically modulate the electrical activity in individual adult-born DG GCs and show that an increase in cell-intrinsic activity of new neurons is sufficient to cause dramatic changes in their connectivity. NaChBac activity-induced connectivity changes in the adult DG appear to be homeostatic, since NaChBac induces an increase in inhibitory inputs and decrease in excitatory outputs. Furthermore, at 13 dpi, when NaChBac$^+$ neurons display a significantly higher number of perisomatic VGAT$^+$ puncta, more NaChBac$^+$ neurons express KCC2 than control neurons (Figure S1B). This observation is consistent with previous reports indicating that the timing of KCC2 expression is activity dependent (Ganguly et al., 2001). Because the upregulation of KCC2 relative to NKCC1 is correlated with the switch between GABAergic inputs being depolarizing to hyperpolarizing (Rivera et al., 1999; Wang et al., 2002), this suggests that the GABAergic input to NaChBac$^+$ neurons becomes inhibitory earlier in their development than in control cells, which could serve to dampen the heightened excitability of these neurons.

The results of a previous study seemed to suggest that global activity alterations are necessary in vitro to effect changes in GABAergic terminals because suppression of single-cell activity in dissociated hippocampal cultures using the potassium channel Kir2.1 did not alter GABAergic inputs (Hartman et al., 2006). Our results show that in new DG neurons in vivo, elevating single-cell activity is sufficient to induce changes in GABAergic input (Figure 1B-D). It is not possible to directly compare the results from these 2 experiments as they were produced in different conditions and systems, namely adult-generated DG neurons in vivo versus embryonic hippocampal cultures. However, when we silenced adult-generated

DG neurons in vivo via retroviral expression of the Kir2.1 channel we did not observe any changes in either dendritic or axonal morphology (data not shown). These observations suggest that the regulation of synaptic input to a single adult-born DG GC may be modulated by increases, but not decreases in intrinsic activity.

In our study, we observed that sEPSCs received by NaChBac$^+$ neurons were of a lower frequency of but increased amplitude than those received by control neurons, and this was consistent with the decreased spine density but increased spine size on their dendrites (Figure 2B and C). The overall excitatory current received was not significantly different compared to controls (Figure 2D, bottom panel, right). In contrast the overall GABAergic current received by NaChBac$^+$ neurons was approximately 10 times that of control neurons (Figure 1D, bottom panel, right). This finding suggests that modulating inhibition may be the primary method by which the activity of an adult-born neuron in the DG is regulated.

**An activity-dependent genetic program involving immediate early gene Npas4 governs neuronal connectivity of adult-born neurons to the mature DG circuit**

Our results reveal an intermediate step between neuronal activity and changes in synaptic connectivity, which involves a transcription factor whose expression is activity-dependent. The connectivity changes triggered by an increase in cell-intrinsic excitability neurons are dependent on the immediate early gene Npas4. The role of Npas4 in these connectivity changes is activity-dependent: deletion of Npas4 does not affect the formation of synapses in control cells which have baseline excitability, but it blocks synaptic alterations triggered by hyperexcitability. Although Npas4 has been shown to regulate the formation of inhibitory inputs to CA1 pyramidal cells *in vitro* (Lin et al, 2008), our results in DG GCs suggests that

knocking out Npas4 alone in individual neurons does not decrease the number of inhibitory $VGAT^+$ contacts on its soma (Figure 4A). Npas4 is expressed at extremely low levels at baseline in DG GCs, but is upregulated with activity, for instance, during kainic acid-induced seizures (Figure S3B). For this reason, it is not surprising that the requirement of Npas4 in inducing an increase in inhibitory contacts is specifically activity-dependent.

Our data also suggests that eliminating cell-intrinsic BDNF in a $NaChBac^+$ GC has no effect on altering the neuronal connectivity of these neurons. This result may be surprising since BDNF is activity-regulated (Ballarin et al., 1991) and is involved in regulating spine formation and size (McAllister et al., 1997; Xu et al., 2000). In addition, BDNF is a major downstream effector of Npas4 and is responsible for formation of inhibitory inputs to CA1 pyramidal neurons (Lin et al., 2008). However, the role of BDNF in dendritic growth varies depending on cell type and synapse location (McAllister et al., 1997). Also, BDNF plays a developmental role in CA1 via Npas4 even at baseline activity levels (Lin et al., 2008), while in the DG Npas4 only plays a significant role in development of synaptic inputs when neuronal activity is raised above baseline levels (Figure 4). This finding indicates that the mechanisms regulating neuronal connectivity may be specific for different neuronal types.

Finally, Npas4 is involved in activity-dependent changes to input connectivity to adult-born DG GCs, but not to their output connectivity in CA3 (Figure 4C). This observation suggests that there are independent programs governing input and output synapses, and this finding could have important implications for the structural alterations triggered by epilepsy.

## ACKNOWLEDGEMENTS

We thank Alberto Stolfi and Drew Friedman for help with the engineering of the viral constructs, David Clapham for providing us with the NaChBac cDNA, Karl Deisseroth for providing the doublefloxed inverse orf vector, Rudolph Jaenisch and Yingxi Lin for providing the conditional BDNF and Npas4 knockout mice respectively. This work was supported by an NIDCD RO1 grant to C.L., an M.I.T. Singleton and Chyn Duog Shiah Memorial fellowships to C.W.L.

## REFERENCES

Acsady, L., Kamondi, A., Sik, A., Freund, T., and Buzsaki, G. (1998). GABAergic cells are the major postsynaptic targets of mossy fibers in the rat hippocampus. J Neurosci *18*, 3386-3403.

Aimone, J.B., Wiles, J., and Gage, F.H. (2006). Potential role for adult neurogenesis in the encoding of time in new memories. Nat Neurosci *9*, 723-727.

Ballarin, M., Ernfors, P., Lindefors, N., and Persson, H. (1991). Hippocampal damage and kainic acid injection induce a rapid increase in mRNA for BDNF and NGF in the rat brain. Exp Neurol *114*, 35-43.

Bean, B.P. (2007). The action potential in mammalian central neurons. Nat Rev Neurosci *8*, 451-465.

Cameron, H.A., and McKay, R.D. (2001). Adult neurogenesis produces a large pool of new granule cells in the dentate gyrus. J Comp Neurol *435*, 406-417.

Chaudhry, F.A., Reimer, R.J., Bellocchio, E.E., Danbolt, N.C., Osen, K.K., Edwards, R.H., and Storm-Mathisen, J. (1998). The vesicular GABA transporter, VGAT, localizes to synaptic vesicles in sets of glycinergic as well as GABAergic neurons. J Neurosci *18*, 9733-9750.

Clayton, G.H., Owens, G.C., Wolff, J.S., and Smith, R.L. (1998). Ontogeny of cation-Cl-cotransporter expression in rat neocortex. Brain Res Dev Brain Res *109*, 281-292.

Erlander, M.G., and Tobin, A.J. (1991). The structural and functional heterogeneity of glutamic acid decarboxylase: a review. Neurochem Res *16*, 215-226.

Freund, T.F., and Buzsaki, G. (1996). Interneurons of the hippocampus. Hippocampus *6*, 347-470.

Galimberti, I., Gogolla, N., Alberi, S., Santos, A.F., Muller, D., and Caroni, P. (2006). Long-term rearrangements of hippocampal mossy fiber terminal connectivity in the adult regulated by experience. Neuron *50*, 749-763.

Ganguly, K., Schinder, A.F., Wong, S.T., and Poo, M. (2001). GABA itself promotes the developmental switch of neuronal GABAergic responses from excitation to inhibition. Cell *105*, 521-532.

Ge, S., Goh, E.L., Sailor, K.A., Kitabatake, Y., Ming, G.L., and Song, H. (2006). GABA regulates synaptic integration of newly generated neurons in the adult brain. Nature *439*, 589-593.

Hartman, K.N., Pal, S.K., Burrone, J., and Murthy, V.N. (2006). Activity-dependent regulation of inhibitory synaptic transmission in hippocampal neurons. Nat Neurosci *9*, 642-649.

Huang, Z.J., Kirkwood, A., Pizzorusso, T., Porciatti, V., Morales, B., Bear, M.F., Maffei, L., and Tonegawa, S. (1999). BDNF regulates the maturation of inhibition and the critical period of plasticity in mouse visual cortex. Cell *98*, 739-755.
Imayoshi, I., Sakamoto, M., Ohtsuka, T., Takao, K., Miyakawa, T., Yamaguchi, M., Mori, K., Ikeda, T., Itohara, S., and Kageyama, R. (2008). Roles of continuous neurogenesis in the structural and functional integrity of the adult forebrain. Nat Neurosci *11*, 1153-1161.
Jakubs, K., Nanobashvili, A., Bonde, S., Ekdahl, C.T., Kokaia, Z., Kokaia, M., and Lindvall, O. (2006). Environment matters: synaptic properties of neurons born in the epileptic adult brain develop to reduce excitability. Neuron *52*, 1047-1059.
Jessberger, S., Clark, R.E., Broadbent, N.J., Clemenson, G.D., Jr., Consiglio, A., Lie, D.C., Squire, L.R., and Gage, F.H. (2009). Dentate gyrus-specific knockdown of adult neurogenesis impairs spatial and object recognition memory in adult rats. Learn Mem *16*, 147-154.
Jessberger, S., and Kempermann, G. (2003). Adult-born hippocampal neurons mature into activity-dependent responsiveness. Eur J Neurosci *18*, 2707-2712.
Jessberger, S., Zhao, C., Toni, N., Clemenson, G.D., Jr., Li, Y., and Gage, F.H. (2007). Seizure-associated, aberrant neurogenesis in adult rats characterized with retrovirus-mediated cell labeling. J Neurosci *27*, 9400-9407.
Johnson, C.P., Fujimoto, I., Rutishauser, U., and Leckband, D.E. (2005). Direct evidence that neural cell adhesion molecule (NCAM) polysialylation increases intermembrane repulsion and abrogates adhesion. J Biol Chem *280*, 137-145.
Kee, N., Teixeira, C.M., Wang, A.H., and Frankland, P.W. (2007). Preferential incorporation of adult-generated granule cells into spatial memory networks in the dentate gyrus. Nat Neurosci *10*, 355-362.
Kelsch, W., Lin, C.W., and Lois, C. (2008). Sequential development of synapses in dendritic domains during adult neurogenesis. Proc Natl Acad Sci U S A *105*, 16803-16808.
Kelsch, W., Lin, C.W., Mosley, C.P., and Lois, C. (2009). A critical period for activity-dependent synaptic development during olfactory bulb adult neurogenesis. J Neurosci *29*, 11852-11858.
Kempermann, G., Kuhn, H.G., and Gage, F.H. (1997). More hippocampal neurons in adult mice living in an enriched environment. Nature *386*, 493-495.
Kron, M.M., Zhang, H., and Parent, J.M. The developmental stage of dentate granule cells dictates their contribution to seizure-induced plasticity. J Neurosci *30*, 2051-2059.
Kron, M.M., Zhang, H., and Parent, J.M. (2010). The developmental stage of dentate granule cells dictates their contribution to seizure-induced plasticity. J Neurosci *30*, 2051-2059.
Lewis, P.F., and Emerman, M. (1994). Passage through mitosis is required for oncoretroviruses but not for the human immunodeficiency virus. J Virol *68*, 510-516.
Lin, C.W., Sim, S., Ainsworth, A., Okada, M., Kelsch, W., and Lois, C. Genetically increased cell-intrinsic excitability enhances neuronal integration into adult brain circuits. Neuron *65*, 32-39.
Lin, C.W., Sim, S., Ainsworth, A., Okada, M., Kelsch, W., and Lois, C. (2010). Genetically increased cell-intrinsic excitability enhances neuronal integration into adult brain circuits. Neuron *65*, 32-39.
Lin, Y., Bloodgood, B.L., Hauser, J.L., Lapan, A.D., Koon, A.C., Kim, T.K., Hu, L.S., Malik, A.N., and Greenberg, M.E. (2008). Activity-dependent regulation of inhibitory synapse development by Npas4. Nature *455*, 1198-1204.
Marty, S., Wehrle, R., and Sotelo, C. (2000). Neuronal activity and brain-derived neurotrophic factor regulate the density of inhibitory synapses in organotypic slice cultures of postnatal hippocampus. J Neurosci *20*, 8087-8095.

McAllister, A.K., Katz, L.C., and Lo, D.C. (1997). Opposing roles for endogenous BDNF and NT-3 in regulating cortical dendritic growth. Neuron *18*, 767-778.
Muller, D., Djebbara-Hannas, Z., Jourdain, P., Vutskits, L., Durbec, P., Rougon, G., and Kiss, J.Z. (2000). Brain-derived neurotrophic factor restores long-term potentiation in polysialic acid-neural cell adhesion molecule-deficient hippocampus. Proc Natl Acad Sci U S A *97*, 4315-4320.
Nitabach, M.N., Wu, Y., Sheeba, V., Lemon, W.C., Strumbos, J., Zelensky, P.K., White, B.H., and Holmes, T.C. (2006). Electrical hyperexcitation of lateral ventral pacemaker neurons desynchronizes downstream circadian oscillators in the fly circadian circuit and induces multiple behavioral periods. J Neurosci *26*, 479-489.
Overstreet-Wadiche, L.S., Bromberg, D.A., Bensen, A.L., and Westbrook, G.L. (2006). Seizures accelerate functional integration of adult-generated granule cells. J Neurosci *26*, 4095-4103.
Parent, J.M., Yu, T.W., Leibowitz, R.T., Geschwind, D.H., Sloviter, R.S., and Lowenstein, D.H. (1997). Dentate granule cell neurogenesis is increased by seizures and contributes to aberrant network reorganization in the adult rat hippocampus. J Neurosci *17*, 3727-3738.
Plotkin, M.D., Snyder, E.Y., Hebert, S.C., and Delpire, E. (1997). Expression of the Na-K-2Cl cotransporter is developmentally regulated in postnatal rat brains: a possible mechanism underlying GABA's excitatory role in immature brain. J Neurobiol *33*, 781-795.
Ren, D., Navarro, B., Xu, H., Yue, L., Shi, Q., and Clapham, D.E. (2001). A prokaryotic voltage-gated sodium channel. Science *294*, 2372-2375.
Ribak, C.E., Tran, P.H., Spigelman, I., Okazaki, M.M., and Nadler, J.V. (2000). Status epilepticus-induced hilar basal dendrites on rodent granule cells contribute to recurrent excitatory circuitry. J Comp Neurol *428*, 240-253.
Rivera, C., Voipio, J., Payne, J.A., Ruusuvuori, E., Lahtinen, H., Lamsa, K., Pirvola, U., Saarma, M., and Kaila, K. (1999). The K+/Cl- co-transporter KCC2 renders GABA hyperpolarizing during neuronal maturation. Nature *397*, 251-255.
Rutherford, L.C., DeWan, A., Lauer, H.M., and Turrigiano, G.G. (1997). Brain-derived neurotrophic factor mediates the activity-dependent regulation of inhibition in neocortical cultures. J Neurosci *17*, 4527-4535.
Schmidt-Hieber, C., Jonas, P., and Bischofberger, J. (2004). Enhanced synaptic plasticity in newly generated granule cells of the adult hippocampus. Nature *429*, 184-187.
Seil, F.J., and Drake-Baumann, R. (2000). TrkB receptor ligands promote activity-dependent inhibitory synaptogenesis. J Neurosci *20*, 5367-5373.
Seki, T., and Arai, Y. (1993). Highly polysialylated neural cell adhesion molecule (NCAM-H) is expressed by newly generated granule cells in the dentate gyrus of the adult rat. J Neurosci *13*, 2351-2358.
Shapiro, L.A., and Ribak, C.E. (2006). Newly born dentate granule neurons after pilocarpine-induced epilepsy have hilar basal dendrites with immature synapses. Epilepsy Res *69*, 53-66.
Tashiro, A., Sandler, V.M., Toni, N., Zhao, C., and Gage, F.H. (2006). NMDA-receptor-mediated, cell-specific integration of new neurons in adult dentate gyrus. Nature *442*, 929-933.
Thind, K.K., Ribak, C.E., and Buckmaster, P.S. (2008). Synaptic input to dentate granule cell basal dendrites in a rat model of temporal lobe epilepsy. J Comp Neurol *509*, 190-202.
Turrigiano, G.G., and Nelson, S.B. (2004). Homeostatic plasticity in the developing nervous system. Nat Rev Neurosci *5*, 97-107.
van Praag, H., Kempermann, G., and Gage, F.H. (1999). Running increases cell proliferation and neurogenesis in the adult mouse dentate gyrus. Nat Neurosci *2*, 266-270.

Wang, C., Shimizu-Okabe, C., Watanabe, K., Okabe, A., Matsuzaki, H., Ogawa, T., Mori, N., Fukuda, A., and Sato, K. (2002). Developmental changes in KCC1, KCC2, and NKCC1 mRNA expressions in the rat brain. Brain Res Dev Brain Res *139*, 59-66.
Wiedenmann, B., and Franke, W.W. (1985). Identification and localization of synaptophysin, an integral membrane glycoprotein of Mr 38,000 characteristic of presynaptic vesicles. Cell *41*, 1017-1028.
Xu, B., Zang, K., Ruff, N.L., Zhang, Y.A., McConnell, S.K., Stryker, M.P., and Reichardt, L.F. (2000). Cortical degeneration in the absence of neurotrophin signaling: dendritic retraction and neuronal loss after removal of the receptor TrkB. Neuron *26*, 233-245.
Yue, L., Navarro, B., Ren, D., Ramos, A., and Clapham, D.E. (2002). The cation selectivity filter of the bacterial sodium channel, NaChBac. J Gen Physiol *120*, 845-853.

Figure 1

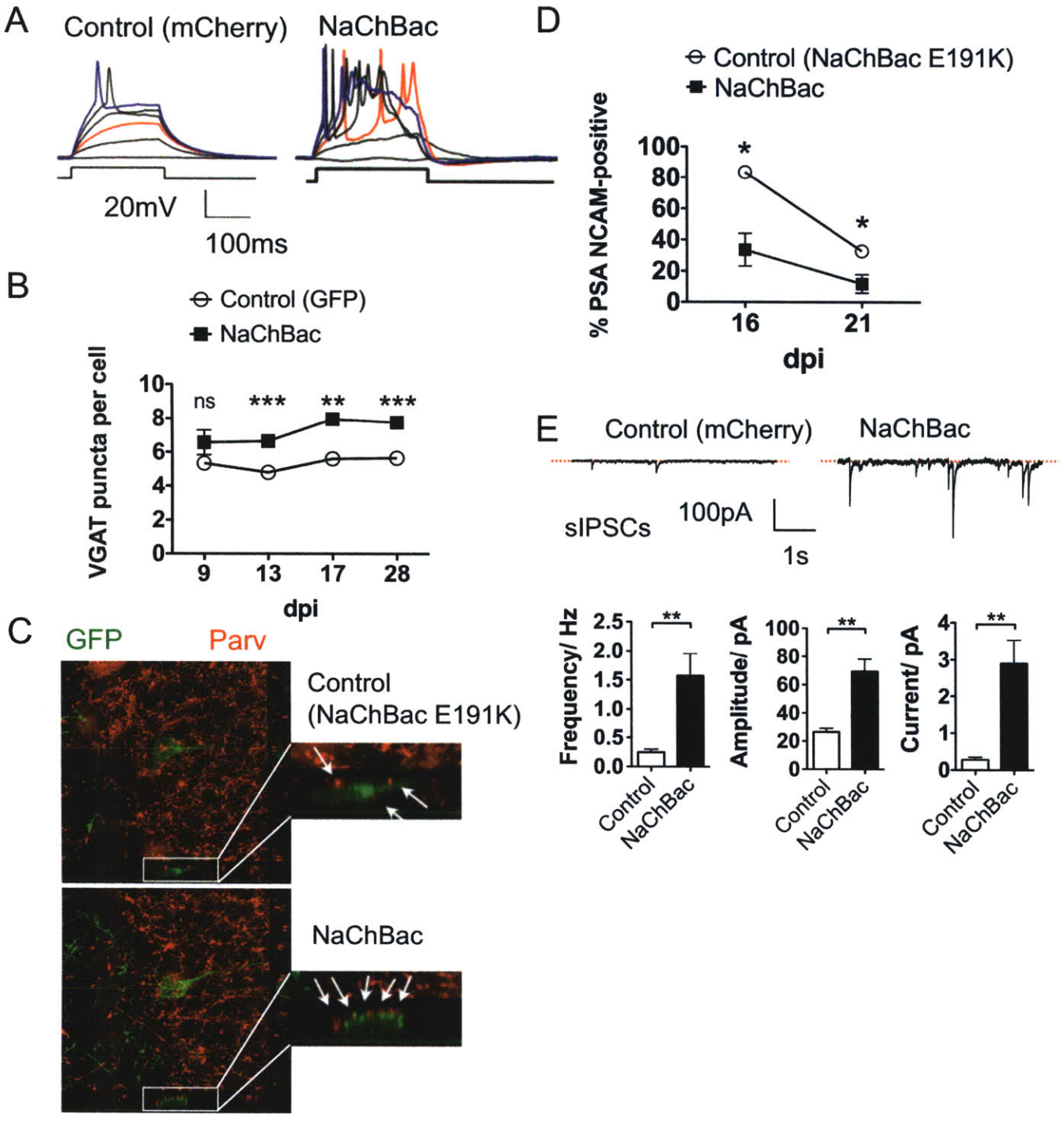
A
Control (mCherry)
NaChBac
20mV
100ms
B
Control (GFP)
NaChBac
VGAT puncta per cell
ns
***
**
***
dpi
C
GFP
Parv
Control
(NaChBac E191K)
NaChBac
D
Control (NaChBac E191K)
NaChBac
% PSA NCAM-positive
dpi
E
Control (mCherry)
NaChBac
sIPSCs
100pA
1s
Frequency/ Hz
Amplitude/ pA
Current/ pA
Control
NaChBac

Figure 2

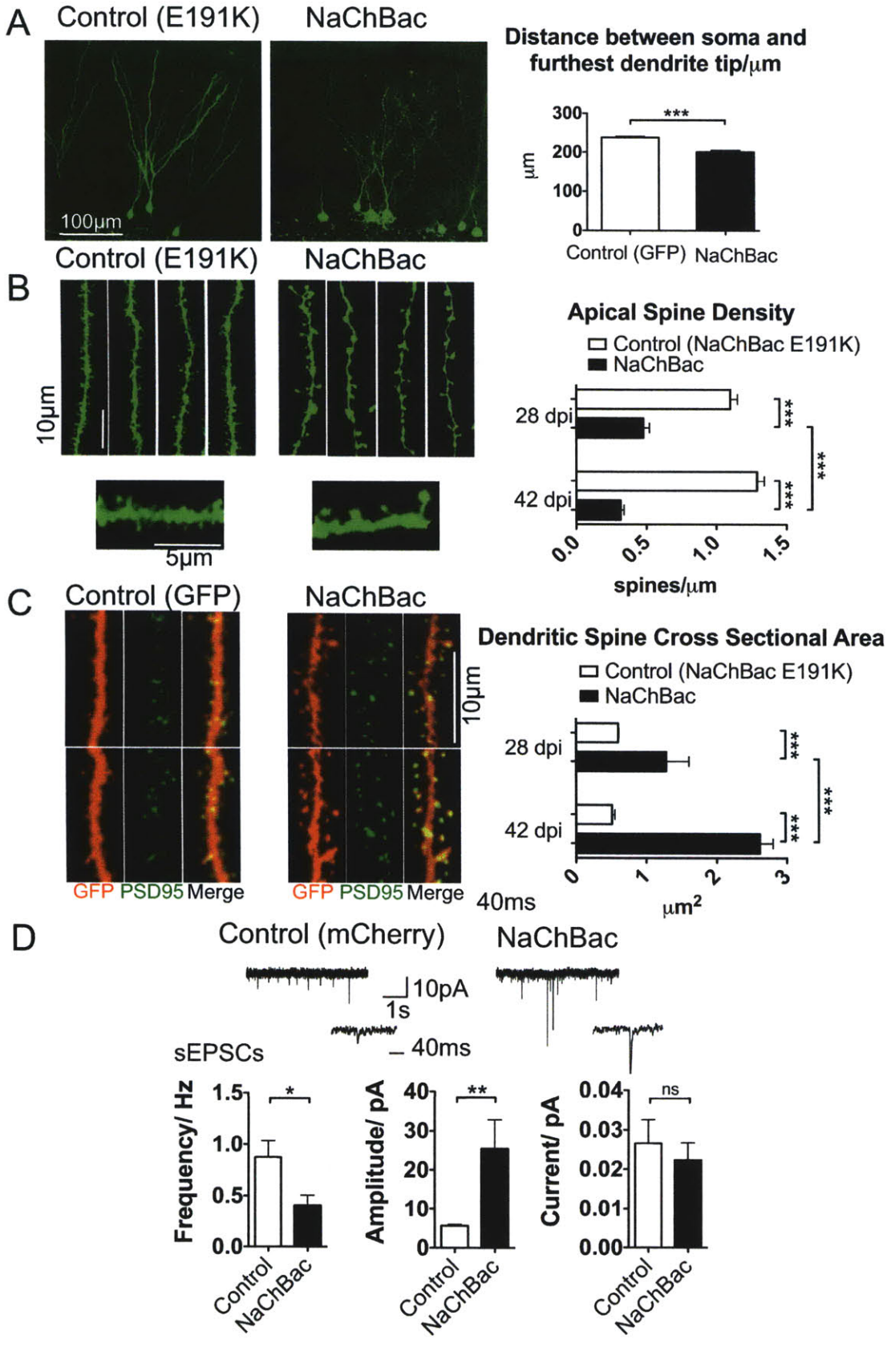
A
Control (E191K)
NaChBac
100μm
Distance between soma and furthest dendrite tip/μm
300
200
100
0
μm
***
Control (GFP)
NaChBac
B
Control (E191K)
NaChBac
10μm
5μm
Apical Spine Density
Control (NaChBac E191K)
NaChBac
28 dpi
42 dpi
***
***
***
0.0
0.5
1.0
1.5
spines/μm
C
Control (GFP)
NaChBac
GFP PSD95 Merge
GFP PSD95 Merge
10μm
Dendritic Spine Cross Sectional Area
Control (NaChBac E191K)
NaChBac
28 dpi
42 dpi
***
***
***
0
1
2
3
μm²
40ms
D
Control (mCherry)
NaChBac
10pA
1s
40ms
sEPSCs
Frequency/ Hz
1.5
1.0
0.5
0.0
*
Control
NaChBac
Amplitude/ pA
40
30
20
10
0
**
Control
NaChBac
Current/ pA
0.04
0.03
0.02
0.01
0.00
ns
Control
NaChBac

Figure 3

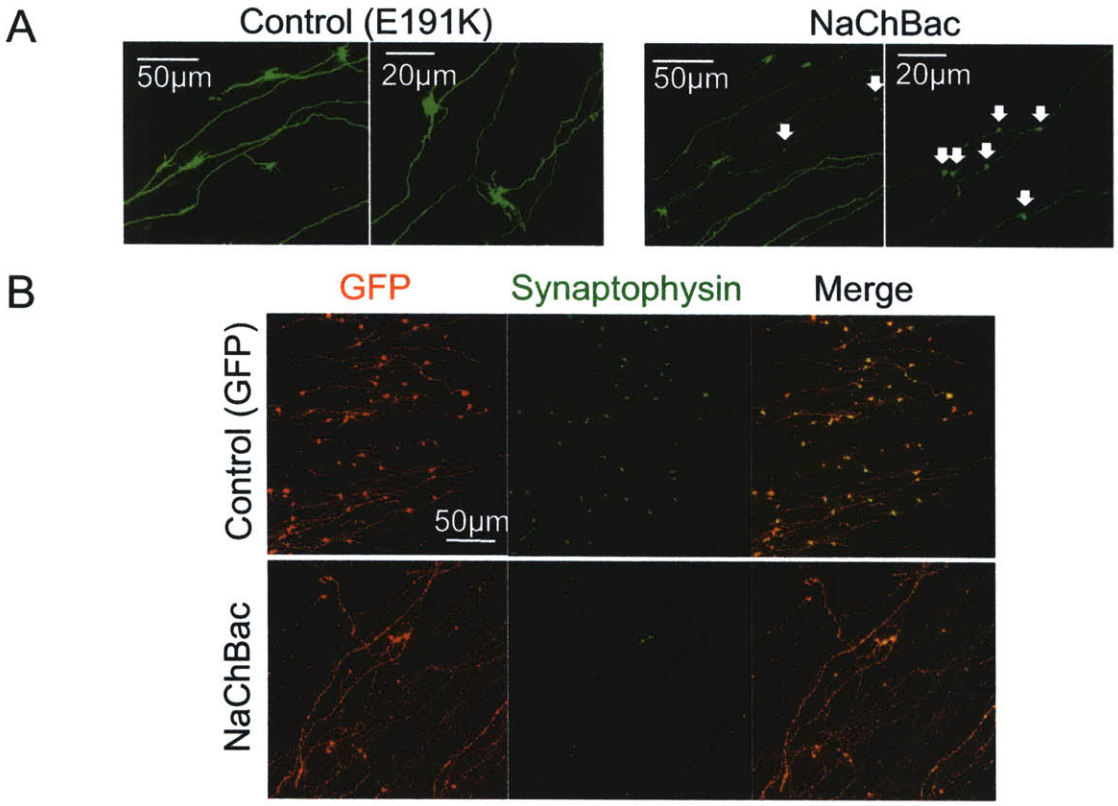
A
Control (E191K)
NaChBac
50µm
20µm
50µm
20µm
B
GFP
Synaptophysin
Merge
Control (GFP)
NaChBac
50µm
C
Control (NaChBac E191K)
NaChBac
# presynaptic sites/µm
0.015
0.010
0.005
0.000
*
***
28 dpi
42 dpi
D
Control (NaChBac E191K)
NaChBac
#LMT/µm
0.010
0.008
0.006
0.004
0.002
0.000
**
***
***
28 dpi
42 dpi
E
% Presynaptic terminals that are LMT at 28 dpi
%
100
80
60
40
20
0
*
Control (NaChBac E191K)
NaChBac

Figure 4

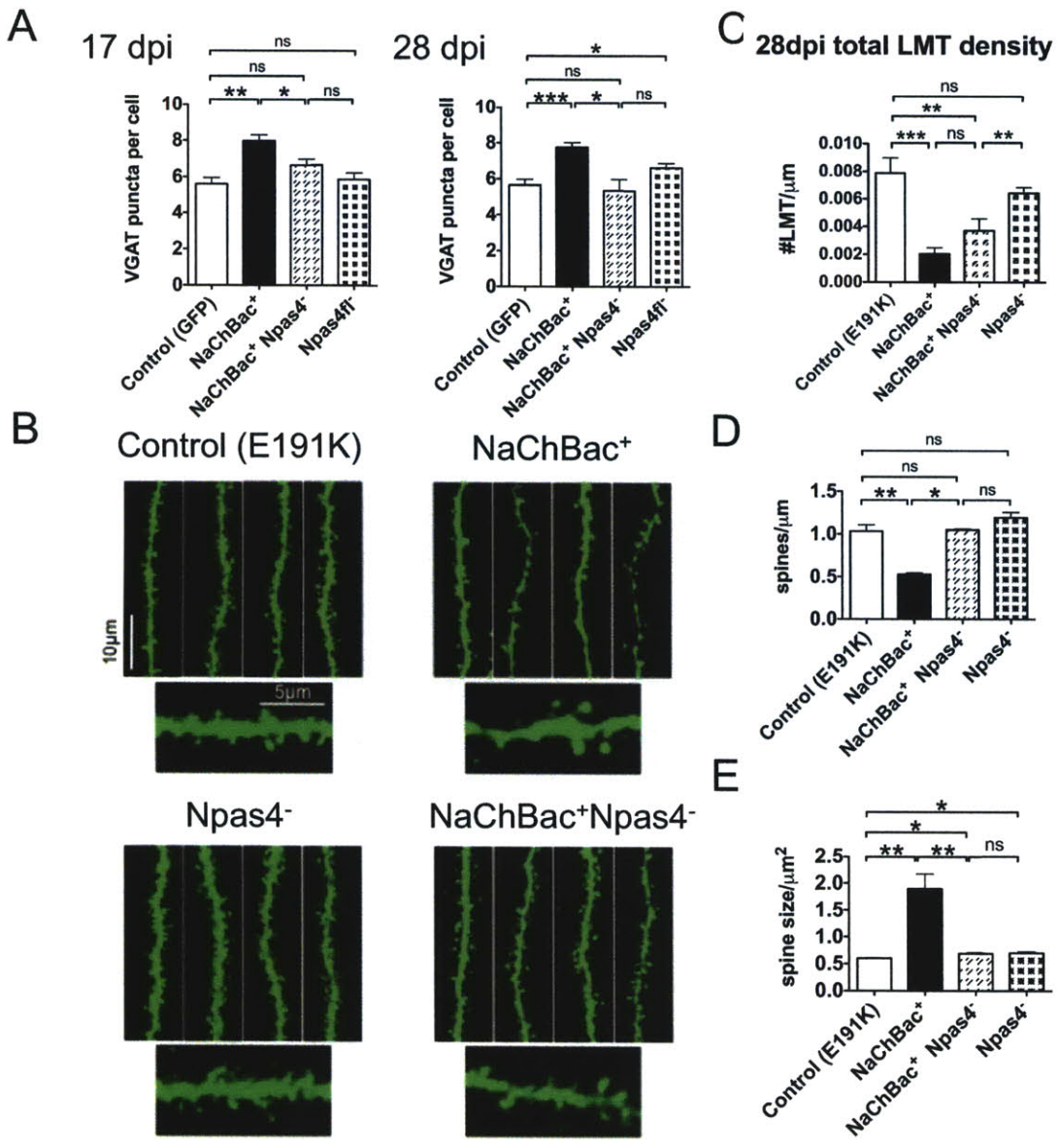
A
17 dpi
28 dpi
VGAT puncta per cell
Control (GFP)
NaChBac+
NaChBac+ Npas4-
Npas4fl-
B
Control (E191K)
NaChBac+
Npas4-
NaChBac+Npas4-
10µm
5µm
C
28dpi total LMT density
#LMT/µm
Control (E191K)
NaChBac+
NaChBac+ Npas4-
Npas4-
D
spines/µm
E
spine size/µm2
ns

## FIGURE LEGENDS

**Figure 1. Expression of NaChBac in adult-born DG granule cells elevates neuronal excitability and results in additional perisomatic GABAergic inputs**

(A) Intrinsic membrane excitability of control ($mCherry^+$) and $NaChBac^+$ neurons at 17 dpi. Neurons were injected with stepwise 5pA current to induce membrane potential change. 15pA of current did not induce any action potentials in control neurons (left panel) but triggered action potentials and long depolarization's in $NaChBac^+$ neurons (right; red trace). 25pA of current induced a single action potential in control neurons but induced repetitive action potentials in $NaChBac^+$ neurons (blue trace).

(B) $NaChBac^+$ neurons displayed increased numbers of perisomatic $VGAT^+$ inhibitory terminals at from 13 dpi onwards (9 dpi GFP: 5.341 ± 0.269 $VGAT^+$ puncta/soma, n = 94 neurons from 5 DGs, NaChBac: 6.57 ± 0.733 $VGAT^+$ puncta/soma, n = 72 neurons from 5 DGs, p = 0.176; 13 dpi GFP: 4.794 ± 0.322 $VGAT^+$ puncta/soma, n = 100 neurons from 8 DGs, NaChBac: 6.648 ± 0.217 $VGAT^+$ puncta/soma, n = 109 neurons from 8 DGs, ***p = 0.0005; 17 dpi GFP: 5.6098 ± 0.342 $VGAT^+$ puncta/soma, n = 56 neurons from 4 DGs, NaChBac: 7.96 ± 0.339 $VGAT^+$ puncta/soma, n = 115 neurons from 4 DGs, **p = 0.0045; 28 dpi GFP: 5.65 ± 0.325 $VGAT^+$ puncta/soma, n = 121 neurons from 6 DGs, NaChBac: 7.76 ± 0.258 $VGAT^+$ puncta/soma, n = 115 neurons from 6 DGs, ***p = 0.0005).

(C) Confocal z-stack images of parvalbumin staining of control and $NaChBac^+$ neurons.

(D) In voltage-clamp mode, control neurons (top panel, left trace) experienced few spontaneous inhibitory synaptic events while NaChBac$^+$ neurons (top panel, right trace) had frequent spikes of inhibitory inputs that were of higher amplitudes. Both frequency (bottom panel, left) and amplitude (bottom panel, middle) of spontaneous IPSCs received by NaChBac$^+$ neurons are higher than those received by control neurons (mCherry control frequency: 0.248 ± 0.054 Hz, n = 7 neurons, NaChBac frequency: 1.571 ± 0.381 Hz, n = 9 neurons, **p = 0.009; mCherry control amplitude: 26.42 ± 2.68 pA, n = 7 neurons, NaChBac amplitude: 69.28 ± 8.9 pA, n = 9 neurons, **p = 0.001). Overall current received by NaChBac$^+$ neurons is about 10 times that received by control neurons (mCherry control: 0.281 ± 0.071 pA, n = 7 neurons; NaChBac: 2.9 ± 0.63, n = 8 neurons; bottom panel, right).

(E) Significantly fewer NaChBac$^+$ neurons expressed PSA-NCAM at both 16 and 21 days post infection (dpi) compared to controls (16 dpi E191K control: 83.5% ± 1.35%, n = 2 DGs, NaChBac: 33.57% ± 10.5%, n = 3 DGs, *p = 0.0347; 28 dpi E191K control: 32.67% ± 3.6%, n = 3 DGs, NaChBac: 11.81% ± 5.9%, n = 3 DGs, *p < 0.05)

Two-tailed t-test used for statistical analysis. Error bars represent SEM.

See also Figure S1.

**Figure 2. Elevated neuronal excitability in DG granule neurons leads to changes in excitatory glutamatergic inputs**

(A) Low magnification confocal images showing decreased dendritic length of NaChBac$^+$ neurons compared to control neurons (pore-dead NaChBac E191K; left

panels). The distance between the furthest dendrite tip to the base of the apical dendrite is significantly lower in NaChBac$^+$ neurons than controls at 28 dpi (far right panel; GFP control: 238.6 ± 3.23 μm, n = 71 neurons, NaChBac: 200.8 ± 4.35 μm, n = 56 neurons, ***p < 0.0001).

(B) High magnification confocal images showing the decreased spine density and increased spine size in NaChBac$^+$ neurons (left panels). NaChBac$^+$ neurons have significantly fewer spines per length of dendrite than control (NaChBac E191K) neurons (far right panel; 28 dpi E191K control: 1.1 ± 0.05 spines/μm n = 21 images, NaChBac: 0.478 ± 0.044 spines/μm, n = 40 images, ***p < 0.0001; 42 dpi E191K control: 1.29 ± 0.052 spines/μm, n = 17 images, NaChBac: 0.316 ± 0.024 spines/μm, n = 9 images, ***p < 0.0001; 28 versus 42 dpi E191K *p = 0.014).

(C) All dendritic protrusions on both control and NaChBac$^+$ neurons cluster PSD95-GFP, suggesting they represent functional excitatory input synapses. Larger spines also exhibit correspondingly larger PDS95-GFP$^+$ puncta (left panels). NaChBac$^+$ neurons have significantly larger spines than control neurons at both 28 and 42 dpi (far right panel; 28 dpi E191K control: 0.636 ± 0.073 μm$^2$ n = 52 images from 4 DGs, NaChBac: 1.298 ± 0.15 μm$^2$, n = 24 images from 4 DGs, ***p < 0.0001; 42 dpi E191K control: 0.513 ± 0.042 μm$^2$, n = 75 images from 5 DGs, NaChBac: 2.618 ± 0.18 μm$^2$, n = 35 images from 8 DGs, ***p < 0.0001; 28 versus 42 dpi NaChBac ***p < 0.0001).

(D) Spontaneous excitatory postsynaptic currents (sEPSCs) were recorded in control (mCherry$^+$) neurons and NaChBac$^+$ neurons at 28 dpi (top panel). At 28 dpi the frequency of sEPSCs was significantly lower for NaChBac$^+$ neurons than control (mCherry Control:

0.876 ± 0.158 Hz, n = 6 neurons, NaChBac: 0.408 ± 0.098, n = 5 neurons, *p = 0.041; bottom panel, left) while the average amplitude was higher (mCherry Control: 5.653 ± 0.387 pA, n = 6 neurons, NaChBac: 25.46 ± 7.4 pA, n = 5 neurons, *p = 0.016; bottom panel, middle). The overall excitatory current received by NaChBac was not significantly different from controls (mCherry Control: 0.0266 ± 0.0059 pA, n = 6 neurons, NaChBac: 0.0224 ± 0.0043, n = 4 neurons, *p = 0.62; bottom panel, right).

Two-tailed t-test used for statistical analysis. Error bars represent SEM.

See also Figure S2.

**Figure 3. Elevated neuronal excitability in DG granule neurons leads to changes in excitatory output targets at CA3**

(A) Confocal maximal projection images showing large mossy terminals (LMTs; arrowheads) and *en passant* boutons on the axons of NaChBac$^+$ and control neurons.

(B) Axons of NaChBac$^+$ neurons showed an overall decrease in the total number of presynaptic sites compared to controls at both 28 and 42 dpi (28 dpi E191K control: 0.0087 ± 0.0011 sites/μm n = 11 images, NaChBac: 0.0059 ± 0.00068 sites/μm, n = 11 images, *p < 0.05; 42 dpi E191K control: 0.01 ± 0.00075 sites/μm, n = 10 images, NaChBac: 0.0056 ± 0.00059 sites/μm, n = 12 images, ***p = 0.0001).

(C) NaChBac$^+$ neurons had significantly fewer LMTs on their axons compared to controls at both 28 and 42 dpi (28 dpi E191K control: 0.0079 ± 0.0011 LMT/μm n = 11 images, NaChBac: 0.0031 ± 0.00043 LMT/μm, n = 11 images, **p = 0.0013; 42 dpi

E191K control: 0.0074 ± 0.00068 LMT/μm, n = 10 images, NaChBac: 0.0007 ± 0.00029 LMT/μm, n = 12 images, ***p < 0.0001; 28 versus 42 dpi NaChBac ***p = 0.0001).

(D) The percentage of presynaptic sites that were LMTs at 28 dpi was much lower in $NaChBac^+$ neurons than neurons expressing the pore-dead channel (E191K control: 88.24% ± 1.95%, n = 17 images, NaChBac: 40.66% ± 7.05%, n = 19 images, *p < 0.03).

(E) Structures resembling presynaptic terminals on the axons of both control and $NaChBac^+$ neurons accumulated synaptophysin-GFP, suggesting the change in density of the different structures correlates with a change in presynaptic sites.

Two-tailed t-test used for statistical analysis. Error bars represent SEM.

**Figure 4. Excitability-induced changes in input connectivity are dependent on cell-autonomous Npas4 signaling**

(A) Deletion of Npas4 blocked the increase in $VGAT^+$ perisomatic contacts observed in $NaChBac^+$ neurons at both 17 and 28 dpi. (17 dpi, GFP control: 5.61 ± 0.34 $VGAT^+$ puncta/soma, n = 56 neurons from 4 DGs, $NaChBac^+$: 7.96 ± 0.34 $VGAT^+$ puncta/soma, n = 115 neurons from 4 DGs, $NaChBac^+Npas4^-$: 6.64 ± 0.32 $VGAT^+$ puncta/soma, n = 84 neurons from 5 DGs; GFP control versus $NaChBac^+$ **p < 0.005; $NaChBac^+$ versus $NaChBac^+Npas4^-$ *p = 0.03; 28 dpi, GFP control: 5.65 ± 0.33 $VGAT^+$ puncta/soma n = 121 neurons from 6 DGs, $NaChBac^+$: 7.8 ± 0.26 $VGAT^+$ puncta/soma n = 115 neurons from 6 DGs, $NaChBac^+Npas4^-$: 5.33 ± 0.64 $VGAT^+$ puncta/soma n = 70 neurons from 5 DGs; GFP control versus $NaChBac^+$ ***p = 0.0005; $NaChBac^+$ versus $NaChBac^+Npas4^-$ *p = 0.017). Absence of Npas4 alone did not decrease the number of contacts and caused

a slight increase at 28 dpi (17 dpi, Npas4$^-$: 5.84 ± 0.37 VGAT$^+$ puncta/soma, n = 85 neurons from 4 DGs; E191K control versus Npas4$^-$ p = 0.67; 28 dpi, Npas4$^-$: 6.61 ± 0.26 VGAT$^+$ puncta/soma, n = 130 neurons from 5 DGs; E191K control versus Npas4$^-$ *p < 0.05).

(B) High magnification confocal maximal projection images showing that eliminating Npas4 signaling from NaChBac$^+$ neurons effectively restored spine density and size to resemble that of controls.

(C) Deletion of Npas4 from NaChBac$^+$ neurons had no change on the decrease in LMT density observed (NaChBac$^+$: 0.002 ± 0.00046 LMT/μm, n = 11 images; NaChBac$^+$Npas4$^-$: 0.0037 ± 0.00086 LMT/μm, n = 18 images, p = 0.1; E191K control versus NaChBac$^+$ ***p = 0.0003; E191K control versus NaChBac$^+$Npas4$^-$ **p = 0.006; NaChBac$^+$Npas4$^-$ versus Npas4$^-$ **p = 0.008)

(D) Absence of Npas4 signaling prevented decrease in spine density resulting from NaChBac activity; there was no significant difference between the spine density on control neurons and that of NaChBac$^+$ neurons lacking Npas4 (E191K control: 1.05 ± 0.001 spines/μm, n = 21 images from 4 DGs; NaChBac$^+$Npas4$^-$: 1.03 ± 0.075 spines/μm, n = 47 images from 4 DGs, p = 0.83; E191K control versus NaChBac$^+$ **p = 0.007; NaChBac$^+$ versus NaChBac$^+$Npas4$^-$ *p = 0.0235). Deletion of Npas4 alone did not increase spine density (Npas4$^-$: 1.19 ± 0.063 spines/μm, n = 51 images from 5 DGs; E191K control versus Npas4$^-$ p = 0.158).

(E) Deletion of Npas4 from NaChBac$^+$ neurons decreased dendritic spine size to almost as low as control levels. (E191K control: 0.6 ± 0.009 μm$^2$, n = 24 images from 3 DGs;

$NaChBac^{+}Npas4^{-}$: 0.69 ± 0.018 $\mu m^2$, n = 37 images from 4 DGs, *p = 0.01). Deletion of Npas4 alone did not decrease spine size, but led to a very small increase ($Npas4^{-}$: 0.71 ± 0.027 $\mu m^2$, n = 50 images from 5 DGs; E191K control versus $Npas4^{-}$ *p = 0.02; $NaChBac^{+}Npas4^{-}$ versus $Npas4^{-}$ p = 0.69).

Two-tailed t-test used for statistical analysis. Error bars represent SEM.

See also Figure S3.

## SUPPLEMENTAL FIGURES

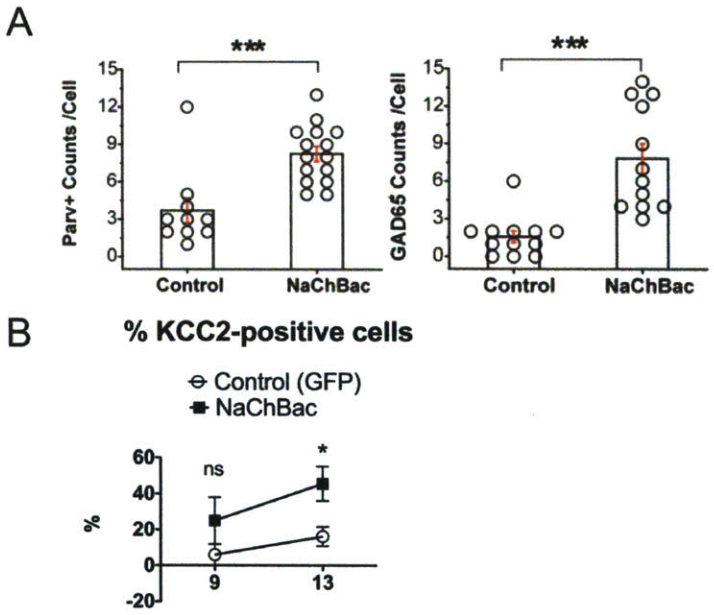


**Figure S1. NaChBac activity alters the development of DG GCs**

(A) Consistent with the increase in $VGAT^+$ perisomatic contacts, $NaChBac^+$ GCs have more parvalbumin- and GAD65-positive contacts on their cell bodies.

(B) A larger proportion of neurons expressing NaChBac are KCC2-positive compared to control neurons at both 9 and 13 dpi, suggesting KCC2 is upregulated earlier in development in $NaChBac^+$ GCs. *p = 0.023.

Two-tailed t-test used for statistical analysis. Error bars represent SEM.

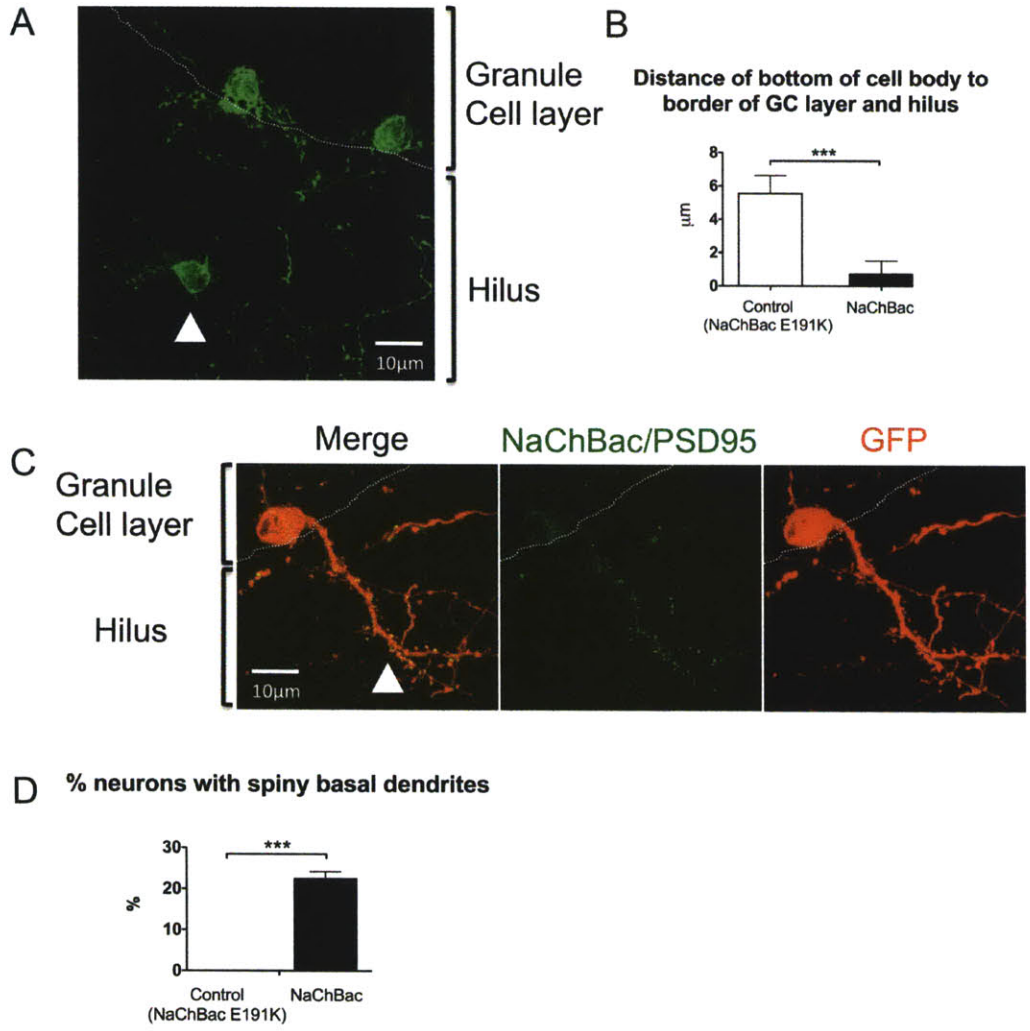


**Figure S2. Increased electrical activity via NaChBac results in ectopic localization of DG GCs, reduced migration and persistence of basal dendrites**

(A) NaChBac$^+$ GCs were occasionally found in the hilar region of the DG where control neurons are never found.

(B) NaChBac$^+$ GCs have cell bodies that are located lower within the granule cell layer of the DG compared to control neurons expressing the pore-dead NaChBac E191K. ***p = 0.0004.

(C) Basal dendrites on NaChBac$^+$ GCs displayed PSD95-positive spines.

(D) Some NaChBac$^+$ GCs displayed basal dendrites compared to none of age-matched control neurons. *p < 0.0001.

Two-tailed t-test used for statistical analysis. Error bars represent SEM.

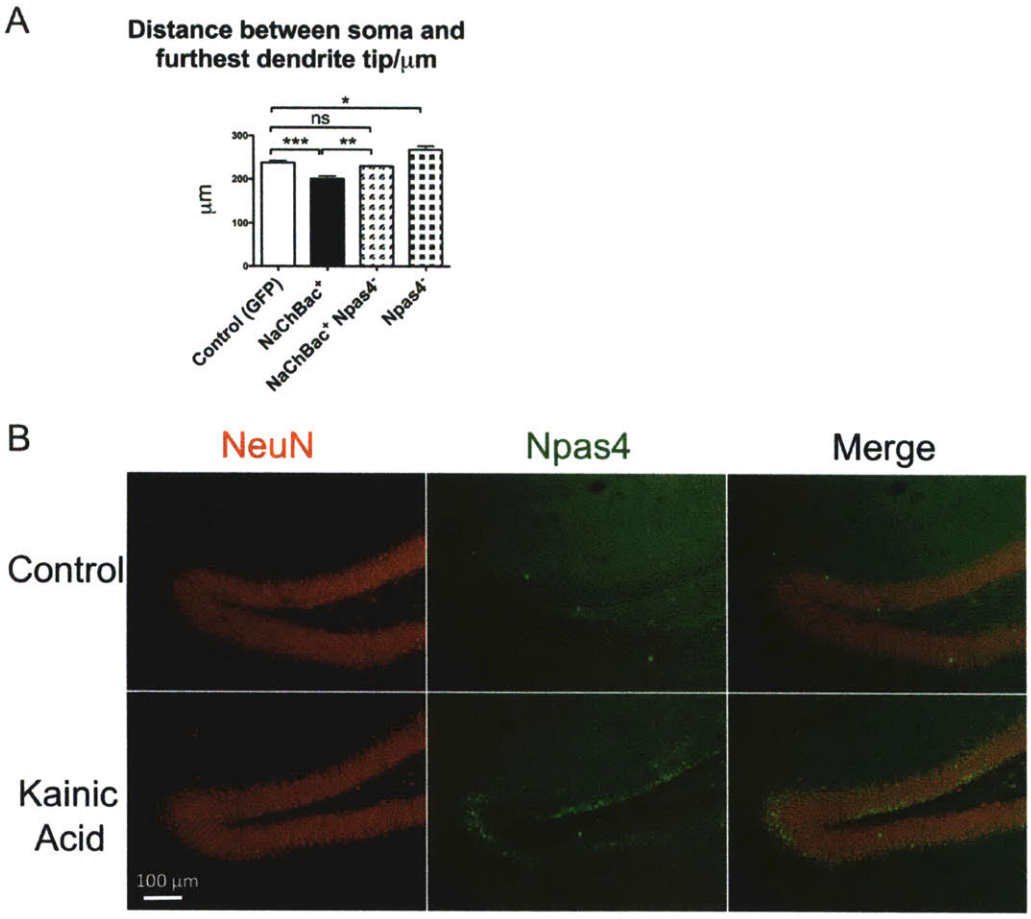


**Figure S3. Npas4 regulates activity-dependent input synaptic morphology**

(A) Absence of Npas4 signaling blocks the decrease in dendritic length observed in NaChBac$^+$ GCs. *p = 0.0203, **p = 0.0041, *** p = 0.0009.

(B) Npas4 expression is extremely sparse among GCs in the DG under control conditions, but is upregulated upon neuronal activation, such as with application of kainic acid.

Two-tailed t-test used for statistical analysis. Error bars represent SEM.

## SUPPLEMENTAL EXPERIMENTAL PROCEDURES

### Retroviral vectors

Cloning of the different constructs was performed using standard molecular techniques. The cDNA for NaChBac was obtained from David Clapham (HHMI, Children's Hospital, Harvard Medical School, Boston). NaChBac E191K was generated by PCR based on previously published sequences (Taglialatela et al., 1995; Yang et al., 1995; Yue et al., 2002). Retroviral vectors were derived from a Moloney leukemia virus with an internal promoter derived from the Rous sarcoma virus (Molar) (Kelsch et al., 2007). Retroviral particles were produced and stored as previously described (Lois et al., 2002). The viral titers were approximately 107 infectious units/μl. Viral constructs were generated as follows. NaChBac-EGFP: the stop codon of NaChBac was eliminated by PCR and fused in frame to the cDNA of EGFP. NaChBac-Cre: the stop codon of the NaChBac-EGFP fusion was eliminated by PCR, and linked by a foot-and-mouth disease (FMDV) virus 2A sequence to the cDNA of Cre Recombinase. PalmEGFP-NaChBac: the palmitoylation sequence from the GAP43 gene was first added to the N-terminus of EGFP. The stop codon of the palmitoylated version of EGFP was eliminated by PCR and linked by a FMDV 2A picornavirus sequence to the cDNA of NaChBac. Synaptophysin-GFP: the stop codon of Synaptophysin was eliminated by PCR and fused in frame to the

cDNA of EGFP. Synaptophysin GFP-NaChBac: the stop codon of the Synaptophysin-GFP fusion was removed by PCR and linked by a 2A sequence to the cDNA of NaChBac. PSD95-GFP: the stop codon of PSD95 was eliminated by PCR and fused in frame to the cDNA of EGFP. PSD95GFP-NachBac: the stop codon of the PDS95-GFP fusion was removed by PCR and linked by a 2A sequence to the cDNA of NaChBac. Invertible PalmMCherry: The doublefloxed inverse open reading frame vector was obtained from Karl Deisseroth. The ChR2-EYFP cDNA was excised from the vector and replaced with the cDNA of Palmitoylated mCherry, which was made by adding the palmitoylation sequence from the GAP43 gene to the N-terminus of the mCherry cDNA.

**Retroviral labeling in vivo**

9 to 12-week old female BL6 mice (Charles River), 'floxed' NMDA-receptor subunit 1 mice (Tsien et al., 1996), 'floxed' BDNF mice (REF), 'floxed' Npas4 mice (REF), p75 knockout mice (REF) and their respective wildtype littermates, were stereotaxically injected at 2 sites per dentate gyrus with 0.5 μl/site of retroviral vectors, after anesthesia with avertin solution. The stereotaxic coordinates were 2.0 mm posterior from bregma, 1.5 mm lateral from the midline, and 1.95 mm ventral from the brain surface, and 2.7 mm posterior from bregma, 1.9 mm lateral from the midline, and 2.05 mm ventral from the brain surface.

**Histology**

Mice were administered an overdose of avertin, before they were perfused intracardially, first with phosphate buffer saline (PBS) and then with 3% paraformaldehyde (PFA). The brains were incubated with 3% PFA overnight, and cut with a Leica vibratome into 40

μm frontal sections. For immunocytochemistry, the sections were first blocked with blocking solution containing bovine serum albumin (3 mg/ ml PBS), and 0.25% Triton X-100 in PBS, and incubated overnight in the relevant primary antibody diluted in blocking solution: polyclonal rabbit anti-GFP antibody (Chemicon; AB3080; 1:2000), rabbit anti-RFP antibody (Lifespan; LS-C60076; 1:200), mouse anti-VGAT antibody (SYSY; Cat. No. 131 002; 1:500), mouse anti-parvalbumin (Sigma; P3088; 1:500), rabbit anti-Npas4 (gift from Yingxi Lin; 1:10,000). Sections were washed 4 times in PBS, for 10 min each time, before a 2-hour incubation at room temperature with Alexa Fluor® 488 or 555 goat anti-rabbit or anti-mouse secondary antibody (Molecular Probes) diluted 1:700 in blocking solution. The sections were washed 4 times in PBS, for 10 min each time, before being mounted on slides with mounting medium (VectashieldTM; Vector Labs).

**Survival ratio analysis**

2 viruses were mixed at an approximate 1:1 ratio for survival analysis. One of the viruses carried the construct encoding mCherry, while the other carried either NaChBac or NaChBac E191K fused to EGFP (NaChBac-EGFP or NaChBacE191K-EGFP). Fluorescently labeled cells were quantified with the aid of the Neurolucida software (MicroBright Field Inc.). The survival ratio is defined as the total number of EGFP-positive cells (including double-labeled cells) divided by of the number of singly labeled mCherry-expressing cells. The ratio of EGFP+ to mCherry+ neurons at 7 days post infection (dpi) was used to normalize all data at subsequent time points for comparison, hence ratios at all subsequent time points were relative to the 7 dpi ratio. Ten to 20 entire sections per dentate gyrus were analyzed to collect at least 100 counted cells in each

dentate gyrus. The mean survival ratio from each dentate gyrus was treated as a single sample.

**Electrophysiology**

For electrophysiology, viruses in which NaChBac is directly fused to GFP were used, because they produce strong fluorescent signals in the soma, which is useful for targeting neurons for fluorescence-guided whole cell recordings. A virus containing the mCherry construct is co-injected into the same DG, and mcherry-only expressing neurons are used as controls for recording. Animals were given an overdose of ketamine/xylazine then perfused intracardially with ice-cold slicing solution containing (in mM): 212 sucrose, 3 KCl, 1.25 NaH2PO4, 26 NaHCO3, 7 MgCl2, 10 glucose (308 mOsm, and pH 7.3). Brain slices were incubated in ice-cold cutting solution and cut into 350 μm frontal slices with a Leica microtome at a speed of 0.08 mm/s. Slices were incubated for 30 min at 35°C, for recovery, in carbogenated recording solution containing (in mM): 125 NaCl, 2.5 KCl, 1.25 NaH2PO4, 26 NaHCO3, 1 MgCl2, 2 CaCl2, 20 glucose (312 mOsm, and pH 7.3). Fluorescent-guided whole-cell patch clamp recordings were performed with a MultiClamp 700B amplifier (Axon Instruments). The pipette solution contained (in mM): 2 NaCl, 4 KCl, 130 K-gluconate, 10 HEPES, 0.2 EGTA, 4 Mg-ATP, 0.3 Tris-GTP, 14 Tris-phosphocreatine (pH 7.3). Successful patching onto the target cell was confirmed by identifying a fragment of fluorescent membrane trapped inside the pipette tip during or after the recording. Pipette resistance ranged from 5 to 8 MΩ, and the pipette access resistance was always less than 16 MΩ after series resistance compensation. The junction potential was not corrected throughout the study. For spontaneous EPSC (sEPSC) recording, the neurons were held at -77 mV and synaptic events were collected at 25°C.

sEPSC contributed to the majority of spontaneous events because ~98% of events could be blocked by 100 μM D, L-AP-5 and 20 μM NBQX (Sigma) at the end of the recording. Inhibitory blockers such as bicuculline were not included during sEPSC recording because they triggered frequent EPSC bursting input in granule neurons, which precluded further analysis. To record sIPSCS intracellular 130 K-gluconate was replaced with 130 CsCl and included 20 μM NBQX and 50 μM AP-5 in the recording bath in order to increase the driving force for chloride efflux, enabling us to record spontaneous GABAergic input at -77mV.

**Analysis of electrophysiological data**

Data was acquired and analyzed with pClamp9 software (Axon Instruments), and 2 min traces of sIPSCs and sEPSCs were analyzed with Mini Analysis Program (Synaptosoft Inc.). Overall current was calculated by multiplying the average charge area per spike of each individual neuron by frequency of spikes of the same neuron.

**Morphological and perisomatic inhibitory terminal puncta analysis**

Confocal image stacks of 40 μm-thick dentate gyrus sections were taken with an Olympus Fluoview laser confocal microscope (Olympus) with a 60X objective lens, a zoom of 1.5 and at z-intervals of 0.25 μm. 10-30 neurons were analyzed in each DG for dendritic length, density, spine size and perisomatic inhibitory analysis, and data from 4-7 DGs were collected for each experimental condition. Data was analyzed with the aid of the Neurolucida software (MicroBright Field Inc.) and the MetaMorph® software (Molecular Devices).

**Statistical analysis**

The Mann-Whitney test from OriginPro 8 (Origin Lab Corporation) was used for comparing the frequency of spontaneous firing in $NaChBac^{+}$ and control neurons at resting membrane potential to determine statistical significance. All other data was analyzed with the two-sample two-tailed Student's t-test in Prism 5 (GraphPad Software, Inc). Data was reported as mean ± SEM.

**Supplemental References**

Kelsch, W., Mosley, C.P., Lin, C.W., and Lois, C. (2007). Distinct mammalian precursors are committed to generate neurons with defined dendritic projection patterns. PLoS Biol 5, e300.

Lois, C., Hong, E.J., Pease, S., Brown, E.J., and Baltimore, D. (2002). Germline transmission and tissue-specific expression of transgenes delivered by lentiviral vectors. Science 295, 868-872.

Taglialatela, M., Ficker, E., Wible, B.A., and Brown, A.M. (1995). C-terminus determinants for Mg2+ and polyamine block of the inward rectifier K+ channel IRK1. EMBO J 14, 5532-5541.

Tsien, J.Z., Huerta, P.T., and Tonegawa, S. (1996). The essential role of hippocampal CA1 NMDA receptor-dependent synaptic plasticity in spatial memory. Cell 87, 1327-1338.

Yang, J., Jan, Y.N., and Jan, L.Y. (1995). Control of rectification and permeation by residues in two distinct domains in an inward rectifier K+ channel. Neuron 14, 1047-1054.

Yue, L., Navarro, B., Ren, D., Ramos, A., and Clapham, D.E. (2002). The cation selectivity filter of the bacterial sodium channel, NaChBac. J Gen Physiol 120, 845-853.

Chapter 3

# Increasing heterogeneity in the organization of synaptic inputs of mature olfactory bulb neurons generated in newborn animals

# Increasing heterogeneity in the organization of synaptic inputs of mature olfactory bulb neurons generated in newborn animals

Wolfgang Kelsch, Shuyin Sim, and Carlos Lois

## ABSTRACT

New neurons are added into the mammalian brain throughout life. Continual neuronal addition may provide the circuit with a particular neuronal type that possesses similar characteristics regardless of when cells are generated during an animal's life. Alternatively, new neurons generated at different stages of an animal's life could have specialized properties and process information differently. To begin distinguish these two possibilities, we compared the densities of glutamatergic synapses of olfactory bulb granule cells (GC) generated in newborn and adult rats over extended periods of time. We observed that whereas adult-born GCs maintained stable cell-to-cell variability of synaptic densities soon after they integrated into the circuit, cell-to-cell variability of synaptic densities of neonatal-born GCs increased months after their integration. We then investigated whether mature neonatal- and adult-born GCs differed in activity-dependent reorganization of their synapses by inducing sensory deprivation after new GCs had completed their differentiation. This late sensory deprivation induced qualitatively different and overall more pronounced changes in the synaptic densities of neonatal-born GCs than in adult-born GCs. These observations suggest that synapses of mature neonatal-born GCs retain a high degree of malleability in response to changes in neuronal activity.

*Author Contributions: Wolfgang Kelsch and Shuyin Sim designed the experiments, designed and generated retroviral vectors, performed intracranial injections, collected and analyzed cell survival data. Wolfgang Kelsch, Shuyin Sim and Carlos Lois wrote the manuscript.*

## INTRODUCTION

It is generally believed that adult neurogenesis provides a continuous influx of immature neurons that are highly plastic only while they are integrating into brain circuits, and subsequently lose most of this plasticity necessary for storage of novel information. Adult neurogenesis could thus represent a continual addition of immature neurons with essentially the same set of properties as neurons generated in the developing brain. An alternative hypothesis is that adult-born neurons may have special properties that allow these new neurons to behave differently and perform different functions from neonatal-born neurons.

The vast majority of new neurons added to the olfactory bulb (OB) throughout postnatal life are granule cells (GCs) that are generated in the subventricular zone (SVZ) and migrate to the GC layer where they differentiate and form synapses (Altman, 1962; Lois and Alvarez-Buylla, 1993; Luskin, 1993). GCs are axon-less interneurons that receive different types of glutamatergic inputs onto synapses in distinct dendritic domains. Deprivation of sensory input during neuronal differentiation ("early deprivation") induces changes to the synaptic densities in all dendritic domains of adult-born GCs (Kelsch et al., 2009). In contrast, deprivation starting after these neurons have differentiated ("late deprivation") only evokes limited synaptic reorganization. These observations suggest a critical period for activity-dependent remodeling of synapses in adult-generated GCs in line with a similar temporal window for inducibility of synaptic long-term potentiation in adult-born GCs (Nissant et al., 2009).

We previously observed that neonatal- and adult-born GCs differ in the sequence in which their synapses form while neurons mature and integrate into the circuits of the OB (Kelsch et al., 2008). However, it is not known whether mature neonatal- and adult-born GCs

also differ in how they maintain their synaptic organization over extended periods of time post-maturation. Here we analyze the organization of synaptic inputs to neonatal-born GCs throughout the animal's life and in response to sensory deprivation after the new neurons completed their maturation and observed that mature neonatal-born GCs retain a high degree of malleability in response to changes in neuronal activity.

## MATERIALS AND METHODS

**Generation of retroviral vectors and retroviral labeling *in vivo*.** Recombinant retroviral vectors under the control of the Rous Sarcoma virus promoter for PSD-95:GFP (PSDG) and Synaptophysin:GFP (SypG) (M*psdg* and M*sypg*) were prepared and stored as described (Kelsch et al., 2008). All animal procedures were approved by the local Animal Welfare Committee and NIH guidelines. Retroviruses were injectedAt stereotaxic coordinates: (anterior; lateral; ventral; mm in reference to Bregma) +1.2; ±1.6; -3.1 for adult rats (>P56) and +0.9; ±2.1; -2.1 for neonatal rats (P5). Animals were kept in a 12 h daylight cycle and under the same housing conditions. Experiments for neonatal- and adult-born GCs were performed at the same time and under similar conditions (same housing room, same type of ventilation cage, and two animals per cage after weaning).

**Analysis of synaptic markers.** Tissue processing and analysis of $SypG^+$ and $PSDG^+$ clusters was performed as previously described (Kelsch et al., 2009). For long-term survival, each analyzed data point (e.g. basal domain, 17 days post infection (d.p.i.)) contained normally distributed $PSDG^+$ cluster densities from 42 cells (3 GCs were analyzed from each animal), expect for 1-year-old adult-born GCs of which we only found a total of 19 complete preserved $PSDG^+$ cells in 8 of 11 injected animals. We observed more superficial adult-born

GCs at 1-year than at one month after they had been generated (data not shown), however due to the originally intended low labeling density for reconstructions, we did not statistically quantify this shift towards more superficial GCs amongst these long-term surviving cells. As GCs with deep and superficial dendritic targeting in the external plexiform layer had comparable mean and *s.d.* of synaptic densities in their dendritic domains at the respective time points (data not shown), data were pooled. Statistical differences in the standard deviation (*s.d.*) were determined using a *Bartlett's* test and for pair wise comparisons a F-test for differences in variances (Prism Gaph). For sensory deprivation experiments, unilateral surgical naris occlusion was performed on the day of intracerebral injection of viruses M*psdg and* M*syp* into the subventricular zone (postnatal day 5). Only animals that showed a strong reduction in immunofluorescences of *c-fos* (Oncogene antibody) expression in the granule cell layer and reduction of tyrosine hydroxylase (Chemicon antibody) expression in the glomerular layer in the deprived bulb were included in further analysis.

## RESULTS

### Protracted changes in the synaptic organization of neonatal-born GCs

We compared synaptic densities of neonatal- or adult-born GCs at 1, 2, and 12 months after they were generated in the SVZ to investigate potential long-term changes in synaptic organization (Fig. 1*A*). Synaptic organization is defined here as the density of glutamatergic input synapses in various dendritic domains. We used oncoretroviral vectors to genetically label synapses in new GCs, because retroviral labeling allows reliable birth-dating of new neurons (Sanes, 1989). To measure the density of glutamatergic input synapses, we delivered PSDG, a genetic marker consisting of a fusion protein between PSD-95 and GFP.

PSD-95 is a protein localized to the postsynaptic density of glutamatergic input synapses (Sheng, 2001). PSDG delivered into new neurons with retroviral vectors (M*psdg*) can be used to genetically label these synapses (Niell et al., 2004; Gray et al., 2006; Kelsch et al., 2008; Livneh et al., 2009; Sturgill et al., 2009), and expression of PSDG at modest levels produced by retroviral expression does not alter synaptic properties as measured by electrophysiological methods (Kelsch et al., 2008). $PSDG^+$ clusters were contacted by the presynaptic protein Bassoon both in immature (Kelsch et al., 2008) and 1-year old GCs (data not shown), and PSDG was clustered at asymmetric synapses on an ultra-structural level (Livenh et al., 2009).

We examined the densities of glutamatergic synapses in different dendritic domains of GCs. The apical dendrite can be divided into an unbranched segment emerging from the soma (the proximal 15% of this unbranched segment is referred to as the proximal domain (Kelsch et al., 2008)) followed by a branched segment (distal domain). The proximal domain and basal dendrite (basal domain) receive axo-dendritic glutamatergic input from axon collaterals of the OB's projection neurons and from axons originating in the olfactory cortices (Mori, 1987). Synapses present in the distal domain of the apical dendrite are bidirectional dendro-dendritic synapses where input and output synapses are co-localized and functionally coupled. These synapses receive glutamatergic input synapses from the lateral dendrites of the OB's projection neurons and release GABA back onto these same projection neurons (Mori, 1987).

We compared the densities of input synapses in neonatal- or adult- born GCs 1, 2, and 12 months after they had been generated in the SVZ (Fig. 1*A*). We observed that the variability (*s.d.*) of densities of $PSDG^+$ synapses in the different dendritic domains of adult-born GCs did not change between 1, 2 and 12 months after they were generated (Fig. 1*B*;

Table 1). Similarly in neonatal-born GCs, the variability (*s.d.*) of densities of $PSDG^+$ synapses did not change in the distal domain over time (Fig. 1*B*; Table 1). Interestingly, the variability (*s.d.*) of densities of $PSDG^+$ synapses in neonatal-born GCs increased between the early time points (1 and 2 months old GCs) and 1 year after their birth increased in the proximal and basal domain (Fig. 1*B*; Table 1). The increase in variability (*s.d.*) of however was only significant for the 1-year time point as 1 and 2 months-old GCs displayed similar variability (*s.d.*).

To investigate changes in densities of output synapses over time, we labeled them using SypG, a fusion protein between Synaptophysin and GFP (Fig. 2*A*). Synaptophysin is a protein localized to presynaptic neurotransmitter vesicles (Sudhof and Jahn, 1991) and SypG expressed with retroviral vectors (M*sypg*) can be used to genetically label output synapses (Meyer and Smith, 2006; Kelsch et al., 2008, 2009). Output synapses of GCs are located in their distal dendritic domain, and they are part of dendro-dendritic synapses (Hinds, 1970). We observed that variability (*s.d.*) of densities of $SypG^+$ clusters were stable between 1 month and 1 year for both neonatal- and adult-born GCs (n.s., Bartlett's test; Fig. 2*B*), consistent with stability of densities of $PSDG^+$ synapses in the distal domain.

As we compared 1- to 2-month- and 1-year-old GCs in different animals, we validated whether variability of densities of $PSDG^+$ clusters is biased for same maturation stage (e.g. 1-month-old neonatal-born GCs) by variability in our experimental conditions over time. We therefore labeled new GCs at P5 in separate groups of animals in parallel to the 1-year-observation-period of animals shown Fig. 1 and examined neonatal-born GCs 1 month after they had been generated. Their mean density and variability (*s.d.*) of $PSDG^+$ synapses did not significantly differ (data not shown). In addition, systematically splitting the data sets of Fig. 1 did not reveal any difference in the mean density and variability (*s.d.*) of

$PSDG^+$ synapses for the same maturation stage (data not shown). Finally, we tested whether neonatal-born GCs would increase cell-to-cell variability shortly after the animal reached adulthood (≥P56) that would then suggest that postnatal maturation of the brain environment would largely account for the increase in heterogeneity. We therefore examined the variability (*s.d.*) of densities of $PSDG^+$ synapses of neonatal-born GCs 4 months after they had been generated (basal~ 0.324±0.116, proximal~ 0.458±0.176, distal domain 0.352±0.109 $PSDG^+$ cluster/μm, n=14 GCs). These values tended to increase in variability (*s.d.*), but did not yet differ significantly from 1- and 2-month-old GCs in Fig. 1 (Bartlett's test), suggesting a slow increase over time.

We followed up on this finding by analyzing whether the increased variability in the synaptic density in the basal dendrite of neonatal-born GCs after maturation was accompanied by changes in its arbour length. We did not observe any significant differences in the length of the dendritic arbor length of the basal domain or its variability between samples of neonatal GCs that were either 1-month- or 1-year old (median [inter quartile range]: 77.5 [48.3-123.8] μm and 70.7 [50.3-105.2] μm, n=70 GCs respectively, Mann-Whitney test: p=0.48, Bartlett's test: p=0.51). We also found that the increase in variability of synaptic density in the proximal and basal domains occurred to the same degree in neonatal-generated GCs regardless of whether they had dendrites branching in the deep or superficial layers of the OB (data not shown).

In summary, the cell-to-cell variability in synaptic densities does not significantly increase in adult-born GCs after they acquire their final synaptic density within a month after being generated. In contrast, synaptic densities in the basal and proximal domains of neonatal-born GCs become increasingly variable between cells even up to 1-year after their birth.

**Sensory deprivation continues to change the synaptic organization of mature neonatal-born GCs**

Neonatal- and adult-born GCs differ in the patterns in which they develop synapses in their dendritic domains during maturation (Kelsch et al., 2008), and in the dynamics of synaptic organization in their dendritic domains after maturation. Do neonatal- and adult-born GCs also differ in the manner in which their synapses are affected by manipulations of sensory input? GCs are part of a sensory relay circuit, and we recently observed that immature adult-born GCs change the synaptic densities of all dendritic domains when sensory input is blocked during neuronal integration into the bulb ("early deprivation") (Kelsch et al., 2009). We thus examined how the synaptic organization of immature neonatal-born GCs changes when deprived of sensory input.

We induced early sensory deprivation by performing unilateral naris occlusion at P5 when viral vectors were delivered to label new GCs in the SVZ (Fig. 3*A*), and subsequently examined the synaptic organization of new neonatal-born GCs using the PSDG and SypG markers (M*psdg* and M*sypg*, respectively). After sensory deprivation, significantly fewer $PSDG^+$ input synapses were present in the distal and basal dendritic domains (Fig. 3*A*). In addition, the density of $SypG^+$ output synapses in the distal dendritic domain also decreased significantly for deprived neonatal-born GCs (at 28 d.p.i.: mean density±*s.d.*: control: 0.365±0.067 and deprived: 0.243±0.077, n=14 GCs, $p<0.0001$, *t*-test). These findings are similar to the effects caused by sensory deprivation in immature adult-born GCs. However, whereas early olfactory deprivation increased $PSDG^+$ proximal synapses in adult-born GCs, it did not trigger any changes in the proximal domain of neonatal-born neurons (Fig. 3C).

After synaptic development, 3 weeks of sensory deprivation only evokes changes in densities of glutamatergic synapses in the proximal, but not in the basal and distal domain (Kelsch et al., 2009). As neonatal-born GCs displayed an increase in heterogeneity that occurred slowly over several months (Fig. 1), we first examined whether a longer period of 'late deprivation' might evoke changes in the basal and distal domain of adult-born GCs. We observed that 'late deprivation' of adult-born GCs for 7 to 9 weeks did not cause any change in the synaptic densities in the distal (deprived: 0.322±0.074 and non-deprived: 0.316±0.125 $PSDG^+$ clusters/μm, $p$=0.87, both $n$=14) and basal domains (deprived: 0.349±0.146 and non-deprived: 0.320±0.092 $PSDG^+$ clusters/μm, $p$=0.52, both $n$=14). In addition, synaptic densities of adult-born GCs remained increased in the proximal domain after 9 weeks of sensory deprivation (deprived: 0.746±0.230 and non-deprived: 0.561±0.138 $PSDG^+$ clusters/μm, $p$=0.01, both $n$=14).

In contrast to adult-born GCs, the synaptic densities of neonatal-born GCs become progressively more heterogeneous over extended periods of time. This suggests that neonatal-born GCs may be able to reorganize their synaptic inputs for longer periods of time than adult-born GCs. Thus, we investigated whether neonatal-born GCs, like adult-born GCs, had a restricted period within which extensive changes in their synaptic organization occurred, or whether mature neonatal-born GCs retained the ability to change their synaptic organization in response to sensory deprivation.

We labelled GCs in the SVZ of newborn animals (P5) and started unilateral naris occlusion only when animals reached adulthood. 'Late deprivation' of neonatal-born GCs started at P75 resulted in a significant loss of basal and distal synapses after 7 weeks of sensory deprivation (Fig. 3*B*). In addition, a transient decrease in the density proximal synapses was observed after 3 weeks of deprivation, but this density returned to control

levels after 7 weeks of deprivation (Fig. 3*B*). Thus, late sensory deprivation affected synaptic densities in all dendritic domains of neonatal-born GCs.

These results indicate that mature neonatal-born GCs retain a higher degree of malleability in terms of reorganizing their synaptic densities in response to changes in sensory activity than mature adult-born GCs (Fig. 3*C*), which is consistent with increasing heterogeneity of synaptic densities of mature neonatal-, but not adult-born GCs.

## DISCUSSION

It is generally believed that adult neurogenesis provides a continuous influx of immature neurons that become less plastic as they mature such that the circuit requires subsequent waves of immature neurons to provide plasticity to store novel information. According to this hypothesis, adult neurogenesis represents the continuous addition of immature neurons with the same properties, regardless of whether they are generated in the developing or adult brain. We observed that whereas adult-born GCs maintained stable synaptic densities soon after integrating into the circuit in line with this hypothesis, whereas the density of synaptic inputs in neonatal-born GCs keeps changing for many subsequent months. In addition, mature neonatal-, but not adult-born GCs remained malleable to reorganize their synaptic densities in all dendritic domains in response to manipulation of sensory input. Thus, suggesting neonatal- and adult-born GCs not only differ in their initial pattern of synaptic development, but also thereafter when they function as mature neurons in the OB. Future study may further explore the dynamics of long-term changes in the same neurons over time to also examine subtle differences in addition to changes in cell-to-cell variability.

**Sources of synaptic heterogeneity**

Synaptic densities in the dendritic domains of neonatal-born GCs become increasingly heterogeneous throughout the life of the animal long after these neurons mature. Heterogeneity in the synaptic organization of neonatal-born GCs can be attributed to several factors that shape the formation, stabilization or loss of synapses. These factors include cell-intrinsic factors such as a high intrinsic level of cell-to-cell variability (Raser and O'Shea, 2005), as well as extrinsic factors such as variability in the number of pre-synaptic axons in the immediate proximity of individual synapses (Stepanyants and Chklovskii, 2005). Neonatal-born GCs retain the ability to change their synaptic densities in their basal and proximal dendritic domains over long periods of time in response to changes in activity (Fig 3*C*). Perhaps as a result of this long-lasting synaptic plasticity, their synaptic densities display increasing variability between individual neurons over time. In contrast, adult-born GCs acquire their final density of synapses within 1 month after their birth, and display no change in cell-to-cell variability in the density of their synapses once they mature (Fig 4*B*). Thus, once they mature, adult-born GCs appear to acquire one 'flavor' that under normal circumstances does not change over prolonged periods of time. This suggests that these neurons may become hardwired soon after their differentiation to perform a defined computational task over the neuron's lifetime. In contrast, mature neonatal-born GCs seem to change their 'flavors' over time, suggesting a more dynamic wiring that may reflect changes in their computational demands during their lifespan.

**Neonatal- and adult-born GCs may perform different functions in the olfactory bulb**

Different forms of plasticity of mature adult-born GCs in comparison with neonatal-born GCs are underscored by widespread changes in the synaptic organization of neonatal-born GCs in contrast to the restricted remodeling of adult-born GCs caused by late sensory deprivation. When late sensory deprivation, which is induced post-differentiation, was performed, widespread changes in synaptic wiring of neonatal-born GCs were observed only after a long period of deprivation, in contrast to the rapid changes seen during early sensory deprivation. This is reminiscent of the slow increase in heterogeneity of synaptic densities in these neurons under non-deprived conditions. Interestingly, although we observed a decrease in synaptic density in the distal domain of neonatal-born GCs triggered by late sensory deprivation, in non-deprived animals there was little change in the variability or mean density of these distal synapses over time. It is possible that the distal synapses of neonatal-born GCs only change their density if the activity of the OB circuit is perturbed in an extreme manner, such as by sensory deprivation. Alternatively, it is possible that the changes that occur in dendro-dendritic synapses under non-deprived conditions, in contrast to the changes seen in axo-dendritic synapses, are too subtle to be detected using our methods.

Axonal projections from higher olfactory areas to GCs ('axo-dendritic inputs') are thought to provide context-related information like reward or aversion that shapes early odor processing in the OB (Kiselycznyk et al., 2006; Su et al., 2009). Activation of axo-dendritic inputs depolarizes and globally excites GCs. Global excitation of GCs facilitates inhibition of tufted and mitral cells (Chen et al., 2000; Halabisky and Strowbridge, 2003) and thereby axo-dendritic inputs may shape odor processing (Laurent, 1999). The increasing heterogeneity in the axo-dendritic synaptic densities of neonatal-born GCs and their ability to sustain deprivation-induced plasticity suggest that they can adapt their synaptic wiring to changing

demands over the animals' lifespan. In particular, reorganizing their axo-dendritic inputs may change the context-related information that activates neonatal-born GCs during odor processing at different stages of the animal's life.

In contrast to neonatal-born GC, adult-born GCs may use activity-dependent mechanisms within a restricted window of time to allow sensory information to shape synaptic wiring during their differentiation. After their integration into the circuit, it appears that adult-generated GCs' stereotypical synaptic organization remains mostly unperturbed for the rest of their existence. Such a 'snapshot' model of synaptic wiring would fit with recent observations that adult-born GCs may be involved in forming long-lasting memories acquired at one point in the life of the animal (Mak and Weiss, 2010). Interestingly, whereas few neonatal-born GCs die after they mature throughout life of the animal, adult-born GCs show a continuous turnover throughout life, potentially also explaining the low numbers of 1-year-old adult-Born GCs that we found (Fig. 1). Such differences in turnover would match that 'snapshots' taking adult-born GCs are discarded after some time (Petreanu et al., 2002; Lemasson et al., 2005, Mouret et al., 2009) whereas neonatal-born GCs adapt their wiring over time and stay in the circuit. In summary, the different degrees of plasticity between neonatal- and adult-born GCs suggest a role of neonatal-born GCs as life-long learners and of adult-born GCs as 'capture-and replay' modules in the OB circuit.

## REFERENCES

Altman J (1962) Are new neurons formed in the brains of adult mammals? Science 135:1127-1128.

Chen WR, Xiong W, Shepherd GM (2000) Analysis of relations between NMDA receptors and GABA release at olfactory bulb reciprocal synapses. Neuron 25:625-633.

Gray NW, Weimer RM, Bureau I, Svoboda K (2006) Rapid redistribution of synaptic PSD-95 in the neocortex in vivo. PLoS Biol 4:e370.

Halabisky B, Strowbridge BW (2003) Gamma-frequency excitatory input to granule cells facilitates dendrodendritic inhibition in the rat olfactory Bulb. J Neurophysiol 90:644-654.

Hinds JW (1970) Reciprocal and serial dendrodendritic synapses in the glomerular layer of the rat olfactory bulb. Brain Res 17:530-534.

Kelsch W, Lin CW, Lois C (2008) Sequential development of synapses in dendritic domains during adult neurogenesis. Proc Natl Acad Sci U S A 105:16803-16808.

Kelsch W, Lin CW, Mosley CP, Lois C (2009) A critical period for activity-dependent synaptic development during olfactory bulb adult neurogenesis. J Neurosci 29:11852-11858.

Kiselycznyk CL, Zhang S, Linster C (2006) Role of centrifugal projections to the olfactory bulb in olfactory processing. Learn Mem 13:575-579.

Laurent G (1999) A systems perspective on early olfactory coding. Science 286:723-728.

Lemasson M, Saghatelyan A, Olivo-Marin JC, Lledo PM (2005) Neonatal and adult neurogenesis provide two distinct populations of newborn neurons to the mouse olfactory bulb. J Neurosci. 25:6816-25.

Livneh Y, Feinstein N, Klein M, Mizrahi A (2009) Sensory input enhances synaptogenesis of adult-born neurons. J Neurosci 29:86-97.

Lois C, Alvarez-Buylla A (1993) Proliferating subventricular zone cells in the adult mammalian forebrain can differentiate into neurons and glia. Proc Natl Acad Sci U S A 90:2074-2077.

Luskin MB (1993) Restricted proliferation and migration of postnatally generated neurons derived from the forebrain subventricular zone. Neuron 11:173-189.

Mak GK, Weiss S (2010) Paternal recognition of adult offspring mediated by newly generated CNS neurons. Nat Neurosci 13:753-758.

Meyer MP, Smith SJ (2006) Evidence from in vivo imaging that synaptogenesis guides the growth and branching of axonal arbors by two distinct mechanisms. J Neurosci 26:3604-3614.

Mori K (1987) Membrane and synaptic properties of identified neurons in the olfactory bulb. Prog Neurobiol 29:275-320.

Mouret A, Lepousez G, Gras J, Gabellec MM, Lledo PM (2009) Turnover of newborn olfactory bulb neurons optimizes olfaction. J Neurosci. 29:12302-14.

Niell CM, Meyer MP, Smith SJ (2004) In vivo imaging of synapse formation on a growing dendritic arbor. Nat Neurosci 7:254-260.

Nissant A, Bardy C, Katagiri H, Murray K, Lledo PM (2009) Adult neurogenesis promotes synaptic plasticity in the olfactory bulb. Nat Neurosci. 728-30.

Petreanu L, Alvarez-Buylla A (2002) Maturation and death of adult-born olfactory bulb granule neurons: role of olfaction. J Neurosci. 22:6106-13.

Raser JM, O'Shea EK (2005) Noise in gene expression: origins, consequences, and control. Science 309:2010-2013.

Sanes JR (1989) Analysing cell lineage with a recombinant retrovirus. Trends Neurosci 12:21-28.

Sheng M (2001) Molecular organization of the postsynaptic specialization. Proc Natl Acad Sci U S A 98:7058-7061.

Stepanyants A, Chklovskii DB (2005) Neurogeometry and potential synaptic connectivity. Trends Neurosci 28:387-394.

Sturgill JF, Steiner P, Czervionke BL, Sabatini BL (2009) Distinct domains within PSD-95 mediate synaptic incorporation, stabilization, and activity-dependent trafficking. J Neurosci 29:12845-12854.

Su CY, Menuz K, Carlson JR (2009) Olfactory perception: receptors, cells, and circuits. Cell 139:45-59.

Sudhof TC, Jahn R (1991) Proteins of synaptic vesicles involved in exocytosis and membrane recycling. Neuron 6:665-677.

## FIGURES

### Figure 1

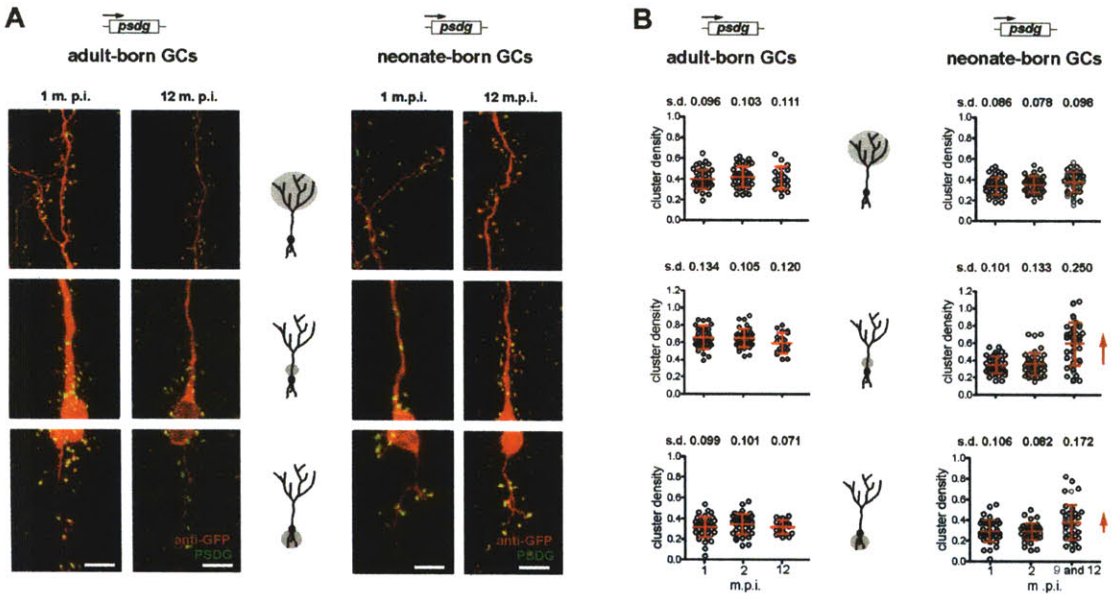


**Figure 1 Neonatal-born GCs show an increasing variability in densities of input synapses in axo-dendritic input domains over time.**

***A***, Adult- and neonatal-born GCs were examined 1-month and 1-year post infection (p.i.). To attribute $PSDG^+$ clusters (green) to a particular GC, dendritic morphology was visualized by immunofluorescence with red secondary antibodies against the diffuse PSDG present in the cytosol that was otherwise undetectable (Kelsch et al., 2008). The 3 main dendritic domains were analyzed separately (from top): distal, proximal and basal domain (scale bar=10 µm).

***B***, Scatter plots of $PSDG^+$ clusters in each dendritic domain (clusters/µm), of adult- and neonatal-born GCs 1-, 2-, and 12-months p.i. (42 GCs each expect for 12-months old adult born GCs (n=19). The 3 dendritic domains are, from top, the distal, proximal, and basal domains. Mean values ± *s.d.* are plotted in red and *s.d.* values are indicated above each time point. Significant increases in the *s.d.* over time were determined with *Bartlett*'s test (*p*-values are indicated if $p<0.05$). Changes in the mean cluster density are indicated by arrows (for statistical analysis see Table 1). 28 GCs from 12 months p.i. and 14 GCs of 9 months p.i. were pooled for the late time point of neonatal-born GCs.

**Table 1**

**A. Adult-born GCs:**

PSDG$^+$ synapses densities

| ~ domain | Bartlett's test: equal variances? | Bartlett's test: *p*-value |
|---|---|---|
| distal | yes | *p*=0.764 |
| proximal | yes | *p*=0.301 |
| basal | yes | *p*=0.318 |

*= In a total of 8 injected animals only 19 complete labeled Gcs were found and analyzed.

**B2. Neonate-born GCs:**

PSDG$^+$ synapses densities:

| ~ domain | Bartlett's test: equal variances? | Bartlett's test: *p*-value | *F*-test for different variances: 1 m.p.i. *vs.* 2 m.p.i. | *F*-test for different variances: 1 m.p.i. *vs.* 12 m.p.i. | *F*-test for different variances: 2 m.p.i. *vs.* 12 m.p.i. |
|---|---|---|---|---|---|
| distal | yes | *p*=0.764 | *p*=0.516 | *p*=0.410 | *p*=0.142 |
| proximal | **no** | ***p*<0.0001** | *p*=0.090 | ***p*<0.0001** | ***p*<0.0001** |
| basal | **no** | ***p*<0.0001** | *p*=0.112 | ***p*=0.0024** | ***p*<0.0001** |

**= The pooled 12 months p.i. sample also contains the 9 months p.i. sample.

## Figure 2

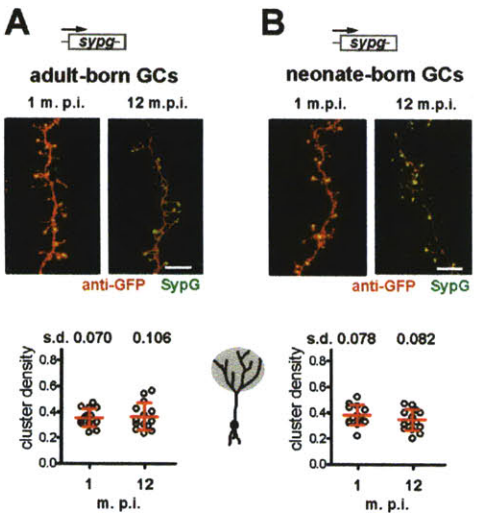


**Figure 2 Density of output synapses does not change after maturation of adult- or neonatal-generated GCs.**

***A***, Synaptophysin:GFP$^+$ (SypG) clusters were examined in the distal domain of adult- and neonatal-born GCs 1-month and 1-year p.i. (scale bar=10 μm).

***B***, Scatter plot of densities of SypG$^+$ clusters (clusters/μm) of adult- and neonatal-born GCs 1- and 12-months p.i.. Their variances did not significantly increase (F-test) for adult- and neonatal-born GCs (p=0.15 and p=0.84).

**Figure 3**

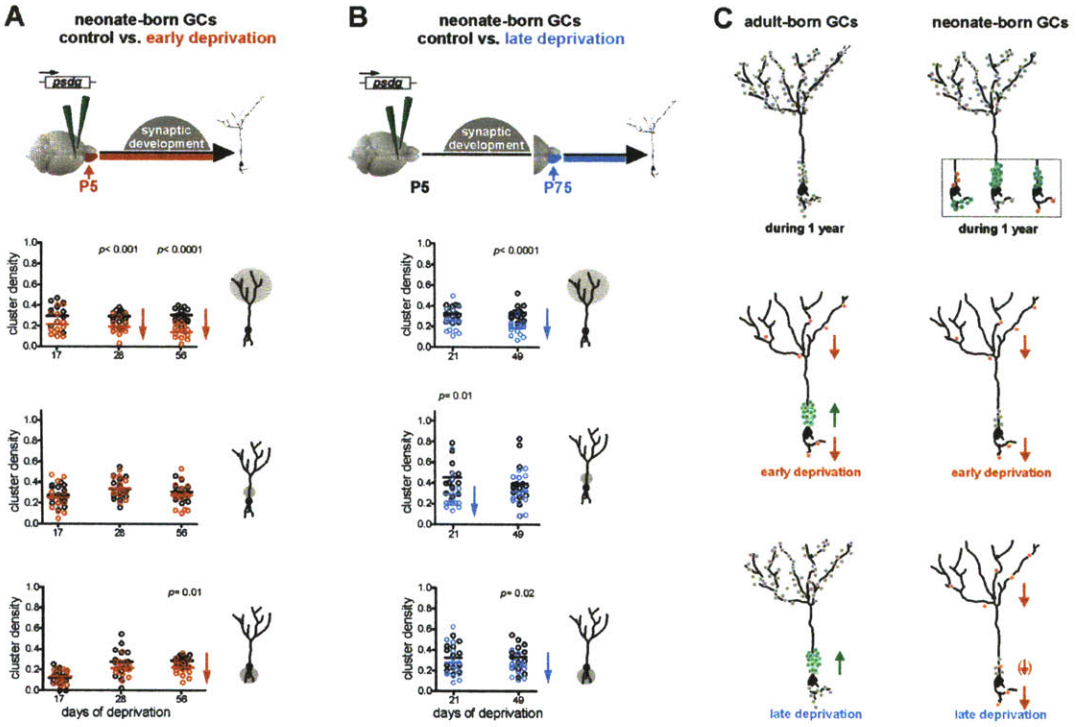


**Figure 3 Glutamatergic input synapse density of neonatal-born GCs is affected by sensory deprivation occurring both during and after their integration in the circuit.**

*A*, Early sensory deprivation: Progenitor cells were infected with retroviruses in the SVZ at P5 on the same day as unilateral naris occlusion was performed. Genetically labeled GCs were examined at different lengths of time after occlusion. Scatter plot and mean density of $PSDG^+$ clusters (clusters/μm) of neonatal-born GCs in sensory deprived and contralateral control olfactory bulbs (red and black circles, respectively). Statistical significance is only indicated if $p<0.05$ (*t*-test).

*B*, Late sensory deprivation: Progenitor cells were infected with retroviruses in the SVZ at P5 and unilateral naris occlusion started at P75. Genetically labeled GCs were examined at different lengths of time after occlusion. Scatter plot and mean density of $PSDG^+$ clusters (clusters/μm) of neonatal-born GCs in sensory deprived and contralateral control olfactory bulbs (blue and black circles, respectively). Statistical significance is only indicated if $p<0.05$ (*t*-test).

*C*, Top row: Adult-born GCs acquire their final density of synapses within 1 month after being generated, and the cell-to-cell variability in their synaptic densities does not increase thereafter. Even months after neonatal-born GCs had been generated, they have not completely acquired a final density of synapses and the values of their synaptic densities in their basal and proximal domains become highly variable from cell-to-cell. Middle row: Early sensory deprivation reduced synaptic densities in the distal and basal

domain of both neonatal- and adult-born GCs. However, early sensory deprivation increased the synaptic density in the proximal domain of adult-born GCs but had no effect in neonatal-born GCs. Bottom row: In adult-born GCs, when sensory deprivation started after the completion of synaptic development, the only detectable changes were increases in the density of glutamatergic input synapses in the proximal domain. In contrast, in neonatal-born GCs, sensory deprivation that started only after their integration into the circuit decreased the density of glutamatergic synapses in their basal and distal domains and transiently in their proximal domain.

# Conclusion

The study of survival and integration of new neurons into mature, active circuits is of interest in the pursuit of neuronal replacement therapies for neurodegenerative diseases, as well as to understand how we might repair an injured brain. Because adult-born neurons are believed to contribute to lifelong learning, an understanding of these phenomena also elucidates how new memories are formed in adulthood while existing memories are kept intact. This thesis presents several novel findings regarding the regulation of synaptic integration of new neurons in the adult olfactory bulb (OB) and hippocampus that furthers the current body of knowledge in the field and presents new directions for future research. Among other implications, our findings indicate that, first, adult neurogenesis may involve the addition of neurons that possess distinct characteristics and perform a complementary function to neurons born during the early development of the brain. Second, survival selection of adult-born neurons is not regulated by specific patterns of spiking activity but by levels of membrane depolarization. Third, alteration of a single neuron's excitability is sufficient to effect changes in synaptic connectivity, which are driven by genetic programs triggered by the activation of immediate early genes.

## ACTIVITY-DEPENDENT REGULATION OF SYNAPTIC CONNECTIVITY OF NEW NEURONS IN THE ADULT BRAIN

In contrast to the notion that adult neurogenesis is merely a continuous addition of the same types of neurons generated during development of the brain, we show in Chapter 3 that neonatal-born neurons display more plasticity in altering their synaptic densities than adult-born neurons. Together with the observation that neonatal-born neurons have a longer

lifespan than adult-born neurons and are less likely to be turned over, these findings support a model of adult-born neurons providing a substrate by which instantaneous new memories are formed. These memory traces become stabilized and intractable after the window of plasticity has closed. Neurons born during the neonatal period, however, may serve to provide flexibility in the circuit to allow for rearrangements of connectivity in response to changing environments and other challenges during the course of an animal's life.

In Chapter 1, our results demonstrate that a certain threshold of membrane depolarization is necessary for survival of adult-born granule neurons in the OB, while precise patterns of neuronal spiking are not essential. In particular, during a critical period during neuronal maturation, the survival of these neurons is sensitive to cholinergic innervation originating from other parts of the brain, which could result from changes in behavioral states such as learning, exercise, or mood changes. This could provide an explanation for how the abovementioned states can affect survival of adult-born neurons (Alonso et al., 2006; Rochefort et al., 2002; van Praag et al., 1999).

Finally, we see in Chapter 2 that although the dentate gyrus (DG) circuit possesses the ability to modulate various aspects of synaptic inputs and outputs of new neurons in response to single-cell activity changes, GABAergic innervation seems to be the primary way in which the excitability of new neurons is regulated. Activity-dependent synaptic changes are effected through a genetic program triggered by immediate early gene Npas4. This activity-dependent genetic program bridges an increase in single-cell activity with the transcriptional activity necessary to bring about changes at synapses, and has no apparent role at baseline conditions in the DG.

Additional data also supports the idea that there is a window of plasticity for synaptic alterations in response to changes in intrinsic activity. When we induce expression NaChBac later in neuronal development of adult-born neurons in the DG, using a Cre-ER system activated by tamoxifen, we see a decrease in the magnitude of synaptic changes compared to when expression is induced earlier (data not shown). This finding corresponds to the observation that as these neurons mature, they display decreasing synaptic plasticity in response to seizure activity (Kron et al., 2010). In addition, not only is there a window of plasticity in the developmental timeframe of each neuron, the brain environment also appears to be less conducive to synaptic plasticity as it ages. When we expressed NaChBac in new neurons born into the brains of middle-aged mice (more than 1 yr old), the decrease in spine density observed was similar to neurons in young adult mice, but the increase in spine size was very much smaller, suggesting that in the aged brains, either the DG environment or the stem cell niche environment has altered the capacity of the new neurons or the surrounding circuit to make morphological changes in response to the neuron's elevated intrinsic excitability.

## DIFFERENCES IN REGULATION OF SYNAPTOGENESIS OF NEW NEURONS IN THE OLFACTORY BULB AND DENTATE GYRUS

Our results demonstrate some differences in the way alteration of intrinsic activity of new neurons affects their integration into the active circuits of the OB and DG. There are fundamental differences present in these two systems, and differences in how new connections are formed may simply reflect differences in the function of the OB and DG in the overall performance of the adult brain. These findings have strong implications on how

scientists should view the function and behavior of adult-born neurons in different parts of the brain.

While granule neurons in the DG are bipolar and possess apical dendrites extending in one direction and a basal axon extending in the opposite direction towards CA3 of the hippocampus, granule cells of the OB are axonless and possess bidirectional dendro-dendritic synapses through which they innervate other tufted and mitral OB neurons. DG granule neurons are excitatory, and exclusively release glutamate onto their target neurons both within the DG and at CA3. OB neurons are inhibitory interneurons that release GABA onto neurons within the OB only. DG neurons migrate a very small distance to their final position (less than 10 microns), while OB neurons spend a long portion of their maturation (almost a week) traveling through the rostral migratory stream to reach the OB from the walls of the lateral ventricle where they are born (Lois et al., 1996). This distance can be as far as 1mm in rodent brains.

Incorporation of new neurons with intrinsic excitability altered with either expression of NaChBac or ESKir2.1 into the OB has dramatic results on their survival, but this survival effect is not observed in the DG. This is surprising especially because the survival of DG granule neurons has been found to be sensitive to single-cell input activity, as demonstrated by the observation that survival decreases by half when the NMDA receptor is deleted (Tashiro et al., 2006). One possibility is that survival of adult-born neurons in the DG is not as sensitive to the extent to which we modulate levels of intrinsic excitability as the granule cells in the OB. Alternatively, our experimental methodology could simply be inadequate to detect the difference. Due to the necessity of sparse infection of neurons in the DG and the low numbers of new neurons, we infect about 200 neurons per DG, which does not provide

sufficient resolution to detect small survival differences. In contrast, we label on the order of several thousand neurons in the adult OB.

NaChBac expression also leads to morphological alterations in DG neurons, many of which recapitulate changes seen in neurons post-seizure, that are not observed in OB neurons. In fact, none of the manipulations of intrinsic excitability affect morphology of OB granule cells, which suggests that for those neurons, changes in extrinsic input is necessary to effect synaptic changes such as those observed in sensory deprivation (Kelsch et al., 2009). The plasticity responses of excitatory and inhibitory neurons differ in many respects (Bi and Poo, 1998), and this could explain the difference in activity-dependent synaptic changes between DG and OB granule neurons.

## FUTURE DIRECTIONS

Several possibilities for future studies emerge from these results. One interesting study would be to examine how reversible changes in synaptic connectivity are if normal excitability levels are restored both within and outside the period of synaptic plasticity. This finding would impact treatments for seizures, as it would determine if neuronal damage is reversible. The observation that increasing inhibitory GABAergic input is the main response to a new neuron with elevated excitability could be followed up by an experiment using RNAi to knockdown components of the GABA receptor in single NaChBac-expressing neurons to study the responses of the neuron and its surrounding circuit if its excitability cannot be dampened through the action of GABA receptors. It would also be interesting to examine real-time changes in the synapses of adult-born as well as neonatal-born neurons while neuronal activity is altered in a temporally-controlled fashion either within a single neuron

e.g. using channelrhodopsin/ halorhodopsin, or circuit wide e,g. via seizures, or stimulation and deprivation paradigms.

## REFERENCES


Alonso, M., Viollet, C., Gabellec, M.M., Meas-Yedid, V., Olivo-Marin, J.C., and Lledo, P.M. (2006). Olfactory discrimination learning increases the survival of adult-born neurons in the olfactory bulb. J Neurosci *26*, 10508-10513.

Bi, G.Q., and Poo, M.M. (1998). Synaptic modifications in cultured hippocampal neurons: dependence on spike timing, synaptic strength, and postsynaptic cell type. J Neurosci *18*, 10464-10472.

Kelsch, W., Lin, C.W., Mosley, C.P., and Lois, C. (2009). A critical period for activity-dependent synaptic development during olfactory bulb adult neurogenesis. J Neurosci *29*, 11852-11858.

Kron, M.M., Zhang, H., and Parent, J.M. (2010). The developmental stage of dentate granule cells dictates their contribution to seizure-induced plasticity. J Neurosci *30*, 2051-2059.

Lois, C., Garcia-Verdugo, J.M., and Alvarez-Buylla, A. (1996). Chain migration of neuronal precursors. Science *271*, 978-981.

Rochefort, C., Gheusi, G., Vincent, J.D., and Lledo, P.M. (2002). Enriched odor exposure increases the number of newborn neurons in the adult olfactory bulb and improves odor memory. J Neurosci *22*, 2679-2689.

Tashiro, A., Sandler, V.M., Toni, N., Zhao, C., and Gage, F.H. (2006). NMDA-receptor-mediated, cell-specific integration of new neurons in adult dentate gyrus. Nature *442*, 929-933.

van Praag, H., Kempermann, G., and Gage, F.H. (1999). Running increases cell proliferation and neurogenesis in the adult mouse dentate gyrus. Nat Neurosci *2*, 266-270.